Università
Ca'Foscari
Venezia

Scuola Dottorale di Ateneo
Graduate School

Dottorato di ricerca
in Economia
Ciclo XXVIII
Anno di discussione 2016

Three Essays In Panel Data Econometrics

Settore scientifico disciplinare di afferenza: SECS-P/05

Tesi di Dottorato di Agudze, Komla Mawulom, Matricola: 840524

Coordinatore del Dottorato
Prof. Michele Bernasconi

Tutore del Dottorando
Prof. Monica Billio

Co-tutore del Dottorando
Prof. Roberto Casarin

Three Essays In Panel Data Econometrics

by

Agudze, Komla Mawulom

Matricola 840524

A thesis submitted in partial fulfillment
for the degree of

Doctor of Philosophy in Economics

Department of Economics

Ca' Foscari University of Venice,

Graduate School of Economics and Management, Veneto

Supervisors :

Prof. Monica Billio
Prof. Roberto Casarin

July, 2016

Declaration

I, Agudze Komla Mawulom, hereby declare that this Ph.D thesis titled " Three Essays In Panel Data Econometrics" is a presentation of my original research work for the degree of Doctor of Philosophy in Economics under the guidance and supervision of Prof. Monica Billio and Prof. Roberto Casarin. Wherever contributions of others are involved, every effort is made to indicate this clearly, with due reference to the literature, and acknowledgement of collaborative research and discussions.

I affirm that this work has not been submitted previously in the same or similar form to another examination committee at another department, university or country.

Signed:

_____

Date:

_____

Abstract

The contributions of this thesis are discussed in three self contained chapters.

Chapter 1 contributes to the literature on regional growth-cycles by developing in a Bayesian framework different notion of multivariate cycle synchronization and proposing an encompassing model combining three dimensions: panel, Markov-switching and multivariate synchronization. The approach is used to study the chronology of provincial growth-cycles in China's economy from March 1989 to July 2009. The estimations reveal the importance of a third regime of rapid-growth in growth-cycle dynamics at both the national and provincial levels. The first regime of recession is of two types: classical recession and growth recession. The third regime of rapid-growth is also of two types: catching or bounce back. We obtain evidence of geographical clusters and qualitative differences among growth rates between coastal and interior provinces. Moreover, this retrospective view sheds some lights on China's 'new-normal' of slower growth since early 2010.

Chapter 2 proposes a new dynamic panel model for large sets of time series with series-specific Markov-switching processes. We introduce a network-based neighbourhood system and allow for local and global interactions between the Markov chains. The paper also contributes to the literature on Markov-switching dynamic panel by developing an efficient Markov-Chain Monte Carlo (MCMC) algorithm for the posterior approximation based on the Metropolis adjusted Langevin (MALA) sampling method. We study the efficiency and convergence of the proposed MCMC through several simulations experiments. The

empirical application of the model is based on the US states coincident indices produced by the Federal Reserve Bank of Philadelphia. We find evidence that the local interactions factor of a state-level cycles with a state neighbours play no role in the common movement of US regional business cycles.

Chapter 3 contributes to the research on the economic impact of diseases that reach epidemic or pandemic proportions. Using a robust production function derived from a panel of 44 Sub-Saharan African countries, it sheds light on the macroeconomic impacts of the Ebola outbreak in Guinea, Liberia and Sierra Leone (GLS). More precisely, the paper shows that the contemporaneous impact of the Ebola outbreak on output growth is largely propagated via the channel of human capital stock. It develops VAR scenario to assess the impact of the shock on various macroeconomic variables with important policy implications.

Contents

List of Tables

List of Figures

Chapter 1

Growth-cycle phases in China's provinces: A Bayesian panel Markov-switching approach

1.1 Introduction

The recent slowdown in China's growth is a widely accepted stylized fact. In order to assess this, it is necessary to look back at China's previous experience. Unlike advanced countries where a slowdown means moving from expansion to recession, China's experience proved that a slowdown comes either from a transition from rapid growth to normal growth or from moderate growth to recession or growth-recession. The rapid-growth regime is generally considered as typical of emerging economies engaged in the catching up of the advanced economies. When looking at the Chinese industrial catching-up process, a too often neglected dimension is the domestic catching-up where backward regions grow more rapidly than their neighbors. The domestic catching-up effect can be examined considering the chronology of the provincial growth-cycles. This paper will primarily focus on two main questions: what are the patterns of provincial growth-cycles? Are growth rates heterogeneous across provinces during the different phases of the growth-cycles? The dating of the cycle's phases is a crucial step to identify the factors which influence the growth-cycle. Studying the Chinese provincial growth-cycles before the years 2009 may even offer

new insights and precursory signals about the entrance of the Chinese economy into a 'new normal' of slower growth since the early 2011's.

Very often, similar research questions have been answered for some countries but not for China. Moreover, the traditional method used to answer such questions is based on a two-stage approach. The first stage is the inference of the cycle's phases and the second stage is the synchronization analysis. While a two step procedure is easy to apply, especially when the number of units of the panel is high, it does not allow the researcher to determine which forms of synchronization characterizes the cycles. Owyang et al. (2005) follow this approach to extract the growth-cycle of each state of the US and provide evidence of a tendency for national recessions to follow geographic patterns. Following a similar inference procedure, Wall (2007) considers quarterly industrial output growth from 1976 to 2005 to determine and to compare national and regional patterns of recession and expansion phases in the Japanese economy. These studies, conducted in Bayesian framework, are based on the popular univariate Markov-switching model of Hamilton (1989).

The second stage of synchronization analysis is usually based on the bivariate (Harding and Pagan (2002)) rather than a multivariate approach (Harding and Pagan (2006)). For example, there is a rich literature on the synchronization of cycles among Chinese provinces conducted under the bivariate approach. Gatfaoui and Girardin (2015) use monthly provincial industrial production indices from 1989 to 2009 and reach the conclusion that the coastal cycles are more synchronized with the national cycles than the interior ones. They also find that the timing and the duration of recessions are province specific. A similar exercise done by Barthélemy and Poncet (2008) over the period from 1990 to 2005 shows that the provincial cycles synchronization increased over time but at a low level compared to that of the U.S. states. Other works in this category include Tang (1998) and Gerlach-Kristen (2009). However, these studies do not distinguish between the

two types of slowdown that characterise the Chinese economy at provincial level. There is no information either on China's international or domestic catching-up processes.

The few works that document the dating of catching-up and bounce back effects a la Friedman (1993) in China's economy, considering the two aspects a of slowdown, have paid attention only to the national level. Girardin (2005) examines the growth-cycle features of East Asian countries including China with quarterly GDP from 1975 to 2002. His study supports the relevance of a third regime of rapid growth for Chinese growth-cycles and that China's national growth-recessions are short and mostly volatile. Other similar examples include Langnana and Hongweib (2007), Liu and Zheng (2008) and Chengyong and Chunrong (2010). Zheng et al. (2010) instead exploit unobserved component methodology with quarterly GDP data from 1978 to 2009 and find evidence of a bounce back effect and a structural break in Chinese economy.

The main contributions of this paper are as follows. First, this paper offers a methodological contribution to the literature of regional growth-cycles by proposing an encompassing model built in a Bayesian framework combining three important dimensions: panel, Markov-switching and synchronization. The panel dimension enables us to take into account interaction among provinces left out in a province-by-province estimation and can be seen as a generalization of the Bayesian univariate Markov-switching model in Owyang et al. (2005). The Markov-switching dimension as usual is helpful for inferring the cycles' phases. The panel model allows for different types of multivariate synchronization and a better understanding of the relationships between provincial cycles (e.g. Hamilton and Owyang (2012), Kaufmann (2010, 2015) and Billio et al. (2016b).

Secondly, we propose a notion of imperfect multivariate synchronization within a Markov-switching framework. This notion can be seen as an intermediate case between perfect multivariate synchronization and strong non-synchronization (see also Çakmaklı et al. (2013)

and Paap et al. (2009) for a different notion of imperfect synchronization). Ideally, in a country like China with more than 60 years of monetary union, one can expect that provincial growth-cycles phases come from homogeneous transition mechanisms even if synchronization is not perfect. In particular, homogeneous transition of provincial growth-cycles phases can be seen as a potential gain from the monetary union.

In principle, the test of multivariate synchronization of Harding and Pagan (2006), modified by Candelon et al. (2009) can be applied. Nevertheless, such a test suffers from a 'boundary value' problem and the distribution of the joint test requires weights that are complex to get and can only be approximated conducting simulation exercises. Thus, we follow a different route and consider a panel of Markov chains with various transitions which allows for different degrees of multivariate synchronization.

One of the main results of this paper is the establishment of a comprehensive chronology of China's growth-cycle phases at the national and provincial levels. Our chronology of the provincial growth-cycles put on evidence a change in the domestic catching-up behaviour of the cycles after the entry of China into the World Trade Organization (WTO).

In addition, we find evidence imperfectly synchronized cycles and of two types of slow-down at the provincial level. The estimations favour the three-regime classification at both the national and provincial levels making very important the third regime for the analysis for heterogeneity across provinces and regime.

The analysis of the mean growth rates in the normal and rapid-growth regimes suggests that the coastal provinces seem to drive the Chinese economy by exhibiting 'Strong' features of growth while the interior provinces present 'Weak' features. The 'Strong rapid-growth' regime prevails only on the coast and can be seen as the 'growth miracle' regime.

The number of provinces in rapid-growth has increased over time while the occurrence and length of growth-recessions decreased over time. As regards the regime heterogeneity,

all provinces exhibit shorter duration of growth-recession or recession than normal and rapid-growth.

The paper is structured as follows. Section 2 presents the Bayesian panel Markov-switching model with three possible degrees of synchronization among the time series and outlines the estimation procedure. In Section 3, we discuss the data and present some evidence supporting its reliability. Section 4 investigates the industrial growth-cycle phases in China's provinces using the proposed model. Section 5 studies the chronology of China's provincial growth-cycles and Section 6 provides conclusions.

1.2 A Bayesian Panel Markov-Switching Model

1.2.1 A panel model with different synchronization possibilities

In the following, since our aim is to date shifts between different growth regimes, we propose a Bayesian panel Markov-switching model with no autoregressive components. This can be seen as a generalization of the Bayesian Markov-switching model in Owyang et al. (2005) to a population of time series. We denote X_{it}, $i = 1, \ldots, N$, $t = 1, \ldots, T$, the observable process, that is the industrial output growth of the province i at time t, with N the total number of units and T the length of the series of the panel. We assume X_{it}, $i = 1, \ldots, N$, $t = 1, \ldots, T$, are conditionally normal with mean and variance depending on the latent process S_{it}, $t = 1, \ldots, T$. The evolution of industrial output growth is described by the following model

$$X_{it} = \sum_{k=1}^{K} \mathbb{1}_{\{k\}}(S_{it})(\mu_{ik} + \sigma_{ik}\varepsilon_{it}), \quad \varepsilon_{it} \overset{i.i.d.}{\sim} \mathcal{N}(0,1), \quad t = 1, \ldots, T \tag{1.1}$$

[1] The first benchmark model used to assess the convergence in industrial output is the growth regression model which involves regressing the current per capita output growth on the initial per capita output plus in some cases a set of conditioning variables. The second model know as distribution approach studies the shape and the inter-temporal dynamics in different time periods.

for $i = 1, \ldots, N$, where K is the number of regimes, and $\mathbb{1}_{\{E\}}(X)$ is the indicator function which takes value 1 if $X \in E$ and 0 otherwise. We assume $Cov(\varepsilon_{it}, \varepsilon_{jt}) = 0$, for all $i \neq j$. The parameters μ_{ik} and σ_{ik} represent the mean growth rate and the output growth volatility, respectively, of province i in state $S_{it} = k$. The latent process S_{it}, $t = 1, \ldots, T$ provides a description of the growth cycle of the i-th province, and each variable S_{it} denotes the province-specific state of economic activity. We assume that S_{it} is a discrete valued Markov (regime switching) process with values in the set $\{1, \ldots, K\}$, and with time-homogeneous transition probability

$$P(S_{it} = j_1 | S_{it-1} = j_2, \ldots, S_{i1} = j_{t-1}) = P(S_{it} = j_1 | S_{it-1} = j_2) = p_{j_1, j_2} \tag{1.2}$$

The model in equation (1.1) is then considered under three different types of assumptions, each assumption leading to a different synchronization models and estimation procedures. The three assumptions naturally take into account different degrees of similarity between the growth-cycle dynamics of the provinces. These are: strong multivariate non-synchronization (Assumption 1), imperfect cycle synchronization with space-homogeneous transition (Assumption 2), and perfect synchronization (Assumption 3). To the three assumptions correspond the following models.

From Harding and Pagan (2006), strong multivariate non-synchronization between states occurs when under Assumption 1, the states of the economy are province-specific and independent across provinces, and their dynamics does not share any similarity. Otherwise stated, the processes S_{it} are independent across provinces and each process has its own transition matrix which is

$$\mathbb{P}\left(S_{it+1} | S_{it}\right) = P_i = \begin{pmatrix} p_{i,11} & \cdots & p_{i,1K} \\ \vdots & \ddots & \vdots \\ p_{i,K1} & \cdots & p_{i,KK} \end{pmatrix} \tag{1.3}$$

The model implied by this assumption is denoted with M_1.

Under Assumption 2, the state of the economy are province-specific, and independent across provinces, but the state transition is the same across provinces. This assumption implies that the processes S_{it}, $t = 1, \ldots, T$ are independent across provinces and follow the same transition matrix

$$\mathbb{P}\left(S_{it+1}|S_{it}\right) = P = \begin{pmatrix} p_{11} & \cdots & p_{1K} \\ \vdots & \ddots & \vdots \\ p_{K1} & \cdots & p_{KK} \end{pmatrix} \tag{1.4}$$

The model implied by this assumption is denoted with M_2 (see also Çakmaklı et al. (2013) and Paap et al. (2009) for a different notions of imperfect synchronization).

The Assumption 3 translates into perfectly synchronized cycles. According to Harding and Pagan (2006), perfect synchronization between states occurs when states are identical, that is $S_{it} = S_t$, $i = 1, \ldots, N$ with transition matrix

$$\mathbb{P}\left(S_{t+1}|S_t\right) = P = \begin{pmatrix} p_{11} & \cdots & p_{1K} \\ \vdots & \ddots & \vdots \\ p_{K1} & \cdots & p_{KK} \end{pmatrix} \tag{1.5}$$

The model implied by this assumption is denoted with M_3.

These three assumptions can be seen as an attempt to diagnose independence, imperfect synchronization and perfect synchronization in the underlying provincial growth-cycles. If the growth-cycles of all the provincial industrial growth-rates are synchronised then our panel Markov switching models based on Assumptions 1 and 2 should be statistically identical.

1.2.2 Bayesian inference

In this paper we follow a Bayesian inference approach. One of the reasons for this choice is that inference for latent-variable models calls for simulation-based methods, which can be naturally included in a Bayesian framework. Moreover, model selection and averaging

can be easily performed in an elegant and efficient way within a Bayesian framework, overcoming difficulties met by the frequency approach in dealing with model selection for non-nested models. In this paper we follow a data augmentation framework and introduce the allocation variables $\boldsymbol{\xi}_{it} = (\xi_{1,it}, \ldots, \xi_{K,it})$, where $\xi_{k,it} = \mathbb{I}_{\{k\}}(S_{it})$ indicates the regime to which the current observation X_{it} belongs. Note that in M_3, $\boldsymbol{\xi}_{it} = \xi_t$, for all i.

The parameter vector and the prior setting for the three models are described as follows. In M_1 the parameter vector is defined as $\boldsymbol{\theta}_1 = (\boldsymbol{\mu}, \boldsymbol{\sigma}, \mathbf{p})$, where $\boldsymbol{\mu} = (\mu_{11}, \ldots, \mu_{1K}, \mu_{N1}, \ldots, \mu_{NK})$, $\boldsymbol{\sigma} = (\sigma_{11}, \ldots, \sigma_{1K}, \sigma_{N1}, \ldots, \sigma_{NK})$, $\mathbf{p} = (\mathbf{p}_1, \ldots, \mathbf{p}_N)$ with $\mathbf{p}_i = (p_{i,11}, \ldots, p_{i,1K}, p_{i,K1}, \ldots, p_{i,KK})$, $i = 1, \ldots, N$. The description of the model is completed by the elicitation of the prior distributions of the parameters (see Appendix A.2 for a summary). We assume normal and inverted gamma priors for μ_{ik} and σ_{ik} and independent Dirichlet prior distributions for the rows of the transition matrices P_i, $i = 1, \ldots, N$. In M_2 and M_3 the parameter vectors are defined as $\boldsymbol{\theta}_2 = \boldsymbol{\theta}_3 = (\boldsymbol{\mu}, \boldsymbol{\sigma}, \mathbf{p})$, where $\boldsymbol{\mu}$, $\boldsymbol{\sigma}$ are defined as in M_1, and $\mathbf{p} = (p_{11}, \ldots, p_{1K}, \ldots, p_{K1}, \ldots, p_{KK})$.

The resulting posterior distribution of the parameters of the Markov-switching model is invariant to permutations in the labelling of the parameters following exchangeable priors. We address the non-identifiability of the parameters (see among others Celeux (1998) and Frühwirth-Schnatter (2001, 2006) for a review), by imposing identification restrictions naturally related to the interpretation of the different states. Thus $\mu_{i1} \leqslant \mu_{i2} \leqslant, \ldots, \leqslant \mu_{iK}$ where $i \in \{1, \ldots, N\}$ (e.g., see Billio et al. (2012, 2016b), Çakmaklı et al. (2013)).

The joint posterior distribution of the parameters and the allocation variables are discussed in Appendix B. Since Bayesian estimators are not easily obtained from analytical computation we follow a Markov-chain Monte Carlo approach to posterior approximation. Samples from the posterior can be obtained by a Gibbs-sampling algorithm. At the d-th iteration, the Gibbs sampler consists of the following steps:

1. Draw the states $S^{(d)}$ from $f(S^{(d)} \mid X, \theta^{(d-1)})$, by using a forward-filtering-backward-sampling procedure.

2. Draw the transition probabilities $\mathbf{p}^{(d)}$ from $f(\mathbf{p}^{(d)} \mid X, S^{(d)})$.

3. Draw the regime specific means $\boldsymbol{\mu}^{(d)}$,from $f(\boldsymbol{\mu}^{(d)} \mid X, S^{(d)}, \boldsymbol{\sigma}^{(d-1)})$.

4. Draw the regime specific volatilities $\boldsymbol{\sigma}^{(d)}$, from $f(\boldsymbol{\sigma}^{(d)} \mid X, S^{(d)}, \boldsymbol{\mu}^{(d-1)})$.

The full conditional distributions of the Gibbs sampler are given in Appendix A.2 together with the sampling procedure for the posterior of the allocation variables using a forward-filtering-backward-sampling (see Frühwirth-Schnatter (2006)) algorithm for the proposed panel Markov-switching models. In order to generate 5000 draws from the posterior distributions, we run the Gibbs sampler for 12000 iterations. Thereafter, we discard the first 2000 draws to avoid dependence from the initial conditions and apply a thinning procedure with a factor of 2 samples to reduce the dependence between consecutive Markov-chain draws.

1.3 Preliminary analysis on the data

In this section, we document the source of our high-frequency data suitable to analyse the growth-cycle phases in China's provinces and eventually the domestic industrial catching-up phenomenon. We carry a first estimation on the national aggregate data considering the Bayesian version of univariate the Markov-switching model. The estimation results confirm the common knowledge of three regimes in growth-cycle dynamics in the Chinese national economy. The dating based on the two-regime model is similar to the benchmark set by OECD for the aggregate Chinese economy. The dating based on the three-regime

model shows that the national rapid-growth regime is characterized by catching-up and bounce back effects. Finally, we attempt a first trial to approximate the cross sectional dimension by looking at the pattern dispersion among the provinces.

1.3.1 Source of the observed data

Our disaggregated data set is the dataset[1] of Gatfaoui and Girardin (2015). It consist of 28 Chinese provincial industrial output series. At this moment, it is the only available monthly industrial output dataset at the provincial level and its covers more than two decades, from March 1989 to July 2009. The data set contains also the aggregated monthly series for the industrial output. We consider the first difference of the logarithm of industrial production of 28 provinces of China and the aggregate Chinese industrial production. The provinces of Chongking, Tibet and Xinjiang are not included in the database because of data unavailability over the full sample.

One of the main hurdles, as described in Holz (2004a,b), when analysing cycles in output, may be the unreliability of China's economic data since provincial-government officials are rewarded for good economic performance. Young (2003) underlines another difficulty, that is the split between volume and prices which is sometimes non-existent since firms often assume that the constant price value of output is equal to the nominal one in order to save time and resources.

The Bayesian panel Markov-switching methodology proposed in this paper is suitable to deal with the issue of possible miss-measurement of the observed provincial industrial output which itself can partly reflect miss-measurement in the actual data or in the reported

[1] The source of this data is CEIC database and China Monthly Statistics, various issues (see Gatfaoui and Girardin (2015), 'Co-movement of Chinese provincial business cycles: Supplementary materials'). A major issue of this dataset is seasonality and the unavailability of data for January or February before February 1993. They considered unobserved components approach with a number of different specifications for the seasonal component to deal with these issues. The dataset is available upon request.

data. Firstly, Markov-switching approaches are less sensitive to the level of the series. In this sense, the obtained cycles will be less sensitive to the level of the observed data and by consequence to any miss-measurement in the observed data. Secondly, the panel dimension proposed in this paper takes into account a joint filtering of the hidden Markov chain to obtain the cycles. Thirdly, we let the data determine the optimal number of regimes and simultaneously select the type of synchronization among the provinces. As consequence, we are able to go deeper in the details to see the things that can be mixed when considering the traditional growth-cycle analysis (e.g., see Burns and Mitchell (1946), Bry and Boschan (1971), Artis et al. (2004) et.)

1.3.2 Classical Markov-switching dating of national cycle

A quick estimation of a two and three-regime models on the national aggregate data shows that the best model is the model with three regimes. This result, in line with the literature on Chinese national initial growth-cycle, does not necessarily discard the issue of the reliability of the database. Hence, we move our analysis one step further, prior to applying our methodology to the available dataset, by comparing (see Table 1.1) the dating of a two regime Markov-switching model with two benchmarks, one given by the Organisation for Economic Cooperation and Development (OECD) and another given by The Conference Board (TCB).

There are differences between the OECD[2] and the TCB[3]national cycles and turning points of China's economy. According to Ozyildirim and Wu (2013), the TCB has national

[2] The OECD Composite leading indicators (CLI) system is based on the growth cycle approach. The growth-cycles and turning points are measured and identified in the deviations from trend in industrial output (see Nilsson and Brunet (2006)). The trend method used by the OECD system is the 'phase-average-trend' method.

[3] The Conference Board built its China leading economic index (LEI) and coincident economic index (CEI) constructed following the NBER approach (see Guo et al. (2009))

industrial value added in addition to four other series making up its coincident indicator while the OECD uses only the national industrial value added as its coincident indicator. Thus we expect that the turning points obtained from our aggregate industrial output to be much closer to the ones of the OECD than that of the TCB. The dating of the recessions and expansions based on the smoothed probabilities from the Markov-switching model with two regime presented in Table 1.1 indicates this expectation.

Recession from Markov-switching with 2 regimes	Recession by OECD	Recession by TCB
1989M03-1991M06	1988M11-1990M07	1988M03-1989M10
1994M06-1999M08	1994M11-1999M08	1993M03-1993M11
2000M08-2001M12	2000M09-2002M01	1995M10-1998M05
2004M06-2005M02	2004M03-2005M01	2000M02-2002M02
2007M11-2008M12	2007M12-2009M2	2004M01-2004M06
		2009M01-2011M02

Table 1.1: Chinese national recessions or growth-recessions chronology based on the two-regime univariate Bayesian Markov-switching model. Data: growth rate of the national index of industrial production. Sample period: March 1989 to July 2009 (month on month). Reference chronology based on the OECD and the TCB composite index is added for comparison purpose.

1.3.3 National growth-recession, catching-up and 'bounce back' episodes

We extract the dating of the national aggregate cycle based on the three-regime model. The results in Table 1.2 indicate that three episodes of growth-recession, four episodes of rapid-growth, and five episodes of normal-growth were present at the national level. Over the period 1989M03-2009M06, the regimes identified are quite stable at the national level.

The first wave of national growth-recession occurred between 1989M03-1990M01. This comes shortly after the 1988-1989 period of turbulence leading to the Tienanmen political crisis. In Table 1.2, the second wave of growth-recession occurred between 1994M08-1997M07. This started before the East Asian crisis of 1997-1998 and was triggered by the

Growth-Recession	Normal-Growth	Rapid-Growth
1989M03-1990M01		
	1990M02-1991M07	
		1991M08-1993M12
	1994M01-1994M07	
1994M08-1997M07		
	1997M08-2002M03	
		2002M04-2004M06
	2004M07-2006M07	
		2006M08-2007M02
	2007M03-2008M03	
2008M04-2008M12		
		2009M01-2009M06

Table 1.2: Chinese national growth-cycle chronology based on the three-regime univariate Bayesian Markov-switching model. Data: growth rate of national index of industrial production. Sample period: March 1989 to July 2009 (monthly information).

austerity package initiated in July 1993 as response to overheating. During the financial crisis of 2008, we identify the third wave of growth-recession between 2008M04-2008M12. Liu (2009) points out that the switch of the national economy to recession around the financial crisis of 2008 was largely due to a 'significant slowdown in external demand and a tight monetary policy to contain inflation in the first three quarters of 2008. The first two episodes of national growth-recession come from internal policy measures of austerity while the last national growth-recession comes from negative external shocks.

The first wave of catching-up started in the third quarter of 1991 and ended in the fourth quarter of 1993. This coincides with the Eighth Five-year plan (1991-1995) that marked the beginning of a renewed economic reform. The second wave of catching-up covered the period 2002M04-2004M06, right after the entry of China into the World Trade Organization (WTO). This overlaps with the Tenth Five-year plan (2001-2005) which contributed to new reforms in terms of domestic and external financial liberalization.

Another interesting result is the disappearance of the East-Asian crisis at the national level among the recession episodes found by the two regime model in Table 1.1. According

to our three regime model which dominates the two regime model, during the East-Asian crisis China experienced normal growth.

Furthermore, the results in Table 1.2, show some evidence supporting Friedman's 'plucking' model[4] (Friedman (1993)) view which states: "a large contraction in output tends to be followed on by a large business expansion; a mild contraction, by a mild expansion". Indeed, early 2009 saw the beginning of a 'bounce back' a la Friedman as a result of a very sizeable monetary and fiscal stimulus (RMB 4 trillions) and a target of 8% growth in national GDP (Tisdell (2009)) leading to a recovery from the global financial crisis, already in the first semester of 2009.

1.3.4 Testing the Pattern of dispersion among provinces

In order to check the heterogeneity in the provincial growth-cycles over time for the coastal and the interior provinces, it is paramount to consider the following measure of cross-sectional dispersion (see Giannone et al. (2008)) of industrial output growth:

$$\frac{1}{2H+1}\sum_{h=-H}^{H}\left[\sum_{i\in R} w_{it}\left(\Delta X_{i,t+h}-\Delta X_{t+h}\right)^2\right]$$

where $\Delta X_{i,t}$ is the first difference of the logarithm of the industrial output of province i during the month t. ΔX_t is the first difference of the logarithm of national aggregate industrial output during the month t. w_{it} represents the industrial output share of province i during the month t and R represents the set of indexes of the provinces. If $R = \{1, \ldots, 28\}$ we obtain the 'global' dispersion. $R = \{1, \ldots, 12\}$ refers to the set of coastal provinces and $R = \{13, \ldots, 28\}$ to the interior ones. In the application we set $H = 6$. Based on this statistic, we distinguish the stylized facts of the dynamics of the dispersion following three

[4] The Friedman's 'plucking' model view was first explored by mean of univariate Markov-switching by Sichel (1994).

perspectives: the coastal, the interior and the aggregate perspectives.

Considering the aggregate perspective (see solid line in Figure 1.1), the sample starts with constant dispersion in provincial growth-cycles from 1989 to 1990, which turns into a period of increasing heterogeneity that culminates at the end of 1996 with a pattern of reversion from 1997 to 1998. A persistent homogeneity of provincial growth-cycles takes place from 1999 to the end of 2002. From 2003, a new pattern of strong heterogeneity in growth-cycles occurs and is more pronounced at mid 2005. A reversion pattern towards reduction of heterogeneity occurs up to the end of 2007 and turns into a period of increasing dispersion in early 2009. Nevertheless, for the first time the patterns of heterogeneity changes after mid 2007 with higher dispersion in the interior than in coastal provinces.

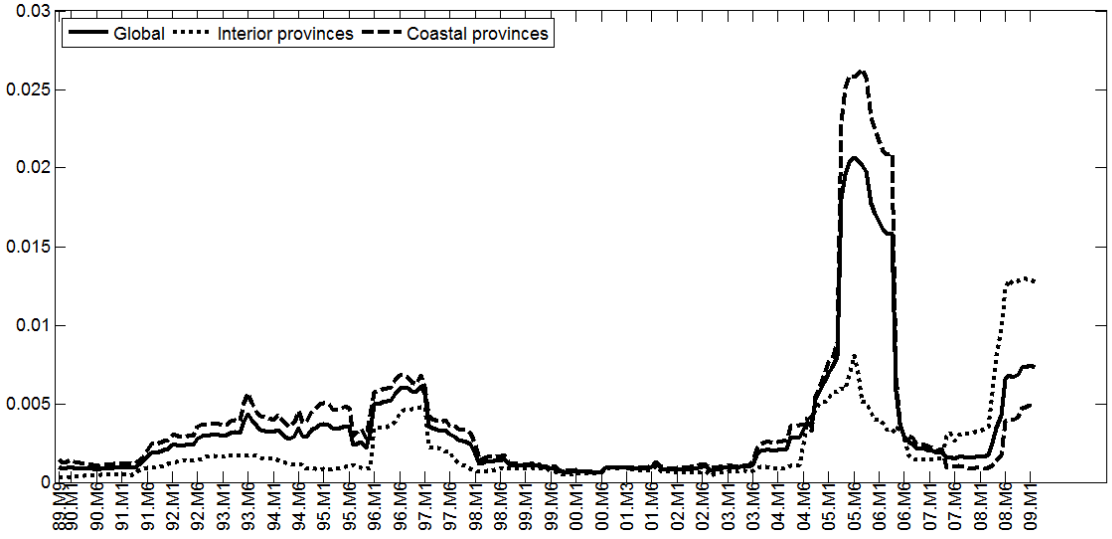

FIGURE1.1: Cross-sectional dispersion of provincial industrial output growth. We indicate by 'national' the dispersion between all the Chinese provinces.

1.4 Provincial growth-cycles analysis

This section presents the results of the estimation of our encompassing model described in section 1.2. In total, 9 versions of the model are estimated. We examine the synchronization model selection and show some special cases of our model. A key result found is that Chinese provinces are characterized by common transitions probabilities but with different dating. Then in the next subsections, we present another two relatively unknown characteristics of the Chinese economy revealed by our model. Firstly, the Chinese provincial growth-cycles phases exhibits 'strong' and 'weak' features. Consequently, the normal growth rate of the coastal provinces equal the rapid growth rate of the inland provinces. Secondly, there is evidence of two types of recessions in the Chinese economy: the classical recession and the growth-recession.

1.4.1 Model selection and growth-cycles synchronization

We describe the model selection procedure in Appendix A.3. In Table 1.3, we present the value of the log marginal likelihood and the Bayesian information criterion (BIC) for different number of regimes of the model corresponding to equation (1.1). This is done by taking into account the synchronization assumptions on the provincial hidden states and transition matrices represented in equations (1.3), (1.4) and (1.5). However, the selection of the best model is based on the BIC. Although from a theoretical viewpoint, the use of the BIC is not as justified for Markov-switching models as the log marginal likelihood, we realised that they often select the same models.

As described, in Table 1.3, if the number of regime K is equal to 2, depending on the assumption on the cycles-synchronization, our general model encompasses a special cases some models already presented in the literature.

On the whole, for all the proposed models (see Table 1.3), the log marginal likelihood

	Model 1. Strong non-synchronization: special case of Owyang et al. (2005) and Harding and Pagan (2006), if K=2	Model 2. Imperfect cycle synchronisation: special case of Candelon et al. (2009), if K=2	Model 3. Perfect synchronisation: special case of Harding and Pagan (2006), if K=2
		Log of marginal likelihood	
K=2	-5.4069e+03	-5.3810e+03	-2.5973e+04
K=3	-4.8188e+03	**-4.8093e+03**	-2.5577e+04
K=4	-5.2670e+03	-5.1116e+03	-2.1054e+04
		BIC	
K=2	1.1770e+04	1.1411e+04	5.2595e+04
K=3	1.1551e+04	**1.0608e+04**	5.2144e+04
K=4	1.3722e+04	1.1565e+04	4.3449e+04

Table 1.3: China's provinces industrial output growth rate, modelled by different Bayesian panel Markov-switching models with different number of state K; log of marginal likelihoods and BIC

and the BIC show the relevance of a third regime in growth-cycle dynamics for the provinces of China. This stylized fact has been found at the national level for many east Asian countries like China, Japan, South Korea, Taiwan, etc., (see Wang and Theobald (2008); Girardin (2005)).

Since synchronization is directly taken into account by the models, the estimation presented in Table 1.3 reveals an important fact: the cycles in the Chinese provinces' are not perfectly synchronized, irrespective of the number of states K. The log of the marginal likelihood and the BIC favour the imperfect-cycles synchronization with three states model to the strong non-synchronization and the perfect synchronization models. Consequently, the provincial dimension is crucial to understand a subcontinent economy like China.

Therefore, in the remaining sections, we examine only the three-regime Bayesian panel Markov-switching model with imperfect synchronization for Chinese provincial industrial output growth rates. We refer to the first regime as growth-recession or recession, the second as normal-growth and the third as rapid-growth.

The estimated absolute value of the mean growth rates of the provinces (except Shaanxi)

during (growth)-recession is smaller than during normal-growth (see Table A.2, in Appendix A.4). This shows the asymmetric feature of slow declines and quick rises of growth in these provinces. The estimated growth rates is almost twice larger during rapid-growth than during normal-growth.

At the national level, the least volatile regime is normal-growth and the most volatile regime is (growth)-recession (see Appendix A.4, Table A.2, row 2 and column 6; row 2 and column 5).

1.4.2 Geographical cluster of provincial growth rates

Our findings suggest that the mean growth rates in the normal-growth and rapid-growth regimes imply a clear geographical cluster between coastal and interior provinces. Figure 1.2 shows that during normal-growth the monthly growth rate is larger than 1% in the coastal provinces (except Zhejiang) and lower than 1% in the interior provinces (except Hunan). In addition, on average monthly growth during the rapid-growth regime is larger than 2% in the coastal provinces except Guangxi, Hebei, Shandong and Shangai, and lower than 1.7% in the interior provinces.

Figure 1.2 also displays a difference in terms of growth rate between the coast and the interior. The magnitude of the growth rate is higher in the coastal than in the interior provinces in both normal and rapid-growth regimes. We identify the area denoted by the rectangle in the Figure 1.2 as the 'growth-miracle' area[5]. Only coastal provinces are found in this area. Although growth rates during rapid-growth differ across China, the regime features accelerated and volatile growth in the coastal provinces found in the 'growth-

[5] The 'growth-miracle' is the term used in the literature to refer to episodes of growth where a backward and poor country experiences a remarkably high growth sustained for decades of real GDP per capita(Hsiao and Mei-Chu (2003). For instance, Yao (2014) mentions the 'growth-miracle' of South Korea Rep. (between 1963 and 1993 with 8.7% growth rate per annum), of China (between 1978 and 2008 with 7.8% per annum), of Japan (between 1950 and 1980 with 7.8% per annum) and of Brazil (between 1950 and 1980 with 7.7% per annum).

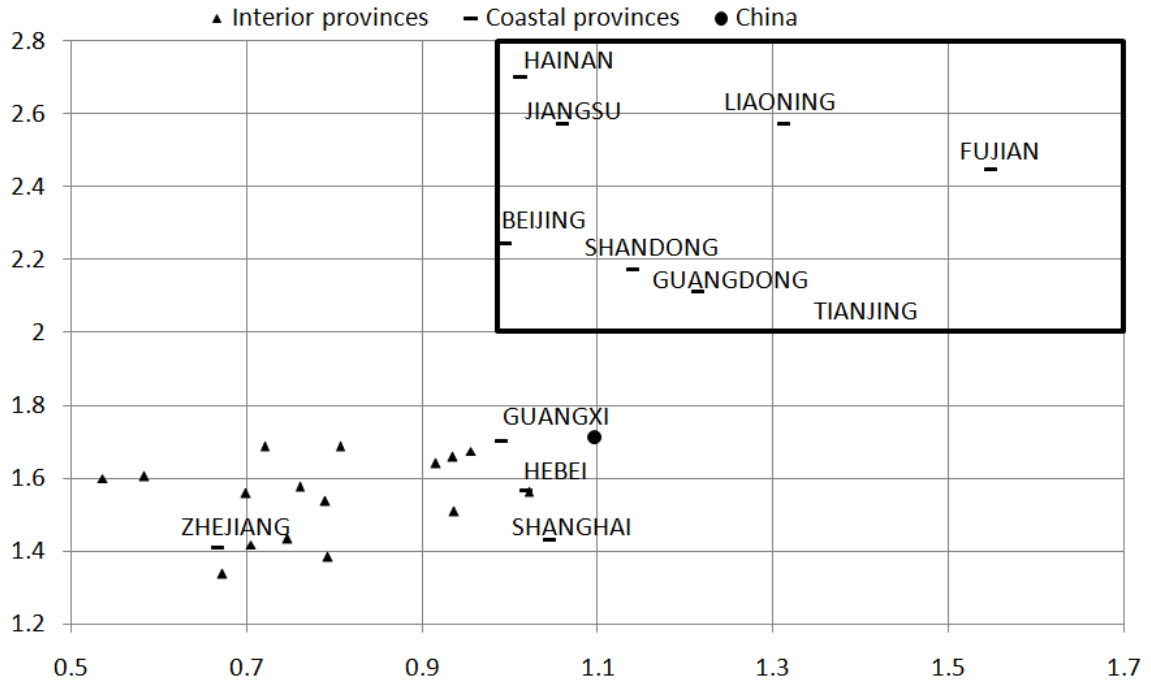

FIGURE1.2: Estimations of monthly provincial mean growth rates with the Bayesian panel Markov-switching model. The vertical axis represents the growth rate in rapid growth and the horizontal axis the growth rate in normal growth. The rectangle delimits the 'growth-miracle' area.

miracle' area of Figure 1.2. In fact, the most volatile regime between the normal and the rapid-growth regimes for the provinces located in the growth miracle area is the rapid-growth regime (Excepted Hainan).

In section 1.5, based on the dating of provincial cycles, we will see if for provinces like at the national level the third regime of rapid-growth is of two types: catching-up and bounce back.

1.4.3 Provincial recession and growth-recession

We find evidence that one fourth of Chinese provinces are characterized by recessions and three fourth by growth-recessions regime. Out of 28 provinces, 7 experienced classical

recessions. These provinces include: Guizhou, Shaanxi, Shanxi, Sichuan and Yunnan, all in the interior and Beijing and Jiangsu on the coast. The average negative growth rate in recession substantially varies among these seven provinces.

The provinces of Guizhou, Jiangsu, Shaanxi, Sichuan and Yunnan experience a fall in output of almost -0.5%. Beijing experiences the lowest fall of -0.1% while Shanxi experiences the largest with -1%. Apparently, these provinces experienced with different intensity of the Tienanmen political crisis of 1988-1989, the East Asian crisis of 1997, the post WTO blues and the global financial crisis of 2008.

1.4.4 From three optimal regimes to six qualitative regimes

Even though the econometric approach selects the three-regime classification as optimal (that best describes the whole economy), a deeper analysis of provincial growth rates suggests the existence of six qualitative regimes.

	'Strong' growth-recession	'Strong' normal growth	'Strong' rapid-growth
Average in the coastal provinces	4.32%	13.59%	24.15%
	'Weak' growth-Recession	'Weak' normal-Growth	'Weak' rapid-Growth
Average in the interior provinces	2.77%	9.90%	18.56%

Table 1.4: Qualitative difference between annualized growth rates in the optimal regimes.

The three regimes, (growth)-recession, normal and rapid-growth feature very different growth rates between coastal and interior provinces (Table 1.4). The provinces on the coast seem to drive China's economy by exhibiting what we will call 'Strong' features while that of the interior present 'Weak' features. The 'Strong rapid-growth' regime can be seen as the 'growth miracle' regime. Overall, we observe high dynamic behaviour among the coastal provinces and a low one among the interior ones.

1.5 Chronology of China's provincial growth-cycles

The objective of this section is to assess the dating of provincial growth-cycles obtained from the imperfect synchronization model. In fact, the notion of imperfect cycles synchronization implies at the same time a bit of heterogeneity as well as a bit of stabilization. Due to heterogeneity, the proportion of provinces experiencing a given regime does not always reflect the proportion of national output in that regime. The analysis of the expected mean growth rate shows the convergence in growth rate induced by domestic catching-up. Finally, we show that one of the root of China's 'new normal' of slower growth is the decline in of the coastal provinces' contribution to the proportion of national output in rapid-growth.

1.5.1 Timing and occurrence of China's provinces growth-cycles

We provide a dating of provincial turning points based on the best model[6] of imperfect cycles synchronization with three regimes in Table 1.6.

The first evidence is the province-specific variation in the timing and length of the occurrence of the regimes. The second evidence is the move of the growth center from the coastal to the interior provinces from the 1990s to the 2000s. The number of coastal provinces experiencing rapid-growth is decreasing over time while it is increasing for the interior provinces suggesting an evidence of a domestic catching-up (see Figure 1.3). Thirdly, the dating of the provincial cycles reveals that the first two national growth-recessions are driven by internal economic factors while the third one is led by external factors. Finally, although the dating of the cycles is based on the three-regime classification, we notice the

[6] As a generalization of the Bayesian univariate Markov switching model in Owyang et al. (2005), our Bayesian panel Markov switching approach delivers also for each province the estimated monthly smoothed probabilities which indicate that the provinces are either in a recession (classical recessions or growth-recessions), normal-growth or rapid-growth (catching-up or bounce back). The dating of the national and province-level regimes is based on such monthly smoothed probabilities (see Krolzig and Toro (2005)).

coexistence of only two regimes where the alternative to normal-growth represents either (growth)-recession or rapid-growth. Between the second quarter of 1991 and the third quarter of 1993 as well as after the entry of China into the WTO, the two coexistent regimes are normal-growth and rapid-growth. By contrast, the period from 1989Q1 to 1990Q1 and that from 1994Q1 to 2001Q4 are characterised by the coexistence of growth-recession and normal-growth regimes.

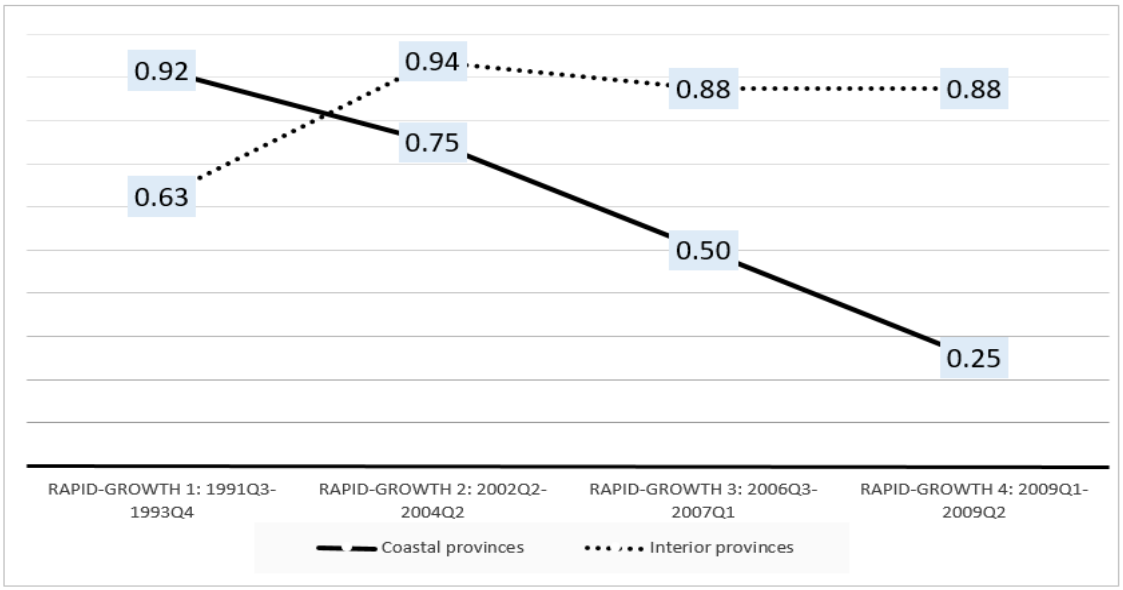

FIGURE1.3: Fraction of provinces in rapid-growth regime.

The 1989Q1-1990Q1 national growth-recession. A total of 19 provinces spread in both coastal and interior regions experienced the growth-recession that started at the beginning of 1989. The rest of the provinces were in normal-growth. Two quarters after the 1989Q1-1990Q1 national growth-recession, 6 provinces -including 4 in the interior- were still in (growth)-recession and one province in the coastal region (Guangdong) entered in rapid-growth.

Catching-up 1: early before the 'Southern Tour'. At the time of the stimulation policy of President Deng (1992), some provinces began showing signs of dynamism by switching from normal growth to rapid-growth. For instance, Guangdong, Jiangsu and Shangai, in coastal provinces, experienced rapid-growth in 1991Q2. At the end of 1992, the southern provinces experienced a massive acceleration in growth after the 'Southern Tour'. Rapid-growth reached almost all the coastal provinces except Tianjin. Only half of the interior provinces experienced rapid-growth, as depicted in Table 1.6 and within this it is persistent only for half of them (Anhui, Henan, Jiangxi, and Yunnan). Once rapid-growth ended at the national level, it ended fairly quickly across all the provinces. Although there were 12 provinces still in rapid-growth at the end 1994Q1, located in the coastal and the interior, this was reduced to only three by the next two quarters (1994Q3).

The 1994Q3-1997Q2 national growth-recession. The geographic pattern of the 1994Q4-1995Q2 national growth-recession is particularly distinct from the one of 1989Q1-1990Q1. As represented in Table 1.6, the 1994Q4-1997Q2 national growth-recession is experienced by few provinces including 7 coastal ones: Beijing, Fujian, Guangxi, Hainan, Jiangsu, Shandong, Tianjing and only 3 of the interior ones: Gansu, Hunan, and Yunnan. Moreover, two quarters after the end of this national growth-recession, 5 interior provinces switched into rapid-growth: Anhui, Guizhou, Henan, Hubei, and Yunan.

The missing East-Asian crisis at the national level. Although the dating based on the three-regime model does not show any recession in China at the national level during the East-Asian crisis, we notice that only few provinces experienced that recession.

Indeed, the results presented in Table 1.6 show that the East Asian crisis of 1997-1998 affected four provinces (Fujian, Guangxi, Liaoning and Tianjing), all located on the coast. In the last quarter of 1997, all the other provinces were in normal-growth except Zheijiang

Weight of Provinces affected by the East Asian crisis	
FUJIAN	0.0282
GUANGXI	0.0170
LIAONING	0.0520
TIANJING	0.0273
Weight of provinces not affected by the East Asian crisis	
OTHERS	0.875

Table 1.5: Share in output of China's provinces in December 1997.

which recorded rapid-growth. Based on our weighting of the provinces, the result shows that although four coastal Chinese provinces were strongly affected by the East Asian Crisis (1997Q4), their total output only accounted for 12.5% of national aggregate output. However, the majority of the provinces denoted as OTHERS in Table 1.5 were identified by normal-growth at the time of the East Asian crisis. This confirms the claim by Chinese officials based on official data that the Chinese national economy globally was in a normal growth regime during the East Asian crisis.

Catching-up 2: after the integration of China into the WTO. As shown in Table 1.6, by the end of 2001, the majority of the interior provinces were experiencing persistent rapid-growth while the coastal provinces were switching between normal-growth, rapid-growth and (growth)-recession. For instance, in the third quarter of 2003, 23 out of 28 provinces recorded rapid-growth. Out of the 5 remaining provinces which were in normal growth, only one is located in the interior.

The post-WTO blues. At the national level, the second and third episodes of catching-up are separated by a period of normal-growth that can be assimilated to the post WTO blues. During this period we record five provincial (growth)-recessions. Three of these provinces are located on the coast (Jiangsu, Liaoning and Zhejiang) and two in the inland (Neimonggu and Shaanxi)

Catching-up 3: after the post-WTO blues. This third episode of catching-up from 2006Q3 to 2007Q1 was supported in majority by the inland provinces. 14 out of 16 of these provinces are in the inland while only half are located on the coast.

The 2008Q2-2008Q4 national growth-recession At the beginning of the national growth-recession of 2008Q2-2008Q4 a total of 8 provinces were in (growth)-recession. This included 4 provinces in the coastal regions: Beijing, Fujian, Guangdong, and Shangai and 4 in the interior: Guizhou, Henan and Shanxi. Due to its openness, Chinese economy was exposed to the sudden collapse of global trade. In 2008, interest rates and reserve requirement rate were reduced and limits on credit growth removed. The government, also, stopped the policy of letting the Yuan appreciate against the US dollar and took the decision to spend 16% GDP in investment. As result, bank lending experienced an extraordinary expansion and early 2009 economic recovery started at the national as well as provincial levels.

National and province-specific bounce back effects a la Friedman. As shown in the preliminary analysis in the section 1.3 industrial output bounce back after the global financial crisis in 2009 at the national level. Typically, in our three regime Markov-switching framework, a bounce back period is a period where the first regime of growth-recession or classical recession is followed by the third regime. Beijing, Hainan and Guizhou experienced a bounce back during the 1994Q3-1997Q2 national growth-recession. During the 2008Q2-2008Q4 national, we also find evidence of provinces (Gansu, Guizhou, Henan and Jiangxi) experiencing a bounce back.

1.5.2 Heterogeneity due to provinces' economic importance

From our best model perspective, Chinese provincial growth-cycles are imperfectly synchronised meaning that the cycles share the same transition probabilities but have differ-

ent dating. Moreover, the provincial cycle's phases are not consistent with the national aggregate dating. Thus, one is left with the issue of building an alternative dating for the national cycle.

We construct the proportion of output (second row of Figure 1.4) by summing up the output share [7] of the provinces in each regime and compare it with the proportion of provinces in each regime (first row of Figure 1.4). The comparison reveals a period where the proportion of provinces in normal-growth (respectively rapid-growth) is higher while the dominant regime of the proportion of national output is rapid-growth (respectively normal-growth). This period covers 1993M08 to 1994M08 (respectively 2006M11 to 2007M12). It follows that the difference between this two proportions is due to the economic importance of the provinces.

The second row of Figure 1.4 shows that the dating of the national aggregate cycle with the three-regime classification (see Table 1.2) is representative of the dominant regime in terms of output. Because the provincial cycles are imperfectly synchronized, the dominant proportion of output in each regime can be seen as an efficient alternative to the dating of the national aggregate cycle. Although the time of occurrence of the provincial regimes differs from the national one, the proportion of provinces experiencing a given regime and the proportion of output in each regime often reflects the regime at work in the national economy.

1.5.3 Stabilisation of provincial output fluctuations

The use of imperfect synchronization instead of the perfect one, allows us to study the convergence of the provincial cycles'. We use the expected mean growth rates to explore

[7] We follow Gatfaoui and Girardin (2015), in using as weights a time varying share of the provinces in the national aggregate industrial output. In this case, each province reflects its economic importance in the country. Byström et al. (2005) use the regional GDP in 2001 to measure the economic importance of the provinces over the time period 1991-2001.

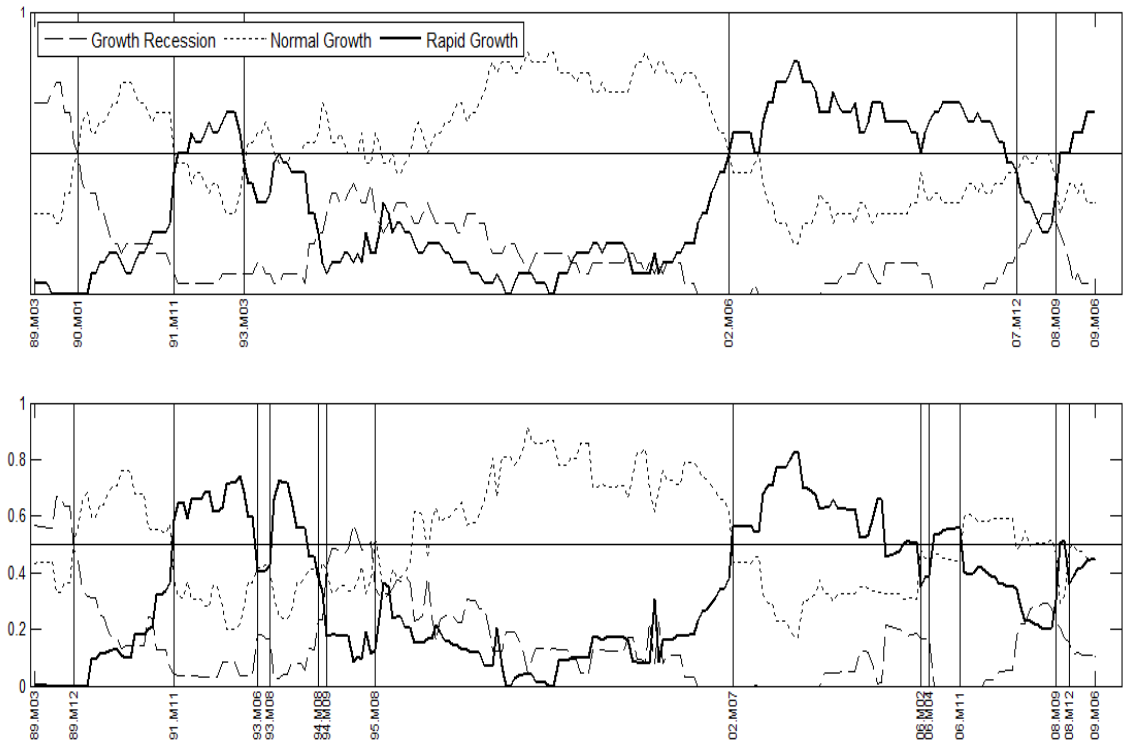

FIGURE1.4: First panel: Fraction of provinces in each regime; Second panel: Proportion of national output in each regime (monthly information). The estimations are based on the Bayesian panel Markov-switching model with imperfect cycle synchronization

that suggestion.

As shown in Figure 1.5, the expected mean growth rate captures in part the convergence in growth rate between coastal and inland provinces. In the early 1990s, expected growth in China's provinces was negative and the proportion of provinces (see Figure 1.4: First panel) in (growth)-recession reached a maximum as a result of inflation. We find evidence that the 1993M03-2002M06 period, between the two first catching up episodes, is characterized by expected growth rates within the range of 0.0% to 1.5%. Indeed, there is a long 'soft landing' period from early 1993 to early 2002 characterized in many provinces by normal-growth. In the period from June 2002 to December 2007, the provinces display higher

expected growth rates above 1.5% which can be attributed to the catching-up effect.

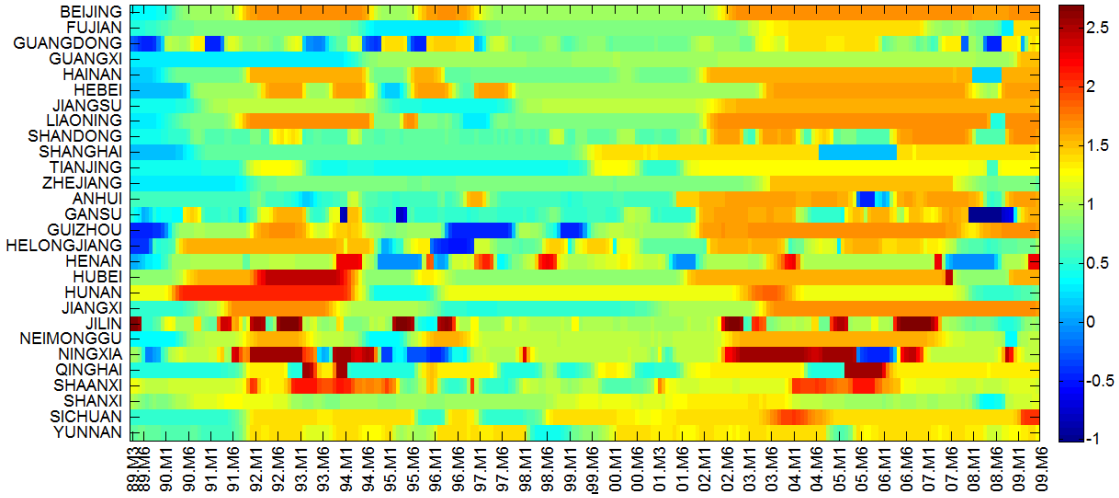

FIGURE1.5: Heat map of expected mean growth over the sample period 1989M3-2009M6. Provinces on the Y-axis are ordered in two groups: coastal provinces from Beijing to Zhejiang and interior provinces from Anhui to Yunnan.

Our time series analysis extends Girardin and Kholodilin (2011) by identifying the convergence patterns between the coastal and the interior provinces.

The survey of literature on the question of convergence in industrial production levels among Chinese provinces in Lemoine et al. (2014) agrees on the rapid convergence, since the end of the 1990s.

1.5.4 One of the roots of China's 'new normal' of slower growth

We weigh the estimated growth rate by the economic importance of the provinces and the operative regime (normal or rapid-growth) in order to isolate the contribution to the proportion of national output in normal and rapid-growth. Overall, we consider four reference periods that belong to the national aggregate rapid-growth episodes: the post 'Southern Tour' (January 1993), the post WTO (September 2003), the post WTO blues

(March 2007) and the post global financial crisis (February 2009). We present the results in Table 1.7.

Table 1.7 shows an evidence of an inversion of the pattern of the contribution to the proportion of output in rapid and normal-growth between coastal and interior provinces. The contribution to the proportion of national output in rapid-growth of the inland provinces increased over time and in February 2009 stabilized at 65%; and this value almost coincides with the one of the coastal provinces in January 1993 (67 %). However, as seen in section 1.4.4, the rapid-growth of inland provinces exhibits 'weak features'. In addition, we saw from Figure 1.2 that only coastal provinces are characterized by 'growth-miracle'; from Figure 1.3 that their fraction in rapid-growth regime is falling over time and from Table 1.7 that their contribution to the proportion of national output in rapid-growth is also declining. Hence, by looking at the Chinese provinces past experience we are able to uncover prior roots to the recent slowdown (since 2011) in China's growth.

1.6 Conclusion

This paper proposes a Bayesian panel Markov-switching framework to study the growth-cycles phases of the unit of the panel. The modelling approach used allows us to propose different multivariate synchronization effect for the unit-specific cycles.

We apply the model to the monthly industrial production of the Chinese provinces over two decades. Our findings suggest that the provincial and national cycles are imperfectly synchronized. The results provide evidence supporting a three-regime classification in the Chinese economy both at national and provincial levels. At the national level there was no classical recession, but only growth-recession episodes, even though seven provinces out of 28 present negatives growth rate.

This paper shows that although from the 1990s to the 2000s the growth center moves

from the coast to the interior, only coastal provinces are characterised by 'growth-miracle'. The coastal provinces display a higher growth rate than that of the interior provinces in both normal-growth and rapid-growth regimes.

The results further indicate that the contribution to the proportion of national output in rapid-growth of the coastal provinces has declined over time while the share of interior provinces has increased. This retrospective insight of Chinese provinces past experience helped us to uncover prior roots to China's 'new normal' of slower growth.

The implications of our results for investors and policy makers are relevant. For the investors, it is important to know provinces which are experiencing especially rapid-growth. For the Chinese fiscal-policy makers, it is important to know which provinces are in recession, normal growth or rapid growth in order to design more uniform counter cyclical policies or to provide stimulus packages across the provinces. Indeed, Barthélemy and Poncet (2008) indicate that stabilization of output fluctuations can be achieved in China by promoting uniform economic policies across the provinces.

A limit of our approach is a possible miss-measurement of the observed provincial industrial output. This miss-measurement can reflect miss-measurement in the actual or in the reported data. Thus, the evidence of convergence in observed provincial growth rates may be attributed to convergence in reported data or actual data.

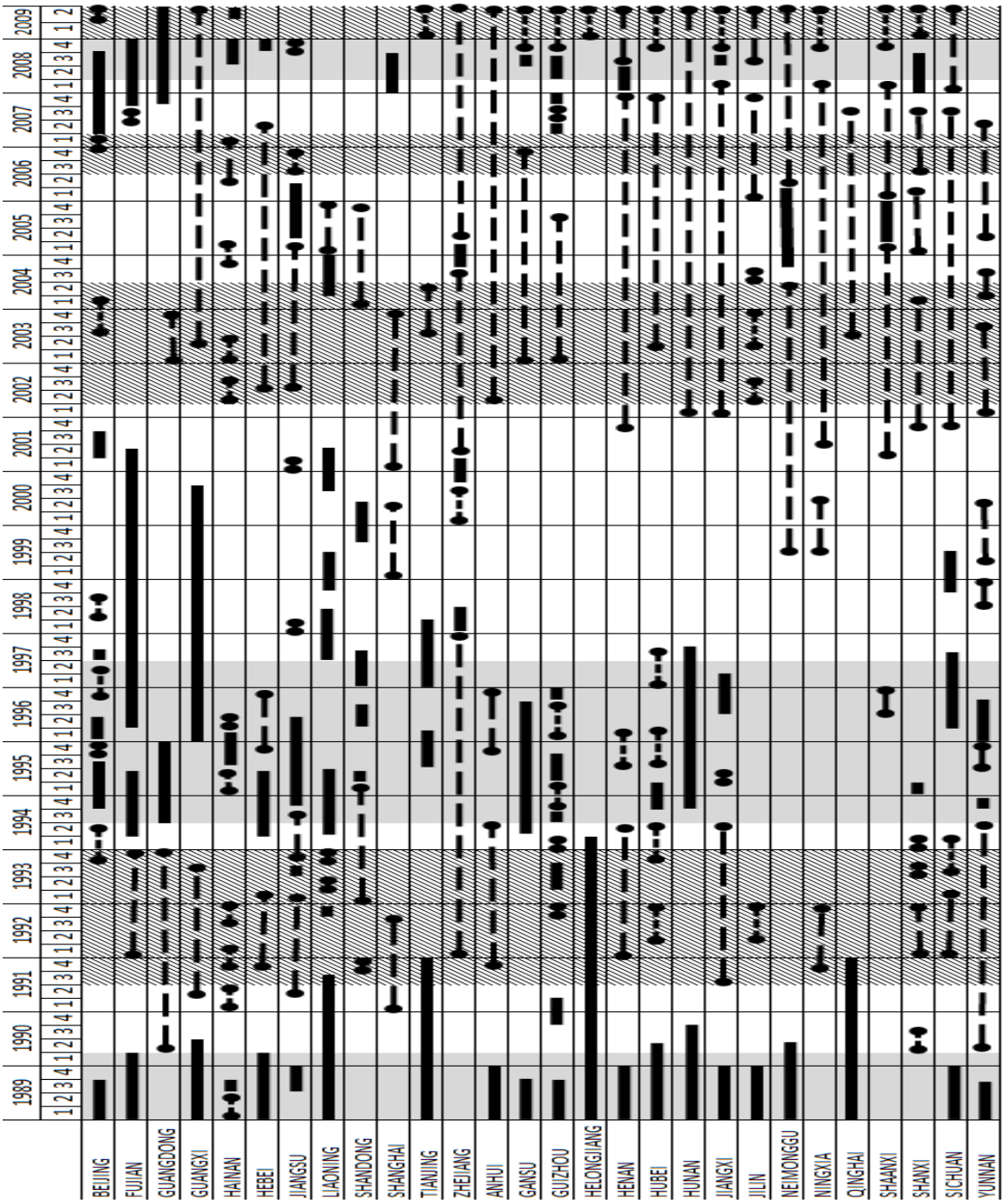

Table 1.6: Chinese provinces (growth)-recession(black bar) and rapid-growth (dotted line) by quarter: 1989Q1-1999Q4 estimated with the Bayesian panel Markov-switching model with imperfect cycle synchronization. Chinese national growth-recession indicated by gray background, normal-growth by white background and rapid-growth simple hatch.

	Post Southern Tour: Jan 1993		Post WTO: Sept 2003		Post WTO Blues: Mar 2007		Post GFC: Feb 2009	
Provinces	Normal-growth	Rapid-growth	Normal-growth	Rapid-growth	Normal-growth	Rapid-growth	Normal-growth	Rapid-growth
BEIJING	10	*0*	0	*6*	0	*24*	0	*16*
FUJIAN	0	*8*	33	*0*	10	*0*	23	*0*
GUANGDONG	0	*6*	0	*6*	7	*0*	0	*0*
GUANGXI	0	*4*	0	*5*	0	*7*	0	*4*
HAINAN	0	*10*	10	*0*	12	*0*	14	*0*
HEBEI	0	*3*	0	*4*	0	*4*	9	*0*
JIANGSU	0	*12*	0	*8*	5	*0*	9	*0*
LIAONING	0	*0*	22	*0*	13	*0*	16	*0*
SHANDONG	0	*18*	19	*0*	23	*0*	2	*0*
SHANGHAI	38	*0*	0	*5*	7	*0*	19	*0*
TIANJING	22	*0*	0	*6*	12	*0*	0	*8*
ZHEJIANG	0	*7*	0	*0*	0	*0*	0	*8*
Total of coastal provinces	(71)	[67]	(84)	[39]	(90)	[35]	(93)	[35]
ANHUI	0	*4*	0	*5*	0	*8*	0	*5*
GANSU	7	*0*	0	*3*	3	*0*	0	*5*
GUIZHOU	0	*3*	0	*2*	2	*0*	0	*4*
HELONGJIANG	0	*0*	16	*0*	5	*0*	0	*4*
HENAN	0	*3*	0	*4*	0	*6*	0	*4*
HUBEI	0	*3*	0	*4*	0	*8*	0	*5*
HUNAN	11	*0*	0	*4*	0	*5*	0	*3*
JIANGXI	0	*3*	0	*5*	0	*6*	0	*6*
JILIN	0	*4*	0	*2*	0	*8*	0	*6*
NEIMONGGU	5	*0*	0	*3*	0	*6*	0	*2*
NINGXIA	0	*2*	0	*4*	0	*3*	0	*4*
QINGHAI	7	*0*	0	*4*	0	*2*	0	*0*
SHAANXI	0	*0*	0	*5*	0	*5*	0	*6*
SHANXI	0	*4*	0	*5*	0	*1*	0	*6*
SICHUAN	0	*4*	0	*5*	0	*6*	0	*4*
YUNNAN	0	*4*	0	*5*	0	*3*	7	*0*
Total of inland provinces	(29)	[33]	(16)	[61]	(10)	[65]	(7)	[65]

Table 1.7: Evolution of the contribution to the proportion of national output in normal-growth and rapid-growth. In the circles, we indicate the total contribution in normal-growth while in the rectangle, we indicate the total contribution in rapid-growth. The estimations are based on the Bayesian panel Markov-switching model with imperfect cycle synchronization

Appendix A

Technical Details of Chapter 1

A.1 Models elicitation

The general panel Markov switching model presented in this paper allows switching in both means and volatilities. It can be written as:

$$X_{it} = \sum_{k=1}^{K} \mathbb{1}_{\{k\}}(S_{it})(\mu_{ik} + \sigma_{ik}\varepsilon_{it}), \quad \varepsilon_{it} \sim \mathcal{N}(0,1)$$

with $i = 1, \ldots, N$ where N is the number of series in the panel and $t = 1, \ldots, T$, T being the length of the series of the panel. The total number of regimes is assumed to be equal to K. The indicator function $\mathbb{1}_{\{E\}}(X)$ takes value 1 if $X \in E$ and 0 otherwise.

A.1.1 Model 1: heterogeneous states with heterogeneous transition mechanism

We assume S_{it} is a Markov chain with transition matrix:

$$\mathbb{P}(S_{it}|S_{i,t-1}) = P_i$$

with $i \in \{1, \ldots, N\}$. The transition matrices of the latent process for unit i can be written as:

$$P_i = \begin{pmatrix} p_{i,11} & \cdots & p_{i,1K} \\ \vdots & \ddots & \vdots \\ p_{i,K1} & \cdots & p_{i,KK} \end{pmatrix} \tag{A.1}$$

where $P_{i,kl}$ represents the conditional probability that unit i moves from the latent regime l at time $t-1$ to the latent regime k at time t. So then, $P_{i,kl} \geqslant 0$, $P_{i,kl} = \mathbb{P}(S_{it} = k | S_{i,t-1} = l)$ and

$$\sum_{l=1}^{K} P_{i,kl} = 1, \quad \forall i \in \{1, \ldots, N\}, \quad \forall k \in \{1, \ldots, K\} \tag{A.2}$$

A.1.2 Model 2: heterogeneous states with homogeneous transition mechanism

Model 2 is presented as follows:

$$X_{it} = \sum_{k=1}^{K} \mathbb{1}_{\{k\}}(S_{it})(\mu_{ik} + \sigma_{ik}\varepsilon_{it}), \quad \varepsilon_{it} \sim \mathcal{N}(0,1)$$

with transition matrix: $\mathbb{P}(S_{it}|S_{i,t-1}) = P, \forall i \in \{1, \ldots, N\}, \forall t \in \{1, \ldots, T\}$

$$\mathbb{P}(S_{it+1}|S_{it}) = P = \begin{pmatrix} p_{11} & \cdots & p_{1K} \\ \vdots & \ddots & \vdots \\ p_{K1} & \cdots & p_{KK} \end{pmatrix} \tag{A.3}$$

A.1.3 Model 3: homogeneous states with homogeneous transition mechanism

Model 3 is presented as follows:

$$X_{it} = \sum_{k=1}^{K} \mathbb{1}_{\{k\}}(S_t)(\mu_k + \sigma_k\varepsilon_{it}), \quad \varepsilon_{it} \sim \mathcal{N}(0,1)$$

with transition matrix: $\mathbb{P}(S_t|S_{t-1}) = P, \forall i \in \{1, \ldots, N\}, \forall t \in \{1, \ldots, T\}$

$$\mathbb{P}(S_{t+1}|S_t) = P = \begin{pmatrix} p_{11} & \cdots & p_{1K} \\ \vdots & \ddots & \vdots \\ p_{K1} & \cdots & p_{KK} \end{pmatrix} \tag{A.4}$$

A.2 Complete data Bayesian inference

A.2.1 Likelihood

The data-augmentation framework applied to the three panel Markov-switching models yields the following completed likelihood functions:

$$\mathcal{L}(X_{1:T}, S_{1:T} \mid \boldsymbol{\theta}_1, M_1) = \prod_{i=1}^{N}\prod_{t=1}^{T}\prod_{l=1}^{K}(2\pi\sigma_{il}^2)^{-\frac{\xi_{l,it}}{2}} \exp\{-\frac{\xi_{l,it}}{2\sigma_{il}^2}e_{itl}^2\} \prod_{k=1}^{K}(p_{i,lk})^{\xi_{l,it}\xi_{k,it-1}} \tag{A.5}$$

$$\mathcal{L}(X_{1:T}, S_{1:T} \mid \boldsymbol{\theta}_2, M_2) = \prod_{i=1}^{N}\prod_{t=1}^{T}\prod_{l=1}^{K}(2\pi\sigma_{il}^2)^{-\frac{\xi_{l,it}}{2}} \exp\{-\frac{\xi_{l,it}}{2\sigma_{il}^2}e_{itl}^2\} \prod_{k=1}^{K}(p_{lk})^{\xi_{l,it}\xi_{k,it-1}} \tag{A.6}$$

$$\mathcal{L}(X_{1:T}, S_{1:T} \mid \boldsymbol{\theta}_3, M_3) = \prod_{i=1}^{N}\prod_{t=1}^{T}\prod_{l=1}^{K}(2\pi\sigma_{il}^2)^{-\frac{\xi_{l,t}}{2}} \exp\{-\frac{\xi_{l,t}}{2\sigma_{il}^2}e_{itl}^2\} \prod_{k=1}^{K}(p_{lk})^{\xi_{l,t}\xi_{k,t-1}} \tag{A.7}$$

where $e_{itl} = X_{it} - \mu_{il}$, $X_t = (X_{1t}, \ldots, X_{Nt})$, $X_{1:t} = (X_1, \ldots, X_t)$, $S_t = (S_{1t}, \ldots, S_{Nt})$ and $S_{1:t} = (S_1, \ldots, S_t)$.

A.2.2 Prior elicitation

A variety of priors can be used to estimate the panel Markov-switching model. For the three models proposed, we assume conjugate independent priors for the parameters. Table A.1 summarizes the different priors.

Model 1: Strong multivariate non-synchronization	Model 2: Imperfect synchronization	Model 3 : Perfect synchronisation
$\mu_{ik} \sim \mathcal{N}(m_{ik}, \tau_{ik}^2)$	$\mu_{ik} \sim \mathcal{N}(m_{ik}, \tau_{ik}^2)$	$\mu_k \sim \mathcal{N}(m_k, \tau_k^2)$
$\sigma_{ik}^2 \sim \mathcal{IG}(\alpha_{ik}, \beta_{ik})$	$\sigma_{ik}^2 \sim \mathcal{IG}(\alpha_{ik}, \beta_{ik})$	$\sigma_k^2 \sim \mathcal{IG}(\alpha_k, \beta_k)$
$(p_{i,k1}, \ldots, p_{i,kK}) \sim \mathcal{D}ir(\delta_{i1}, \ldots, \delta_{iK})$	$(p_{k1}, \ldots, p_{kK}) \sim \mathcal{D}ir(\delta_1, \ldots, \delta_K)$	$(p_{k1}, \ldots, p_{kK}) \sim \mathcal{D}ir(\delta_1, \ldots, \delta_K)$

Note: $i \in \{1, \ldots, N\}$ and $k \in \{1, \ldots, K\}$.

Table A.1: Conjugate priors: normal distribution for the means growth rate; Inverse Gamma distribution for the volatilities of the growth rate; Dirichlet distribution for the transitions probabilities of the regimes.

A.2.3 Posterior simulation

Model 1 (independence cycles synchronization with space-heterogeneous transition)

The posterior distribution of the unit specific mean growth rate of model 1 is proportional to the product of likelihood in (A.5) and the prior in table A.1 (see column 1 and row 2).

$$f(\mu_{il}|X_{1:T}, S_{1:T}, \boldsymbol{\theta}_{1_{-\mu_{il}}}) \propto \mathcal{N}(\overline{m}_{il}, \overline{\tau}^2_{il})$$

with $\overline{m}_{il} = \overline{\tau}^2_{il}(\frac{m_{il}}{\tau^2_{il}} + \frac{1}{\sigma^2_{il}} \sum_{t \in \mathcal{T}_{il}} X_{it})$ and $\overline{\tau}^2_{il} = (\frac{1}{\tau^2_{il}} + \frac{T_{il}}{\sigma^2_{il}})^{-1}$.

We defined $\mathcal{T}_{il} = \{t = 1, \ldots, T | S_{it} = l\}$, $T_{il} = card(\mathcal{T}_{il})$, $X_{1:t} = (X_1, \ldots, X_t)$, $S_t = (S_{1t}, \ldots, S_{Nt})$ and $S_{1:t} = (S_1, \ldots, S_t)$. The notation $\boldsymbol{\theta}_{1_{-\mu_{il}}}$ refer to the parameter in $\boldsymbol{\theta}_1$ without μ_{il}.

The posterior distribution of the unit specific volatilities of model 1 is proportional to the product of likelihood in (A.5) and the prior in table A.1 (see column 1 and row 3).

$$f(\sigma_{il}|X_{1:T}, S_{1:T}, \boldsymbol{\theta}_{1_{-\sigma_{il}}}) \propto \mathcal{IG}(\alpha_{il} + T_{il}, \beta_{il} + \frac{1}{2} \sum_{t \in \mathcal{T}_{il}} (X_{it} - \mu_{il})^2)$$

The posterior distribution of each l-th row of the transition matrix $(p_{i,l1}, \ldots, p_{i,lK})$ of model 1 is proportional to the product of likelihood in (A.5) and the prior in table A.1 (see column 1 and last row).

$$f((p_{i,l1}, \ldots, p_{i,lK})|X_{1:T}, S_{1:T}, \boldsymbol{\theta}_{1_{-(p_{i,l1}, \ldots, p_{i,lK})}}) \propto \mathcal{D}ir(\delta_{i1} + T_{i,l1}, \ldots, \delta_{iK} + T_{i,lK})$$

where $T_{i,lk} = card\{t \in \{1, \ldots, T\} | S_{it} = l \text{ and } S_{it-1} = k\}$.

Model 2 (imperfect cycles synchronization with space-homogeneous transition)

The posterior distribution of the unit specific mean growth rate of model 2 is proportional to the product of likelihood in (A.6) and the prior in table A.1 (see column 2 and row 2). It

can be derived directly from the one of model 1 since the are almost of the same structure:

$$f(\mu_{il}|X_{1:T}, S_{1:T}, \boldsymbol{\theta}_{2_{-\mu_{il}}}) \propto \mathcal{N}(\overline{m}_{il}, \overline{\tau}^2_{il})$$

with $\overline{m}_{il} = \overline{\tau}^2_{il}(\frac{m_{il}}{\tau^2_{il}} + \frac{1}{\sigma^2_{il}} \sum_{t \in \mathcal{T}_{il}} X_{it})$ and $\overline{\tau}^2_{il} = (\frac{1}{\tau^2_{il}} + \frac{T_{il}}{\sigma^2_{il}})^{-1}$.

The posterior distribution of the unit specific volatilities of model 2 is proportional to the product of likelihood in (A.6) and the prior in table A.1 (see column 2 and row 3). Similarly, it can be derived directly from the one of model 1 because the are almost of the same structure:

$$f(\sigma_{il}|X_{1:T}, S_{1:T}, \boldsymbol{\theta}_{2_{-\sigma_{il}}}) \propto \mathcal{IG}(\alpha_{il} + T_{il}, \beta_{il} + \frac{1}{2} \sum_{t \in \mathcal{T}_{il}} (X_{it} - \mu_{il})^2)$$

The posterior distribution of each l-th row of the transition matrix $(p_{l1}, \ldots, p_{lK})$ of model 1 is proportional to the product of likelihood in (A.6) and the prior in table A.1 (see column 2 and last row).

$$f(p_{l1}, \ldots, p_{lK}|X_{1:T}, S_{1:T}, \boldsymbol{\theta}_{2_{-(p_{l1}, \ldots, p_{lK})}}) \propto \mathcal{D}ir(\delta_1 + \sum_{i=1}^{N} T_{i,l1}, \ldots, \delta_K + \sum_{i=1}^{N} T_{i,lK})$$

Model 3 (perfect cycles synchronization)

The posterior distribution of the mean growth rate of model 3 is proportional to the product of likelihood in (A.7) and the prior in table A.1 (see column 3 and row 2).

$$f(\mu_l|X_{1:T}, S_{1:T}, \boldsymbol{\theta}_{3_{-\mu_l}}) \propto \mathcal{N}(\overline{m}_l, \overline{\tau}^2_l)$$

with $\overline{m}_l = \overline{\tau}^2_l(\frac{m_l}{\tau^2_l} + \frac{1}{\sigma^2_l} \sum_{i=1}^{N} \sum_{t \in \mathcal{T}_l} X_{it})$ and $\overline{\tau}^2_l = (\frac{1}{\tau^2_l} + \frac{1}{\sigma^2_l} N T_l)^{-1}$.

The posterior distribution of the volatilities of model 3 is proportional to the product of likelihood in (A.7) and the prior in table A.1 (see column 3 and row 3).

$$f(\sigma_l|X_{1:T}, S_{1:T}, \boldsymbol{\theta}_{3_{-\sigma_l}}) \propto \mathcal{IG}(\alpha_l + NT_l, \beta_l + \frac{1}{2}\sum_{i=1}^{N}\sum_{t\in\mathcal{T}_l}(X_{it} - \mu_l)^2)$$

The posterior distribution of each l-th row of the transition matrix $(p_{l1}, \ldots, p_{lK})$ of model 3 is proportional to the product of likelihood in (A.7) and the prior in table A.1 (see column 3 and last row). It can be derived directly from the one of model 2 because the are almost of the same structure:

$$f((p_{l1}, \ldots, p_{lK})|X_{1:T}, S_{1:T}, \boldsymbol{\theta}_{3_{-(p_{l1},\ldots,p_{lK})}}) \propto \mathcal{D}ir(\delta_1 + NT_{l1}, \ldots, \delta_K + NT_{lK})$$

A.2.4 Forward-filtering and backward-sampling algorithm

The forward-filtering backward-sampling algorithm also known as multi-move Gibbs sampling for hidden Markov chain model has been proposed independently for Markov-switching autoregressive model (Chib (1996), Kim and Nelson (1998), Kim and Nelson (1999)).

Model 1

By means of dynamic factorization, the full conditional distribution of the whole path of the unit specific hidden state is:

$$\begin{aligned}\mathbb{P}(S_{i,1:T}|X_{1:T}, \boldsymbol{\theta}_1) &= \mathbb{P}(S_{iT}|X_{1:T}, \boldsymbol{\theta}_1)\mathbb{P}(S_{i,1:T-1}|S_{iT}, X_{1:T}, \boldsymbol{\theta}_1) \\ &= \mathbb{P}(S_{iT}|X_{1:T}, \boldsymbol{\theta}_1)\prod_{t=1}^{T-1}\mathbb{P}(S_{i,t}|S_{i,t+1:T}, X_{1:T}, \boldsymbol{\theta}_1)\end{aligned}$$

The second term of the RHS can be written as follows:

$$\mathbb{P}(S_{i,t}|S_{i,t+1:T}, X_{1:T}, \boldsymbol{\theta}_1) \propto \mathbb{P}(S_{i,t+1}|S_{i,t})\mathbb{P}(S_{i,t}|X_{1:t}, \boldsymbol{\theta}_1)$$

The second term of the RHS represents the transition probability. By dividing by the normalizing constant we have the following probability mass function:

$$\mathbb{P}(S_{i,t} = k|S_{i,t+1:T}, X_{1:T}, \boldsymbol{\theta}_1) = \frac{\mathbb{P}(S_{i,t+1}|S_{i,t} = k)\mathbb{P}(S_{i,t} = k|X_{1:t}, \boldsymbol{\theta}_1)}{\sum_{l=1}^{K} \mathbb{P}(S_{i,t+1}|S_{i,t} = l)\mathbb{P}(S_{i,t} = l|X_{1:t}, \boldsymbol{\theta}_1)} \tag{A.8}$$

where $\mathbb{P}(S_{i,t} = k|X_{1:t}, \boldsymbol{\theta}_1)$ is calculated by Hamilton filter algorithm.

Firstly, the multi-move algorithm assumes that, by forward recursion $t = 1, \ldots, T$ the unit specific filtered state probability distribution $\mathbb{P}(S_{i,t} = k|X_{1:t}, \boldsymbol{\theta}_1)$ are stored. Secondly, the filtered state $S_{i,T}$ is drawn conditional on $X_{1:T}$ and $\boldsymbol{\theta}_1$. At a third position, given $S_{i,T}$ and based on (A.8), the sampling of the unit specific smoothed state $S_{i,t}$ for $t = T-1, \ldots, 1$ is implemented by backward recursion. The algorithm of the filtering consists of two steps of forward recursion $t = 1, \ldots, T$:

Prediction step We calculate the probability for $i = 1, \ldots, N$ and $l = 1, \ldots, K$

$$\begin{aligned} \mathbb{P}(S_{it} = l|X_{1:t-1}, \boldsymbol{\theta}_1) &= \sum_{k=1}^{K} \mathbb{P}(S_{it} = l|S_{it-1} = k)\mathbb{P}(S_{i,t-1} = k|X_{1:t-1}, \boldsymbol{\theta}_1) \\ &= \sum_{k=1}^{K} p_{i,kl}\mathbb{P}(S_{i,t-1} = k|X_{1:t-1}, \boldsymbol{\theta}_1) \end{aligned} \tag{A.9}$$

where $p_{i,lk}$ is the transition probability of unit i. We initialize for $t = 1$, $\mathbb{P}(S_{i,0} = k|X_0, \boldsymbol{\theta}_1)$ to be equal to the ergodic probabilities.

Update step We calculate the probability for $i = 1, \ldots, N$ and $l = 1, \ldots, K$

$$\mathbb{P}(S_{it} = l|X_{1:t}, \boldsymbol{\theta}_1) = \frac{\mathbb{P}(S_{it} = l|X_{1:t-1}, \boldsymbol{\theta}_1)f(X_{it}|S_{it} = l, X_{1:t-1,-i}, \boldsymbol{\theta}_1)}{\sum_{k=1}^{K} \mathbb{P}(S_{it} = k|X_{1:t-1}, \boldsymbol{\theta}_1)f(X_{it}|S_{it} = k, X_{1:t-1,-i}, \boldsymbol{\theta}_1)} \tag{A.10}$$

The algorithm of the smoothing consists of one step of backward recursion $t = T - 1, \ldots, 1$:

Smoothing step We store the filtered states. We calculate the probability for $i = 1, \ldots, N$ and $l = 1, \ldots, K$

$$\begin{aligned}
\mathbb{P}(S_{it} = l|X_{1:T}, \boldsymbol{\theta}_1) &= \sum_{k=1}^{K} \mathbb{P}(S_{it} = l, S_{it+1} = k|X_{1:T}, \boldsymbol{\theta}_1) \\
&= \sum_{k=1}^{K} \mathbb{P}(S_{it} = l|S_{it+1} = k, X_{1:T}, \boldsymbol{\theta}_1)\mathbb{P}(S_{it+1} = k|X_{1:T}, \boldsymbol{\theta}_1) \\
&= \sum_{k=1}^{K} \frac{p_{i,lk}\mathbb{P}(S_{it} = l|X_{1:t}, \boldsymbol{\theta}_1)\mathbb{P}(S_{it+1} = k|X_{1:T}, \boldsymbol{\theta}_1)}{\sum_{j=1}^{K} p_{i,jk}\mathbb{P}(S_{it} = j|X_{1:t}, \boldsymbol{\theta}_1)} \qquad \text{(A.11)}
\end{aligned}$$

Model 2

The procedure remains typically the same like the case of independence model describes in the above subsection except that in (A.8), (A.9) and (A.11) the unit specific transition probabilities $\mathbb{P}(S_{it}|S_{it-1})$ are identical for all unit that is $\mathbb{P}(S_{it}|S_{it-1}) = P$ exactly like in (1.4).

Model 3

The procedure remains typically the same like the case of imperfect synchronization model describes in the above subsection except that (A.10) of updating step becomes:

$$\mathbb{P}(S_t = l|X_{1:t}, \boldsymbol{\theta}_3) = \frac{\mathbb{P}(S_t = l|X_{1:t-1}, \boldsymbol{\theta}_3) \prod_{i=1}^{N} f(X_{it}|S_t = l, X_{1:t-1,-i}, \boldsymbol{\theta}_3)}{\sum_{k=1}^{K} \mathbb{P}(S_t = k|X_{1:t-1}, \boldsymbol{\theta}_3) \prod_{i=1}^{N} f(X_{it}|S_t = k, X_{1:t-1,-i}, \boldsymbol{\theta}_3)} \qquad \text{(A.12)}$$

A.3 Model Selection for Provincials Growth-Cycles

With regime switching dynamics, the selection of the best model is a difficult task. When the number of regimes is the same in the models being compared, standard testing procedures can be applied. This is not our case because we want to select simultaneously

the number of regimes (two, three or four-states switching model) as well as the type of synchronization driven by the data generating process. Nevertheless, in a fully Bayesian framework, the decision concerning model selection can be based on the log marginal likelihood if the prior distributions of the regime-dependent parameters of interest are proper (see Gelfand and Dey (1994),Frühwirth-Schnatter (2006) for details). In this case, Bayes factors are properly defined.

A.4 Panel Markov-switching model of Imperfect synchronization with 3 regimes for China's provinces

A.4. PANEL MARKOV-SWITCHING MODEL OF IMPERFECT SYNCHRONIZATION WITH 3 REGIMES FOR CHINA'S PROVINCES

	μ_{i1}	μ_{i2}	μ_{i3}	σ_{i1}	σ_{i2}	σ_{i3}
NATIONAL	0.5302	1.0967	1.7117	0.4731	0.3804	0.4390
Coastal Provinces						
BEIJING	-0.0836	1.0000	2.2457	0.5343	0.5087	0.8156
FUJIAN	0.8814	1.5486	2.4498	0.3820	0.3316	0.5585
GUANGDONG	0.3795	1.2150	2.1120	0.5674	0.3244	0.5069
GUANGXI	0.4724	1.0000	1.7007	0.4155	0.3906	0.3456
HAINAN	0.1522	1.0121	2.7025	0.7895	1.1293	0.5120
HEBEI	0.3261	1.0187	1.5649	0.4913	0.3018	0.3347
JIANGSU	-0.4710	1.0603	2.5720	1.4596	0.6691	1.6190
LIAONING	0.4729	1.3129	2.5734	0.4212	0.3863	0.6560
SHANDONG	0.2389	1.1408	2.1750	0.9514	1.3555	3.6761
SHANGHAI	0.0610	1.0456	1.4325	1.1111	1.4282	1.0067
TIANJING	0.5108	1.3724	2.0071	0.4421	0.3342	0.5904
ZHEJIANG	0.1007	0.6674	1.4107	0.7632	0.9599	1.8689
Interior Provinces						
ANHUI	0.3348	0.9554	1.6744	0.5922	0.3525	0.3362
GANSU	0.2625	0.7919	1.3844	0.4533	0.2991	0.4623
GUIZHOU	-0.4749	0.7461	1.4332	0.6214	0.6866	0.4571
HELONGJIANG	0.2708	0.9361	1.5084	0.3975	0.3378	0.6646
HENAN	0.1452	0.7604	1.5778	0.5473	0.3917	0.3134
HUBEI	0.1349	0.9156	1.6416	0.5233	0.3476	0.4024
HUNAN	0.4325	1.0215	1.5623	0.4017	0.3266	0.3285
JIANGXI	0.2448	0.8064	1.6870	0.5746	0.3993	0.3143
JILIN	0.2610	0.7200	1.6867	0.8074	0.9395	0.5221
NEIMONGGU	0.0965	0.7043	1.4180	0.4418	0.3105	0.4302
NINGXIA	0.0678	0.6716	1.3381	0.7231	0.6011	0.4099
QINGHAI	0.2891	0.7887	1.5385	0.4550	0.2908	0.4189
SHAANXI	-0.4515	0.5832	1.6042	0.9213	0.5193	0.5440
SHANXI	-1.0158	0.5356	1.5995	0.6705	0.7839	0.5466
SICHUAN	-0.4637	0.9349	1.6598	0.6884	0.4594	0.3488
YUNNAN	-0.5047	0.6985	1.5580	0.6691	0.8056	0.4933

Note: All estimated value are significant at the 5% level. μ_{i1}, μ_{i2} and μ_{i3} denote respectively the province specific mean growth rate in slowdown, normal-growth and catching-up regime. σ_{i1}, σ_{i2} and σ_{i3} denote respectively province specific volatility in slowdown, normal-growth and catching-up regime

Table A.2: Estimation of the Panel Markov-switching model of Imperfect synchronization with 3 regimes for China provinces'.

Chapter 2

Bayesian Panel Markov-Switching model with interacting Markov chains

2.1 Introduction

Markov-switching (MS) models have been extensively used in macroeconomic and finance to extract the different phases or regimes in the market behaviour. The extension to a multivariate set-up with multiple chains is still a challenging issue due to the difficulties in modelling dependence between the chains. Moreover, in the last years, the modelling of large set of time series (Bańbura et al. (2010), Stock and Watson (2014)) become important and Markov-switching models proposed in the literature were designed for medium size panel, (e.g., Billio et al. (2016a)), or use a number of Markov chains that is smaller than the number of series (e.g., Kaufmann (2015), Kaufmann (2010), Hamilton and Owyang (2012)).

In this paper, we propose a new dynamic panel model for large set of time series with series-specific and interacting Markov-switching processes. The interaction mechanism between the series-specific Markov chains is designed to be either local (in some neighbourhood) or global (regarding all the series) or both. The neighbourhood system or the network structure of the individual time series can be a priori known by the researchers or

endogenous to the model and therefore need to be inferred. The local interactions between the Markov chains is based on a system of neighbourhoods. We assume that the state transition of each chain depends on the previous state of the series in its neighbourhood.

Another contribution is the introduction of a convenient parametrization of the transition matrix. The first advantage in using this parametrization is on the inference side. The multivariate logistic transformation widely used in the literature for the endogenous transition models implies a non-linear transformation of the parameters which makes the inference task more difficult. In a Bayesian setting, the non-linear parametrization can lead to a poor performance of the Markov Chain Monte Carlo (MCMC) sampling used for posterior approximation (e.g., see Scott (2011)). The endogenous linear time-varying transition instead is not exposed to these inferential difficulties. The drawback of the linear parametrization relies on the constraints one needs to introduce on the parameters but in our models these constraints can be easily handled through the use of standard prior distributions defined on the parameter space.

The second advantage of the linear assumption for the time-varying transition is that it allows us to provide some theoretical properties of our multiple-chain model under the assumption of a broader class of interaction mechanisms allowing for idiosyncratic, local and global interactions (Föllmer and Horst (2001)). The global interactions parameter assesses the importance of common movement in all the units-specific Markov-chains while the local one the common movement with the neighbours of the units-specific Markov-chains.

This paper also contributes to the literature on Markov-switching dynamic panel by developing an efficient MCMC algorithm for the posterior approximation. The standard approach based on Metropolis-Hastings algorithm becomes inefficient due to difficulties in setting the scale of multivariate proposal distribution. The scale of the parameter

posterior distribution can be different along the directions of the parameter space and hand-tuning the proposal scale can be a difficult task even for a small or moderate number of parameters. To solve this problem we consider the Metropolis adjusted Langevin (MALA) sampling method (Girolami and Calderhead (2011)) which is exploiting the information on the gradient of the target distribution. This method has been used in many fields such as statistics, physics and recently applied also in econometrics by Burda and Maheu (2013), Burda (2015) and Virbickaite et al. (2015).

Our modelling approach presents several advantages also in terms of applications. The model is parsimonious compared to a traditional time varying multivariate MS model and the coefficients of the linear parametrization make sense in term of theirs interpretations.

In terms of macro application, the model helps (1) to better characterize the synchronization of regional business cycles, (2) to identify which of the local and global interactions plays a substantial role for the common movement, (3) to shed light on how the co-movements that are common propagate to the rest of the economy (see Hamilton and Owyang (2012), Camacho and Leiva-Leon (2014), Leiva-Leon (2014)).

The remainder of the paper is structured into seven sections. Section 2 describes the panel Markov-switching model, the regime switching transition and its relationship to systemic risk. In section 3, we discuss some properties of the proposed model. In section 4 and 5, we present some simulation experiments and the estimation procedures under Bayesian framework. In section 6, we conduct some applications on both simulated and real data. Section 7 provides conclusions.

2.2 Panel Markov Switching with interacting Markov chains

In our panel MS model with interacting chains (PMS-IC), we assume each series $\{X_{it}\}$, $t = 1, \ldots, T$ in a panel of N units $i = 1, \ldots, N$; is a conditionally linear and Gaussian

process with mean and variance driven by a unit-specific Markov chain S_{it} which takes value in the finite set $\{0, \ldots, K-1\}$.

The measurement equation is written as:

$$X_{it} = \sum_{k=1}^{K} \mathbb{I}_{\{k\}}(S_{it}) \left[\Psi_{ik}' Z_{it} + \sigma_{ik}\varepsilon_{it}\right], \quad \varepsilon_{it} \overset{\text{iid}}{\sim} \mathcal{N}(0,1) \tag{2.1}$$

where $Z_{it}' = (1, Z_{2it}, \ldots, Z_{mit})$ is a vector of covariates and Ψ_{ik} a m-dimensional parameters vector. K represents the number of unobserved latent regimes and the symbol $\mathbb{I}_E(X)$ is the indicator function which takes value 1 if $X \in E$ and 0 otherwise.

The K by K transition matrix P_{it} of the i-th chain is time-varying and has l-th row and k-th column element $P_{it,lk}$ defined as:

$$P_{it,lk} = \mathbb{P}\left(S_{it+1} = l | S_{it} = k, S_{-i,t}\right) \tag{2.2}$$

which represents the conditional probability that unit i moves to the regime $l \in \{1, \ldots, K\}$ at time $t+1$. $S_t = (S_{1t}, S_{2t}, \ldots, S_{Nt}) \in \mathbf{S}$ is all configurations at time t, with $\mathbf{S} = \{0, \ldots, K-1\}^N$ and $S_{-i,t} = \{S_{jt}, j = 1, \ldots, N; \quad j \neq i\}$.

Following Kaufmann (2010) and Billio et al. (2016a), we assume that the transition probabilities of each chain do not only depend on their own past values but involve also the past regimes of other other chains in the panel. In this paper we propose a new interaction mechanism:

$$P_{it+1,lk} = \alpha p_{lk} + \beta m_{i,k}\left(S_t\right) + \gamma m_k\left(S_t\right) \tag{2.3}$$

with, $0 < \alpha \leqslant 1, \quad 0 \leqslant \beta < 1, \quad 0 \leqslant \gamma < 1$, interactions parameters such that $\alpha + \beta + \gamma = 1$ and p_{lk} fixed transition probability parameter such that $\sum_{k=1}^{K} p_{lk} = 1$. The second term on the right-hand side represents the local interactions mechanism and the third term defines

the global interactions. In our model, $m_{i,k}(S_t)$ is the local interaction factor and measures the proportion of chains belonging to the neighbourhood of chain i which are in the state k at time t, that is:

$$m_{i,k}(S_t) = \frac{1}{|N(i)|} \sum_{j \in N(i)} \mathbb{I}_{\{k\}}(S_{jt}) \tag{2.4}$$

where $N(i) \in \mathcal{N}$ is the neighbourhood of the chain i, and $\mathcal{N} = \{N(i)\}_{i=1,\dots,N}$ is a neighbourhood system with $N(i)$ subset of $D = \{1, \dots, N\}$ (see Brémaud (2013), Chap. 7) and $\mathcal{G} = (\mathcal{N}, D)$ is called graph or topology.

The global interaction factor $m_k(S_t)$ is given by the proportion of chains in regime k at time t that is:

$$m_k(S_t) = \frac{1}{N} \sum_{j=1}^{N} \mathbb{I}_{\{k\}}(S_{jt}) \tag{2.5}$$

These specifications of the global and local interactions allow us to assess the dependence between the time series of the panel. Modelling dependence by interactions effects is appealing in many contexts. In financial econometrics, the interactions represent linkages between financial institutions and the PMS-IC synchronization has the interpretation of contagion effect. One way of capturing these effects is via the network of connections of the individual series. Allen and Babus (2009) provide a review of network model application in economics and finance. Vesper (2013) complements existing measures of systemic risk, by introducing the combination of MS model with a latent network structure of financial institutions. In macro perspective, our PMS-IC has the potential to analyse the co-movement of regional business cycles. It does not only helps to characterize the units-specific cycles but also shows the importance of global component (global interactions), regional component

(local interactions) and fixed time independent transition in business cycles synchronization. In this vein, Kose et al. (2003, 2008) document the common dynamic properties of the world business cycles fluctuations employing a Bayesian dynamic latent factor model. Their results suggest that the regional components play only minor role in explaining cycles fluctuations. However, Francis et al. (2012) find that when the regional component is defined differently from simple geography, its effect becomes more important. Leiva-Leon (2014) proposed a new model that combines several bivariate Markov-switching models and network of synchronisation in order to create a link of interdependencies business cycles. However, the model cannot assess the importance of global and regional components in the cycles fluctuations.

The behaviour of unit i of the panel at time $t+1$ is influenced by idiosyncratic interaction, an empirical average at t and by the situation in some neighbourhood $N(i)$ at t. For instance, an individual that has in its network at t a high proportion of series in regime k will tend to transition in regime k or will remain in regime k at time $t+1$. α reflects the intensity of idiosyncratic interaction from time t to time $t+1$ and γ reflects the intensity of global interactions between the collection of time series from time t to time $t+1$. Parameter β captures the level of local interactions.

The transition probabilities satisfy the condition:

$$\sum_{k=1}^{K} P_{it,lk} = 1, \quad \forall i \in \{1,\dots,N\}, \quad \forall l \in \{0,\dots,K-1\}, \quad \forall t \in \{1,\dots,T\}$$

The linear parametrization of the regime switching transition matrix presents twofold advantages. First, the parametrization allow for idiosyncratic, global interactions and interaction in the neighbourhood of the Markov chains. Hence, if the population of time series presents high global interactions at time t then the panel MS model will more likely

exhibit episodes of contagion at time $t+1$. Secondly, formulating linearly over unit specific interaction and global interaction; the new endogenous transition matrix can be seen as solution to the usual critique to exogenous transition matrix and as well as generalisation of the fixed transition matrix. In fact, if the parameter α which measure the intensity of unit specific interaction is equal to 1 then we are back to the case of exogenous fixed transition matrix.

2.3 Properties of the model

The use of linear parametrization to model the evolution of the endogenous time-varying transition matrix insures the convergence of the Markov processes transition probabilities to unique ergodic probabilities.

Let $\mathbf{S} = \{0, 1, \ldots, K-1\}^N$ be the finite set of all configurations of $S_t = (S_{it})_{1 \leqslant i \leqslant N}$ with $S_{it} \in \{0, 1, \ldots, K-1\}$, $i = 1 \ldots, N$. The following result provides a characterization of the macroscopic dynamic of the set of Markov chains for diverging N and shows that the interacting transition kernel defined in Equation 2.3 is generating a deterministic sequence of empirical averages. These quantities can be used to find the limiting behaviour of the set of chains as t tends to infinity and to give an interpretation to the parameters of the transition probabilities.

The theoretical relationship between the local interactions factor and the global one is summarised by the following. Let us define the empirical averages:

$$\overline{m}\left(S_t\right) = \left(\overline{m}_0\left(S_t\right), \ldots, \overline{m}_{K-1}\left(S_t\right)\right)\prime$$

and the proportion of regime in some finite neighbourhood $N(i)$ of i:

$$\overline{m}_i\left(S_t\right) = \left(\overline{m}_{i0}\left(S_t\right), \ldots, \overline{m}_{iK-1}\left(S_t\right)\right)\prime$$

where

$$\overline{m}_k\left(S_t\right) = \lim_{N\to\infty} \frac{1}{N} \sum_{i=1}^{N} \mathbb{I}_{\{k\}}(S_{it}), \quad k = 0, 1, \ldots, K-1$$

$$\overline{m}_{ik}\left(S_t\right) = \frac{1}{|N(i)|} \sum_{j\in N(i)} \mathbb{I}_{\{k\}}(S_{jt}), \quad k = 0, 1, \ldots, K-1$$

with S_{it} is a Markov chain with transition probabilities

$$\pi_i(S_{it+1} = k|S_t) = \alpha p_{S_{it}k} + \beta m_{i,k}\left(S_t\right) + \gamma m_k\left(S_t\right)$$

where $\sum_{k=0}^{K-1} \pi_i(S_{it+1} = k|S_t) = 1$ Then the sequence of empirical averages of $\overline{m}_i\left(S_t\right)$ converge to $\overline{m}\left(S_t\right)$

The theoretical relationship between the global interactions factor and the fixed transition probability matrix is given in Proposition 1.

Proposition 1. Let $\mathbf{S_1} = \{S_t \in \mathbf{S}|\exists m_{t+1}\}$ and $\Pi(\cdot|S_t) = \prod_{i=1}^{\infty} \pi_i(\cdot|S_t)$ the product kernel of the population of chains, then

$$\lim_{N\to\infty} \frac{1}{N} \sum_{i=1}^{N} \mathbb{I}_{\{k\}} S_{it+1} = \lim_{N\to\infty} \frac{1}{N} \sum_{i=1}^{N} \pi_i\left(S_{it+1} = k|S_t\right) \quad \Pi(\cdot|S_t) - a.s., \tag{2.6}$$

the sequence of empirical averages satisfies almost surely the recurrence relation

$$\overline{m}_k\left(S_{t+1}\right) = \alpha \sum_{j=0}^{K-1} p_{jk}\overline{m}_j\left(S_t\right) + (1-\alpha)\overline{m}_k\left(S_t\right) \tag{2.7}$$

and the global interaction process $\{\overline{m}\left(S_t\right)\}_{t\in\mathbf{N}}$ converges almost surely to the unique invariant probability of the fixed transition probability matrix

$$P = \begin{pmatrix} p_{01} & \cdots & p_{K-1,0} \\ \vdots & \ddots & \vdots \\ p_{0,K-1} & \cdots & p_{K-1,K-1} \end{pmatrix}$$

Proof. See Appendix B.1.1.

Finally, a third proposition on the convergence of the Markov-chain process of the population of time series with time-varying transition probabilities is present in the following with Proof in Appendix B.1.2.

Proposition 2. The process $\{S_t\}_{t\in\mathbf{N}}$ converges in law to the unique product kernel

$$\Pi_{\overline{m}}(\cdot|S_t) = \prod_{i=1}^{\infty} \pi_{\overline{m}i}(\cdot|S_t)$$

2.4 Simulation examples

Figure 2.1 shows how the endogenous transition probabilities vary with the parameter α. If the fixed component of the transition probabilities is larger than the global interaction term at time t (Figure 2.1 right) then the probability to stay in one state or to switch to another state is increasing with α.

In the opposite case, if the fixed component of the transition probabilities is less than the global interaction at time t (Figure 2.1 left) then the time-varying transition probability is decreasing with respect to α. It comes out that in presence of important global interactions and persistence over time, the PMS-IC model exhibits a large scale globalisation of episodes of one regime.

In order to show qualitatively the dynamic behaviour of the panel of series under our PMS-IC model, we provide some simulated examples. We isolate the contribution of the global and local interaction mechanism and specify six parameters settings which are summarized in Table 2.1.

The difference between the six settings is on the choice of the underlying parameters α, β and γ. We distinguish six cases. In Model 1, all the interactions are null and the overall

FIGURE2.1: Different shape of the time varying probabilities $P_{it,lk} = \alpha P_{lk} + \gamma m_{t,k}$ at a given time t in function of α. Note that in this case the presence of local interaction is not allowed, $\beta = 0$

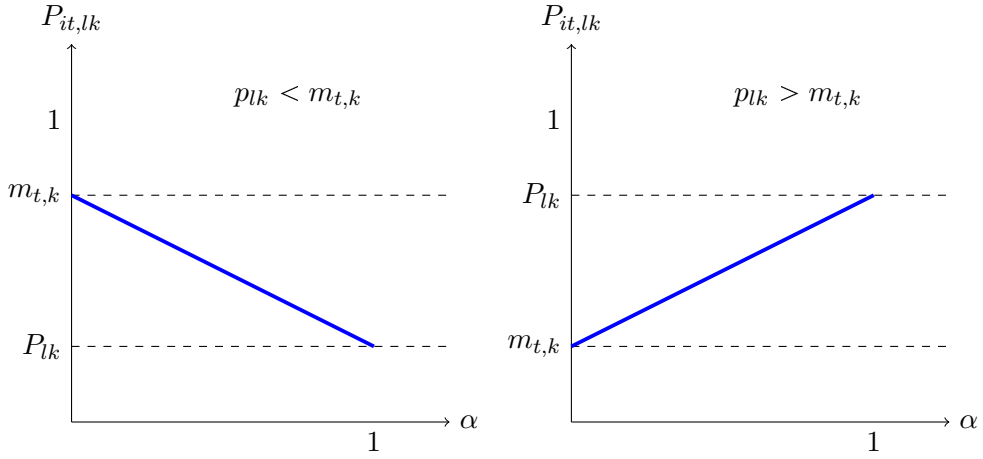

Settings label	α	β	γ
Setting 1 (No interaction)	1.00	0.00	0.00
Setting 2 (Weak global interaction)	0.70	0.00	0.30
Setting 3 (Strong global interaction)	0.30	0.00	0.70
Setting 4 (Weak local interaction)	0.70	0.30	0.00
Setting 5 (Strong local interaction)	0.30	0.70	0.00
Setting 6 (Both local and global interaction)	0.50	0.25	0.25

Table 2.1: Parameter value of idiosyncratic, global and local interaction mechanism.

effect is given by the fixed component of the transition matrix. We assume a weak global interaction among the Markov-chains for Model 2 and a stronger one for Model 3. On the other side, we consider a weak global interaction among the Markov-chains for Model 4 and a stronger one for Model 5. The global and local effect are simulated in Model 6 assuming for them an equal weight. In all the experiments, we consider a population of 50 time series following PMS-IC generated with 5000 time horizon. Furthermore, we assume the following model specification with three regimes (ie, $K = 3$):

$$X_{it} = \sum_{k=1}^{K} \mathbb{I}_{\{k\}}(S_{it}) \left[\mu_{ik} + \sigma_{ik}\varepsilon_{it}\right], \quad \varepsilon_{it} \overset{i.i.d.}{\sim} \mathcal{N}(0,1)$$

for $i = 1, \ldots, 50$ and $t = 1, \ldots, 5000$, and the fixed transition component:

$$P = \begin{pmatrix} 0.98 & 0.02 & 0.00 \\ 0.01 & 0.98 & 0.01 \\ 0.00 & 0.02 & 0.98 \end{pmatrix} \tag{2.8}$$

$\mu_{i1} = -2, \quad \mu_{i2} = 0, \quad \mu_{i3} = 2, \quad \sigma_{i1} = .3, \quad \sigma_{i2} = .05, \quad \sigma_{i3} = .3$

Note that the ergodic probability associate with P is $\pi_i = (.25 \quad .5 \quad .25)$.

The first scope of Figure 2.2 is to show the different impact of the parameter values on the level of synchronization among the series. The second aspect we study is the convergence of the global interaction chain to the invariant transition matrix of the fixed transition matrix. Figure 2.2 highlights the ability of our PMS-IC model to account for various degree of synchronization of chains. The value of α, β and γ corresponding to our six parameters settings were carefully chosen in order to represent a wide variety of possible interactions. A look at the heat-maps shows that the level of synchronization has augmented with the level of the local and global parameters. In all the different cases, the convergence to the ergodic of the fixed transition probabilities is reached with different speed.

The shape of the time varying transition is given in Figure 2.3. Without loss of generality, we present only the simulation of the probabilities to stay in regime 1, regime 2 and regime 3 for the first unit in the panel. The evidence emerging from these plots is that the global and local parameters play an important role: the higher the levels of these parameters the higher the volatility of the time varying transition probabilities is.

In conclusion, we provide a Monte Carlo estimate of the synchronization level for different values of the local and global interactions parameters. We use the bivariate concordance index of Harding and Pagan (2002) to assess the impact of the local and global parameters on the synchronization of chains. This index describes the fraction of time two chains

spend in the same phase. Let us define $c_{i,j}$ as the proportion of time the series i is in the same phase as the series j. It can be expressed by the following equation:

$$c_{i,j} = \frac{1}{T}\sum_{t=1}^{T}\sum_{k=0}^{K-1}\mathbb{I}_{\{k\}}(S_{it})\mathbb{I}_{\{k\}}(S_{jt}) \tag{2.9}$$

The relationship between the local and global interactions parameters and the level of synchronization among the chains can be measured by:

$$\overline{c} = \frac{1}{\frac{N(N-1)}{2}}\sum_{i=1}^{N}\sum_{j=i+1}^{N} c_{i,j} \tag{2.10}$$

which is in the unit interval. The closer the value of $\overline{c}$ is to one the greater the extent of synchronization within the panel of series.

A panel of 200 series is simulated from our PMS-IC using the settings presented for the underlying specification detailed in Equation 2.8. A system of three neighbourhoods is designed for the model with only local interactions. The neighbours selected are made up with 4, 16 and 24 units. Figures 2.4a and 2.4b reveal that the rate of synchronization increases with the size of the neighbourhood and the value of β as well as γ. Hence, the level of synchronization is positively related to the parameter β (resp. γ) that reflect the importance of common movement with the units-specific chains in the neighbourhood (resp. of the importance of common movement in all the units-specific chains).

2.5 Bayesian inference

2.5.1 Likelihood function and prior distributions

Let $\theta = (\mu_1, \ldots, \mu_K, \sigma_1, \ldots, \sigma_K, vec(P_1)', \ldots, vec(P_N)', \alpha, \beta, \gamma)$ be the vector of parameters with $\mu_l = (\mu_{1l}, \ldots, \mu_{Nl})$, $\sigma_l = (\sigma_{1l}, \ldots, \sigma_{Nl})$. Let us define $\xi_{k,it} = \mathbb{I}_{\{k\}}(S_{it})$. $\xi_{k,it}$ = refer to the regime k that the observation X_{it} belongs to.

By using the sequential factorization of the likelihood, the complete likelihood of the PMS-IC model writes as:

$$\begin{aligned}\mathcal{L}(X_{1:T}, S_{1:T} \mid \theta) &= \prod_{i=1}^{N}\prod_{t=1}^{T}\prod_{l=1}^{K}\prod_{k=1}^{K} f(X_{it}|S_{it},\theta)^{\xi_{l,it}} P_{it,lk}^{\xi_{l,it}\xi_{k,it-1}} \\ &= \prod_{i=1}^{N}\prod_{t=1}^{T}\prod_{l=1}^{K}\prod_{k=1}^{K}(2\pi\sigma_{il}^2)^{-\frac{\xi_{l,it}}{2}} \exp\{-\frac{\xi_{l,it}}{2\sigma_{il}^2}(X_{it}-\mu_{il})^2\} \\ &\qquad (\alpha P_{lk} + \beta m_{it,k} + \gamma m_{t,k})^{\xi_{l,it}\xi_{k,it-1}}\end{aligned} \tag{2.11}$$

In order to complete the specification of the Bayesian model, we discuss the prior choice. A variety of priors can be used to estimate the panel Markov switching model. We consider conjugate priors which are based on proper distributions. We assume conjugate independent priors for the unit specific parameters:

$$\mu_{il} \sim \mathcal{N}(m_{il}, \tau_{il}^2) \tag{2.12}$$

$$\sigma_{il}^2 \sim \mathcal{IG}(\alpha_{il}, \beta_{il}) \tag{2.13}$$

$$(P_{l1}, \ldots, P_{lK}) \sim \mathcal{D}ir(\delta_1, \ldots, \delta_K) \tag{2.14}$$

$$(\alpha, \beta, \gamma) \sim \mathcal{D}ir(\varphi_1, \varphi_2, \varphi_3) \tag{2.15}$$

with $l = 1, \ldots, K$ and $i = 1, \ldots, N$, where $\mathcal{IG}(\alpha, \beta)$ denote the inverse gamma distribution with parameters: α and β and $\mathcal{D}ir(\delta_1, \ldots, \delta_K)$ the K dimensional Dirichlet distribution with parameters: $\delta_1, \ldots, \delta_K$.

One of the main problems of Bayesian analysis using Markov-switching processes, is the non-identifiability of the parameters. That is, the posterior distribution of parameters of Markov switching model resulting is invariant to permutations in the labelling of the parameters, if this latter follow exchangeable priors. Consequently, the marginal posterior distributions for the parameters are identical for each switching component and the symmetries of the posterior distribution affect the MCMC simulation and the interpretation of the

labels switch. For more details about the effects that label switching and non-identification have on the results of a MCMC based Bayesian inference, see among other Celeux (1998), Frühwirth-Schnatter (2001),Frühwirth-Schnatter (2006). One way to address the label switching problem is to consider under some specific condition the permutation sampler proposed by Frühwirth-Schnatter (2001). Another alternative is to impose identification constraints on the parameters. This practice is widely used in macroeconomics because it is naturally related to the interpretation of the different states (e.g. recession and expansion) of the business cycle. We follow the latter approach and impose identification restrictions that $\mu_{i1} \leqslant \mu_{i2} \leqslant, \ldots, \leqslant \mu_{iK}$.

2.5.2 Posterior simulation

We are able to conduct Bayesian inference, knowing the likelihood function and the prior distribution. By means of Baye's rule, the posterior distribution in a general form follows the relationship:

$$\pi(\theta \mid X, S) \propto \mathcal{L}(X, S \mid \theta) p(S \mid X, \theta) \pi(\sigma) \pi(\mu) \tag{2.16}$$

where $\pi(\theta \mid X)$ is the posterior distribution, $\mathcal{L}()$ the completed likelihood function $\pi(\theta)$ and the prior distribution.

Our sampling algorithm is based on conditional posterior distributions described in appendix 2 The model in equation (2.1) is estimated by adapting the multi-move Gibbs-sampling procedure for Bayesian estimation of Markov switching models presented in Frühwirth-Schnatter (2006). The Gibbs sampler iterates according to the following steps:

1. Draw $S_i^{(d)}$ from $f(S_i^{(d)} \mid X, \theta^{(d-1)})$, $i = 1, \ldots, N$.

2. Draw $(\alpha, \beta, \gamma)^{(d)}$, from $f((\alpha, \beta, \gamma)^{(d)} \mid X, S^{(d)}, (p_{it,l1}, \ldots, p_{it,lK})^{(d-1)})$. where $S^{(d)} = (S_1^{(d)}, \ldots, S_N^{(d)})$.

3. Draw $(p_{l1}, \ldots, p_{lK})^{(d)}$ from $f((p_{l1}, \ldots, p_{lK})^{(d)} \mid X, S^{(d)}, (\alpha, \beta, \gamma)^{(d-1)})$, $i = 1, \ldots, N$, $l = 1, \ldots, K$.

4. Draw $\mu_{il}^{(d)}$,from $f(\mu_{il}^{(d)} \mid X, S_i^{(d)}, \sigma_{il}^{(d-1)}$, $i = 1, \ldots, N$, $l = 1, \ldots, K$.

5. Draw $\sigma_{il}^{(d)}$, from $f(\sigma_{il}^{(d)} \mid X, S_i^{(d)}, \mu_{il}^{(d-1)})$ $i = 1, \ldots, N$, $l = 1, \ldots, K$.

2.5.3 Gibbs iterations mains issues

Firstly, the multi-move sampling of the hidden state cannot be directly implemented:

1. the full conditional posterior distribution of the unit specific hidden state depends on proportionality factor that need to be taken into account by introducing Metropolis-Hastings adjustment, where

2. the proposal distribution is identical to forward filtering backward sampling (FFBS) of the states.

Secondly, the standard sampler based on independent proposal poorly estimates the parameter (α, β, γ):

1. the posterior distribution of (α, β, γ) is prior dependent, and

2. a straightforward implementation of Metropolis-Hastings algorithm with the proposal distribution equal to the prior distribution becomes inefficient, resulting in high rate of acceptance followed by poor mixing of the chain.

In the following section we present Metropolis adjusted Langevin sampling algorithms as an efficient option to solve the issues described above when using independent proposal. In this case, the Gibbs sampler changes slightly according to the following steps:

1. Draw $S_i^{(d)}$ from Metropolis-Hastings adjusted FFBS (see Appendix B.4).

2. Draw $(\alpha, \beta, \gamma)^{(d)}$, from Metropolis adjusted Langevin algorithm (MALA) .

3. Draw $(p_{l1}, \ldots, p_{lK})^{(d)}$ from $f((p_{l1}, \ldots, p_{lK})^{(d)} \mid X, S^{(d)}, (\alpha, \beta, \gamma)^{(d-1)})$, $i = 1, \ldots, N$, $l = 1, \ldots, K$ by using a Metropolis-Hastings algorithm.

4. Draw $\mu_{il}^{(d)}$,from $f(\mu_{il}^{(d)} \mid X, S_i^{(d)}, \sigma_{il}^{(d-1)}$, $i = 1, \ldots, N$, $l = 1, \ldots, K$.

5. Draw $\sigma_{il}^{(d)}$, from $f(\sigma_{il}^{(d)} \mid X, S_i^{(d)}, \mu_{il}^{(d-1)})$ $i = 1, \ldots, N$, $l = 1, \ldots, K$.

We simulate (α, β, γ) from $f\left(\alpha, \beta, \gamma | X_{1-T}, S_{1-T}, \theta_{-(\alpha,\beta,\gamma)}\right)$ where the prior is chosen to be Dirichlet $\mathcal{D}ir(\varphi_1, \varphi_2, \varphi_3)$. Since by definition $(\alpha, \beta, \gamma) \in [0; 1]^3$; when dealing with random walk proposals we need to use transformation of α, β and γ to the real line which introduces a Jacobian factor into the acceptance probability of the Metropolis adjusted Langevin. We assume

$$\alpha = \frac{1}{1 + exp(-\alpha')}\beta = \frac{1}{1 + exp(-\beta')}\gamma = \frac{1}{1 + exp(-\gamma')}$$

For the Metropolis-adjusted Langevin algorithm (MALA) we need the partial derivatives of the complete log-likelihood with respect to the transformed parameters (see Appendix B.5).

The proposal mechanism of Metropolis adjusted Langevin algorithm is given by the following equation

$$\omega^* = \omega^n + \frac{\epsilon^2}{2} M \nabla_\omega l\left(\omega^n\right) + \epsilon\sqrt{M} z^n \tag{2.17}$$

where $\omega = (\alpha, \beta, \gamma)'$, $l = log\{\mathcal{L}(X, S, \theta)\}$ is the complete data joint log-likelihood, ϵ is the integration step and $z \sim \mathcal{N}(0, 1)$. M is a preconditioning matrix which helps to circumvent issues that appear when the elements of ω have very different scales or if they are strongly correlated. $\sqrt{M}$ can be obtained via Cholesky decomposition such that

$M = UU'$ and $\sqrt{M} = U$. The convergence to invariant distribution $p(\omega)$ is ensure by employing Metropolis acceptance probability after each integration step. The proposal density is

$$q(\omega^*|\omega^n) = \mathcal{N}\{\omega^*|\mu(\omega^n, \epsilon), \epsilon^2\mathbf{I}\}$$

with $\mu(\omega^n, \epsilon) = \omega^n + \frac{\epsilon^2}{2}\nabla_\omega L(\omega^n)$ and acceptance probability of standard form if given by $\min\{1, p(\omega^*)q(\omega^n|\omega^*)/p(\omega^n)q(\omega^*|\omega^n)\}$. The choice of the preconditioning matrix does not follow any systematic and principled manner. For instance, Christensen et al. (2005) showed that a global level of preconditioning can be inappropriate for the transient phase of Markov process.

2.6 Empirical studies

2.6.1 Posterior densities of the regression parameters

We assess the efficiency of our proposed estimation algorithm using the mean square error (MSE) for the parameters and the hidden states.

Setting label	Model 1	Model 2	Model 3	Model 4	Model 5	Model 6
The unit-specific regression parameters (in total 50 parameters for each regime)						
$\mu_{.,1}$	1.323e-02	6.144e-04	0.762e-03	0.866e-03	8.078e-04	6.954e-04
$\mu_{.,2}$	1.977e-02	0.750e-04	0.009e-03	0.009e-03	0.161e-04	0.119e-04
$\mu_{.,3}$	0.357e-02	4.031e-04	0.731e-03	0.632e-03	4.402e-04	9.807e-04
$\sigma_{.,1}$	0.740e-03	4.000e-04	0.001e-03	0.313e-03	5.044e-04	0.000e-04
$\sigma_{.,2}$	0.120e-03	1.600e-04	0.000e-04	0.005e-03	0.090e-04	0.000e-04
$\sigma_{.,3}$	0.109e-03	2.000e-04	0.000e-04	0.757e-03	2.013e-04	0.001e-04
Idiosyncratic, local and global parameters						
(α, β, γ)	1.976e-07	3.5535e-04	5.5682e-04	1.540e-02	3.09e-02	4.110e-02
The unit-specific Markov chains (in total 50 parameters for each regime)						
Regime 1	5.000e-04	1.200e-03	2.000e-03	1.400e-03	1.600e-03	1.900e-03
Regime 2	1.300e-04	2.200e-03	3.800e-03	2.100e-03	2.100e-03	2.800e-03
Regime 3	6.000e-04	1.600e-03	2.400e-03	1.200e-03	2.200e-03	1.600e-03

Table 2.2: Mean square error (MSE) for the parameters estimated using the proposed PMS-IC algorithms.

MSE is evaluated on 5000 iterations after convergence. Table 2.2 reports for each model the average MSE for the 50 units in our panel. The first message of the table is that precision of the inferences of the unit-specific regression parameters decreases with the parameters β and γ. The second message is that precision of the inferences of the unit-specific Markov chains increases with the parameters β and γ.

2.6.2 US States coincident indices datasets

We consider the US states monthly coincident indices datasets produced by the Federal Reserve Bank of Philadelphia. At the moment of this study, its covers the 50 States of US and starts from October 1979 to December 2015. The data set contains also the State-level diffusion indexes. This index of business cycle diffusion is constructed on the scale -100 to 100 where a negative number is related to the spread of national recession and positive one to national expansion. This dataset is used in Owyang et al. (2005) under a Bayesian univariate independent Markov-switching model. In order to check the importance of the local and global interactions across the US states, we consider two settings. The first setting assume only global interactions among the US states coincident indices while the second one assume both the global and local interactions effects. In order to investigate the local interactions among the states-level cycles, we use also a geographic proximity matrix exogenously defined. The results presented in Table 2.3, favour the hypothesis that only the global interactions of the cycles prevail.

	Marginal log-likelihood	α	β	γ
Model with only global interactions	879.726	0.724	–	0.276
		(0.712, 0.733)	–	(0.267, 0.288)
Model with the global and local interactions	438.976	0.526	0.000	0.474
		(0.506, 0.543)	(0.000 0.000)	(0.458, 0.494)

Table 2.3: Comparison in terms of marginal log likelihood between different PMS-IC on the US states regional data. In parenthesis the 95% high posterior density interval

In the remainder of this subsection, we will analyse the model with only global interactions. We plot in Figure 2.5 the global interactions of recessions of the US-States business cycles together with the diffusion index of the US national cycle phases published by the Federal Reserve Bank of Philadelphia.

Our proposed PMS-IC with global interactions of cycles is able to capture all the national recessions given by the NBER. The second point is that the diffusion index of the FED and our global interactions capture the same downturns point of the national cycle. However, our model shows that the degree of synchronization of the US states cycles plays a role in making the slowdowns and the recessions costs faster and deeper than the FED diffusion index reveals. The 'great recession' has been different from the previous ones because of its duration, deepness, real and financial consequences. It has been a global and wide spread crisis across the States. The global component explains a substantial portion of the cyclical movements for most states. The linkages between the financial institutions increase the strength of the connections of the States. Our global interactions factor catches the great recession downturn as the FED diffusion index does. However, our PMS-IC model can study the effects of States specific-recessions and shows that global connections can strengthen the consequences of a national recession.

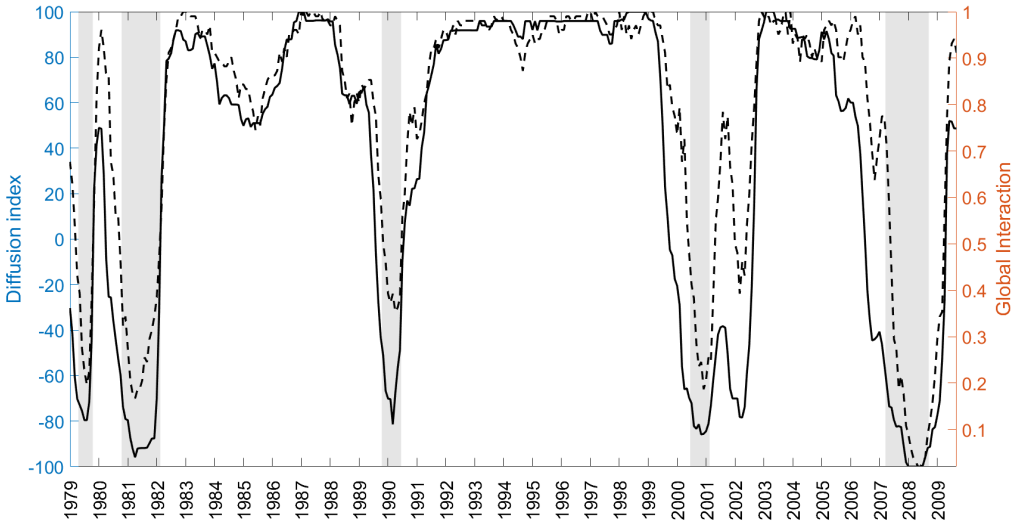

FIGURE2.5: Evolution of the global interactions factor (solid line) from the PMS-IC model and the diffusion index of the Federal Reserve of Philadelphia (dashed line). Gray bars represent the US national recession periods following the official dating of the National Bureau of Economic Research (NBER)

The scatter plot (see Figure 2.6) of the estimated mean growth rates and volatilities shows a clear separation between the two phases of the regional cycles. For every state, the expansion growth rates is positive and the recession growth rate negative.

The regression line shows a negative relationship between the state coincident index mean growth rates and the relative volatilities during recessions. On the contrary in the expansion regime the volatilities are quite low and there are positively correlated with the mean growth rates. As the state coincident index summarize current economic conditions we can conclude that during deep recession the uncertainty is much more higher and can slow the recovery itself. From Table B.1 in the Appendix, the volatilities of the recession growth rates are always higher than the ones of expansion regimes.

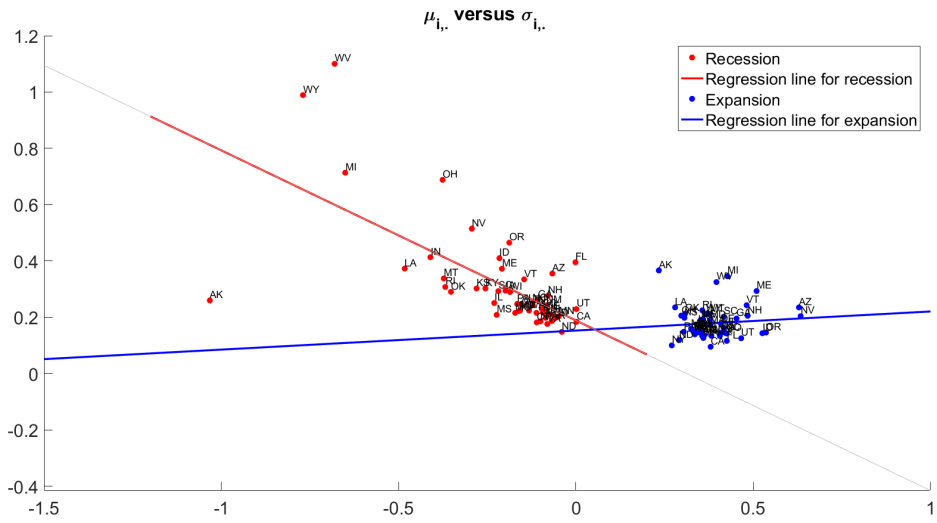

FIGURE2.6: Estimations of monthly State-level coincident index mean growth rates and volatilities with the Bayesian PMS-IC model. The horizontal axis represents the mean growth rates and the vertical axis the volatilities. Sample period: October 1979 to December 2015 (month on month). The label of the US-States is added for clarity purpose

2.7 Conclusion

The motivation for this paper comes from the idea that there might be a presence of interactions mechanism among a population of time series. These interactions can either be local (ie in some neighbourhoods) or global (ie for all the units in the panel). Thus, to investigate these interactions, we propose a new dynamic panel Markov switching with interacting chains (PMS-IC) model and provide an efficient Markov Chain Monte Carlo algorithm for the posterior approximation.

We introduce a linear time-varying transition probabilities for the unit-specific Markov chains. Theses transition probabilities linearly depend on three factors. The first factor, the fixed transition matrix, assumes that all the series share a time independent common movement. The intensity of this factor is captured by the parameter denoted α. The second

factor, the local interactions factor, assumes that each unit-specific Markov chain shares a time dependent common movement with its neighbours. The importance of this factor is measured by the parameter β. The third factor, the global interactions factor, assumes that all the unit-specific Markov chains share a time dependent common movement. The importance of this factor is assessed by the parameter γ.

The Markov Chain Monte Carlo algorithm for the posterior approximation follows a four steps algorithm: (1) run a Metropolis-adjusted Forward-Filtering Backward-Sampling for the hidden states (2) apply a Metropolis-adjusted Langevin (MALA) sampling method for (α, β, γ) (3) use a standard Metropolis-Hastings to draw the fixed transition probabilities and (4) draw the unit-specific regression parameters from their posterior distribution.

We illustrate the usefulness of our PMS-IC model by conducting simulation exercises and regional business cycle application. Our simulation experiments reveal that the proposed model is able to capture several levels of synchronization. In fact, the level of synchronization among the time series is positively correlated to the parameter β and γ. The macro application is based on the US states regional business. The PMS-IC is able to capture all the national recessions given by the NBER. Most importantly, the estimations reveal that the local interactions factor play no role in the US regional business cycles. Only the global interactions of the cycles prevail. The global interactions factor of the US states cycles play a role in making the recession cost faster and deeper than the FED diffusion index reveals.

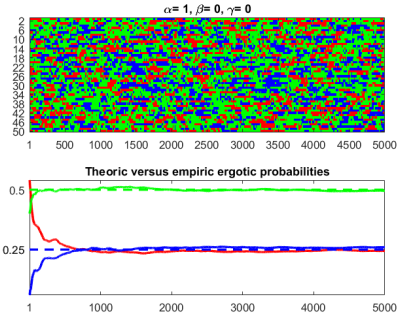

(a) Setting 1: no interaction

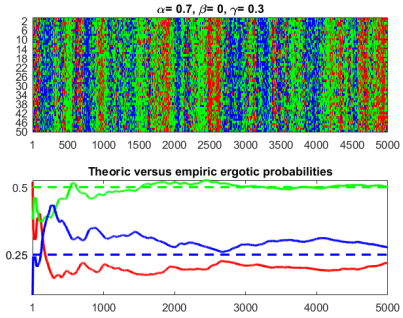

(b) Setting 2: weak global interactions

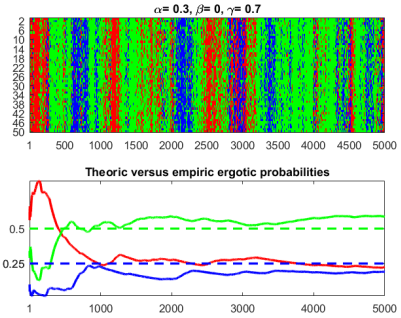

(c) Setting 3: strong global interactions

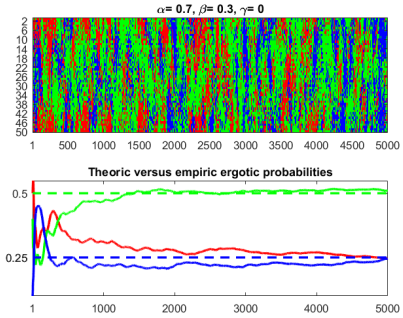

(d) Setting 4: weak local interactions

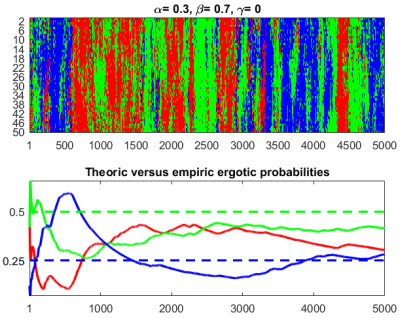

(e) Setting 5: strong local interactions

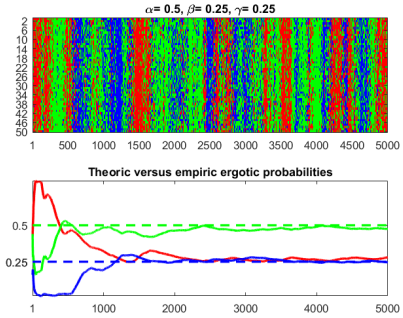

(f) Setting 6: both local and global interactions

FIGURE2.2: Population of 50 time series generated. For each model, the top plot is a heat-maps of the time series. In each plot, colors blue mean that the serie is in expansion regime; colors green refer to moderate expansion regime and colors red refer to recession regime. For each model: the bottom plot describes the evolution of the global interaction chain of the linear time varying transition matrix together with the horizontal lines given by the elements of theoric ergotic probabilities of the fixed transition matrix.

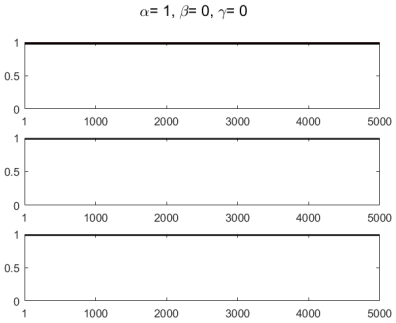

(a) Setting 1: no interaction

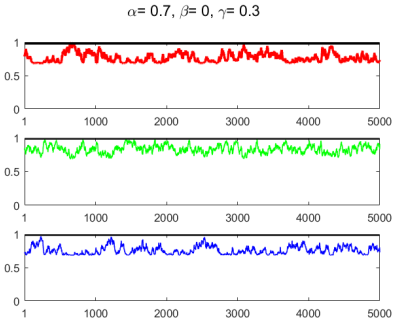

(b) Setting 2: weak global interactions

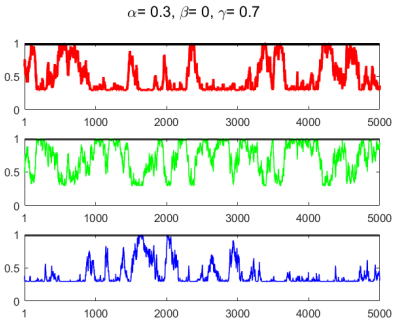

(c) Setting 3: strong global interactions

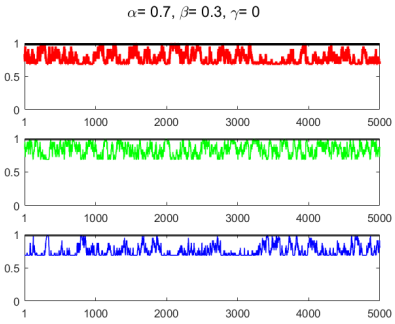

(d) Setting 4: weak local interactions

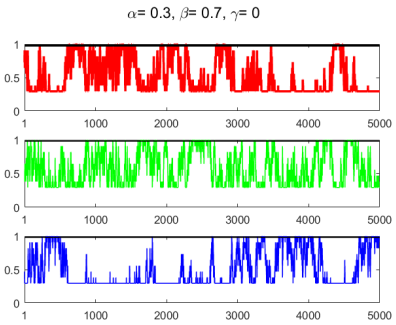

(e) Setting 5: strong local interactions

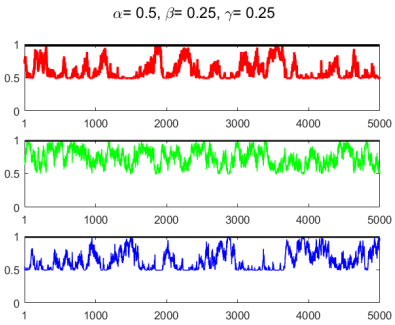

(f) Setting 6: both local and global interactions

FIGURE2.3: Evolution of elements of both fixed and time varying transition matrices for the first chain of the panel for each model. Probabilities to be in regime 1 at time t. Colours blue is for $P_{1t,11}$; colors green refer $P_{1t,22}$ and colors red refer to $P_{1t,33}$. For all plots, horizontal black lines represent the fixed transition probabilities defined in equation 2.8 .

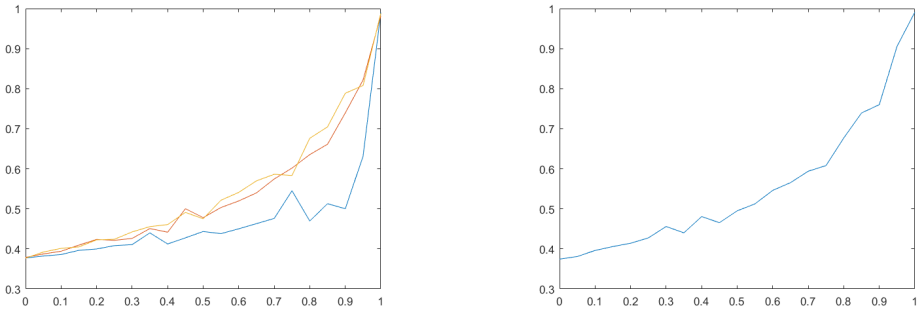

(a) $0 \leqslant \beta \leqslant 1$ (b) $0 \leqslant \gamma \leqslant 1$

FIGURE2.4: Relationship between the local parameter β, the global parameters γ and the synchronization of chains. The vertical axis represents the value taken by $\bar{c}$ in function of β the local interaction parameter for panel (a) and in function of γ the global interaction parameter for panel (b). The horizontal axis represents the value of α.

Appendix B

Technical Details of Chapter 2

B.1 Properties of the PMS-IC

B.1.1 Proof of Proposition 1

Proof. Without loss of generality let assume K=2.

Define $W_{it,1} = S_{it} - \mu_{it}$ where $\mu_{it} = \pi_{it}(S_t, 1)$ and $S_t \in \mathbf{S_1}$. Then $\{W_{it,1}\}_{i \geqslant 1}$ is a sequence of independent random variables, conditioning on $\mathcal{F}_{t-1} = \sigma(\{S_u\}_{u \leqslant t-1})$, such that $\mathbb{E}(W_{it,1}|\mathcal{F}_{t-1}) = 0$ and $\mathbb{V}(W_{it,1}|\mathcal{F}_{t-1}) = \mu_{it}(1-\mu_{it})$ which satisfies $\sum_{i=1}^{\infty} \frac{\mu_{it}(1-\mu_{it})}{i^2} < \infty$. Then by the strong law of large numbers it follows that $\sum_{i=1}^{N} W_{it,1}$ converge a.s. to zero for $N \to \infty$ (see Williams (1991), p. 118, Theorem 12.8).

From the previous result we have

$$\begin{aligned} \overline{m}_{t+1,1} &= \lim_{N\to\infty} \frac{1}{N} \sum_{i=1}^{N} \pi_{it}(S_t, 1) \qquad \text{(B.1)} \\ &= \lim_{N\to\infty} \frac{1}{N} \sum_{i=1}^{N} (S_{it}\alpha p_{11} + (1 - S_{it})\alpha p_{01} + \beta \overline{m}_{it,1} + \gamma \overline{m}_{t,1}) \\ &= (\overline{m}_{t,1}\alpha p_{11} + (1 - \overline{m}_{t,1})\alpha p_{01} + (1 - \alpha - \gamma)\overline{m}_{t,1} + \gamma \overline{m}_{t,1}). \end{aligned}$$

The limits of the recursion can be easily find by setting $\overline{m}_t = \overline{m}^*$ and solving the equation

$$\overline{m}^* = \alpha\left(\overline{m}^* p_{11} + (1 - \overline{m}^*)p_{01}\right) + (1-\alpha)\overline{m}^*$$

in $\overline{m}^*$. □

B.1.2 Proof of Proposition 2

See Föllmer and Horst (2001)

B.2 Linear time varying transition mechanism

We assume a linear parametrization of the transition probabilities. The transition matrix P_{it} of unit i at time t is linear with respect to the fixed transition matrix P the local interactions indices $m_{it,k}$, $k = 1, \ldots, K$ and the global interactions index $m_{t,k}$, $k = 1, \ldots, K$.

We define a global interaction mechanism as a map:

$$m_{t,k}\left(S_{1t}, \ldots, S_{Nt}\right) : \Delta^N_{[0,1]^K} \longrightarrow \Delta_{[0,1]^K}$$

where $\Delta_{[0,1]^K}$ is the standard K-dimensional simplex. The local interaction is defined as a map:

$$m_{it,k}\left(S_{1t}, \ldots, S_{Nt}\right) : \Delta^{|N(i)|}_{[0,1]^K} \longrightarrow \Delta_{[0,1]^K}$$

where $|N(i)|$ is the cardinal of the set $N(i)$ of neighbourhood of unit i, $i = 1, \ldots, N$.

The matrix representation of the linear time varying transition probabilities is:

$$\mathbb{P}\left(S_{it}|S_{it-1}\right) = P_{it} = \alpha P + \beta \mathbf{1}_K m_{it}\left(S_{1t}, \ldots, S_{Nt}\right) + \gamma \mathbf{1}_K m_t\left(S_{1t}, \ldots, S_{Nt}\right),$$

$$0 < \alpha \leqslant 1, \quad 0 < \beta \leqslant 1, \quad 0 < \gamma \leqslant 1, \quad \alpha + \beta + \gamma = 1$$

We denote $\mathbf{1}_K = \begin{pmatrix} 1 \\ \vdots \\ 1 \end{pmatrix}$, $m_t\left(S_{1t}, \ldots, S_{Nt}\right) = \left(m_{t,1}, \ldots, m_{t,K}\right)$, $m_{it}\left(S_{1t}, \ldots, S_{Nt}\right) = \left(m_{it,1}, \ldots, m_{it,K}\right)$,

with $m_{t,l} = \frac{1}{N} \sum_{j=1}^{N} \mathbb{I}_{\{l\}}(S_{jt-1})$, $\forall k = 1, \ldots, K$

P the fixed transition probabilities matrix is defined by

$$P = \begin{pmatrix} P_{11} & \cdots & P_{1K} \\ \vdots & \ddots & \vdots \\ P_{K1} & \cdots & P_{KK} \end{pmatrix}$$

where P_{lk} represents the fixed conditional probability that unit i moves from the latent regime k at time $t-1$ to the latent regime l at time t. So then, $P_{lk} \geqslant 0$, $P_{lk} = \mathbb{P}(S_{it} = l | S_{i,t-1} = k)$.

B.3 Parameters full conditional distribution

1. The posterior distribution of the regime dependent intercept μ_{il} (where $l = 1, \ldots, K$ and $i = 1, \ldots, N$) according to the likelihood in equation (2.11) and the prior in

equation (2.12) has a normal distribution with density function:

$$
\begin{aligned}
f(\mu_{il}|X_{1:T}, S_{1:T}, \theta_{-\mu_{il}}) &\propto \exp\{-\frac{1}{2\tau_{il}^2}\left(\mu_{il}-m_{il}\right)^2\}\prod_{t=1}^{T}\exp\{-\frac{\xi_{l,it}}{2\sigma_{il}^2}\left(X_{it}-\mu_{il}\right)^2\} \\
&\propto \exp\{-\frac{1}{2\tau_{il}^2}\left(\mu_{il}-m_{il}\right)^2\}\prod_{t\in\mathcal{T}_i}\exp\{-\frac{1}{2\sigma_{il}^2}\left(X_{it}-\mu_{il}\right)^2\} \\
&\propto \exp\{-\frac{1}{2\tau_{il}^2}(\mu_{il}^2-2\mu_{il}m_{il})\}\exp\{-\sum_{t\in\mathcal{T}_{il}}\frac{1}{2\sigma_{il}^2}(\mu_{il}^2-2\mu_{il}X_{it})\} \\
&\propto \exp\{-\frac{1}{2}\mu_{il}^2\left(\frac{1}{\tau_{il}^2}+\frac{T_{il}}{\sigma_{il}^2}\right)-2\mu_{il}\left(\frac{m_{il}}{\tau_{il}^2}+\frac{\sum_{t\in\mathcal{T}_{il}}X_{it}}{\sigma_{il}^2}\right)\} \\
&\propto \mathcal{N}(\overline{m}_{il},\overline{\tau}_{il}^2)
\end{aligned}
$$

with $\overline{m}_{il}=\overline{\tau}_{il}^2\left(\frac{m_{il}}{\tau_{il}^2}+\frac{\sum_{t\in\mathcal{T}_{il}}X_{it}}{\sigma_{il}^2}\right)$ and $\overline{\tau}_{il}^2=\left(\frac{1}{\tau_{il}^2}+\frac{T_{il}}{\sigma_{il}^2}\right)^{-1}$.

We defined $\mathcal{T}_{il}=\{t=1,\ldots,T|S_{it}=l\}$, $T_{il}=card(\mathcal{T}_{il})$, $X_{1:T}=(X_1,\ldots,X_T)$ and $S_{1:T}=(S_1,\ldots,S_T)$. The notation θ_{-r} indicates that element r is excluded from the vector θ.

2. The posterior distribution of the regime dependent volatility σ_{il} (where $l=1,\ldots,K$ and $i=1,\ldots,N$) according to the likelihood in equation (2.11) and the prior in equation (2.13) has inverse gamma distribution with density function:

$$f\left(\sigma_{il}|X_{1:T},S_{1:T},\theta_{-\sigma_{il}}\right)\propto\left(\frac{1}{\sigma_{il}^2}\right)^{(\alpha_{il}+1)}\exp\{-\frac{\beta_{il}}{\sigma_{il}^2}\}\prod_{t\in\mathcal{T}_{il}}\frac{1}{\sigma_{il}^2}exp\{-\sum_{t\in\mathcal{T}_{il}}\frac{1}{2\sigma_{il}^2}(X_{it}-\mu_{il})^2\}$$

$$\propto\left(\frac{1}{\sigma_{il}^2}\right)^{(\alpha_{il}+T_{il}+1)}\exp\{-\frac{1}{\sigma_{il}^2}\{\beta_{il}+\sum_{t\in\mathcal{T}_{il}}(X_{it}-\mu_{il})^2\}\}$$

$$\propto\mathcal{IG}\left(\alpha_{il}+T_{il},\beta_{il}+\sum_{t\in\mathcal{T}_{il}}(X_{it}-\mu_{il})^2\right)$$

3. The posterior distribution of each l-th row of the transition matrix $P_{l,1:K}=(P_{l1},\ldots,P_{lK})$ according to the likelihood in equation (2.11) and the prior in equation (2.14) density function:

$$f\left(p_{l,1:K}|X_{1:T},S_{1:T},\theta_{-(p_{l,1:K})}\right)\propto\left(\prod_{k=1}^{K}p_{lk}^{(\delta_k-1)}\right)\prod_{t=1}^{T}\prod_{i=1}^{N}\prod_{k=1}^{K}(\alpha p_{lk}+\beta m_{it,k}+\gamma m_{t,k})^{\xi_{k,it}\xi_{l,it-1}}$$

$$\propto\left(\prod_{k=1}^{K}p_{lk}^{(\delta_k-1)}\right)\prod_{k=1}^{K}\prod_{i=1}^{N}\prod_{t\in\mathcal{T}_{ilk}}(\alpha p_{lk}+\beta m_{it,k}+\gamma m_{t,k})$$

$$\propto\prod_{k=1}^{K}\left(p_{lk}^{(\delta_k-1)}\prod_{i=1}^{N}\prod_{t\in\mathcal{T}_{ilk}}(\alpha p_{lk}+\beta m_{it,k}+\gamma m_{t,k})\right)$$

4. The posterior distribution of (α,β,γ) according to the likelihood in equation (2.11) and the prior in equation (2.15) density function:

$$f\left(\alpha,\beta,\gamma|X_{1-T},S_{1-T},\theta_{-(\alpha,\beta,\gamma)}\right)\propto\left(\alpha^{\varphi_1-1}\beta^{\varphi_2-1}\gamma^{\varphi_3-1}\right)\prod_{t=1}^{T}\prod_{i=1}^{N}\prod_{l=1}^{K}\prod_{k=1}^{K}(\alpha p_{lk}+\beta m_{it,k}+\gamma m_{t,k})^{\xi_{k,it}\xi_{l,it-1}}$$

$$\propto\left(\alpha^{\varphi_1-1}\beta^{\varphi_2-1}\gamma^{\varphi_3-1}\right)\prod_{k=1}^{K}\prod_{l=1}^{K}\prod_{i=1}^{N}\prod_{t\in\mathcal{T}_{ilk}}(\alpha p_{lk}+\beta m_{it,k}+\gamma m_{t,k})$$

B.4 Forward-filtering backward-sampling (FFBS) algorithm

The FFBS algorithm also known as multi-move sampling, is needed to sample from the joint posterior distribution $f(S_{i,1:T}|S_{-i,1:T}, X_{1:T}, \theta)$. By means of dynamic factorization, the full conditional distribution of the unit specific hidden state is

$$\begin{aligned}
\mathbb{P}(S_{i,1:T}|S_{-i,1:T}, X_{1:T}, \theta) &= \mathbb{P}(S_{iT}|S_{-i,1:T}, X_{1:T}, \theta)\mathbb{P}(S_{i,1:T-1}|S_{iT}, S_{-i,1:T}, X_{1:T}, \theta) \\
&= \mathbb{P}(S_{iT}|S_{-i,1:T}, X_{1:T}, \theta) \prod_{t=1}^{T-1} \mathbb{P}(S_{i,t}|S_{i,t+1:T}, S_{-i,1:T}, X_{1:T}, \theta) \\
&\propto \mathbb{P}(S_{iT}|S_{-i,1:T}, X_{1:T}, \theta) \prod_{t=1}^{T-1} \mathbb{P}(S_{i,t+1}|S_{i,t}, S_{-i,t})\mathbb{P}(S_{i,t}|S_{-i,1:T}, X_{1:t}, \theta) \\
&\propto \left(\mathbb{P}(S_{iT}|S_{-i,1:T}, X_{1:T}, \theta) \prod_{t=1}^{T-1} \mathbb{P}(S_{i,t}|S_{-i,1:t}, X_{1:t}, \theta)\right)\left(\prod_{t=1}^{T-1} \mathbb{P}(S_{i,t+1}|S_{i,t}, S_{-i,t}, \theta)\right)
\end{aligned}$$

With this factorization, a Metropolis-Hasting (M.-H.) procedure is needed to take into account the proportionality factor with the FFBS algorithm as proposal for the unit specific hidden state. The filtering probability for unit i at time t, $t = 1, \ldots, T$, algorithm gives the prediction probability, the one step-ahead forecast density and the updated probability. The prediction probability is: for $l = 1, \ldots, K$

$$\begin{aligned}
\mathbb{P}(S_{it} = l|S_{-i,1:t}, X_{1:t-1}, \theta) &= \sum_{k=1}^{K} \mathbb{P}(S_{it} = l|S_{it-1} = k, S_{-it-1})\mathbb{P}(S_{i,t-1} = k|S_{-i,1:t-1}, X_{1:t-1}, \theta) \\
&= \sum_{k=1}^{K} P_{it-1,kl}\mathbb{P}(S_{i,t-1} = k|S_{-i,1:t-1}, X_{1:t-1}, \theta)
\end{aligned} \tag{B.2}$$

where $P_{it-1,lk}$ is the conditional probability that unit i moves from regime k at time $t-1$ to regime l at time t. $S_{-i,t} = \{S_{jt}, j = 1, \ldots, N j \neq i\}$. We initialize for $t = 1$, $\mathbb{P}(S_{i,0} = k|X_0, \theta)$ to be equal to the ergodic probabilities.

The filtered probability is computed such as: for all $l = 1, \ldots, K$ we have

$$\begin{aligned}\mathbb{P}(S_{it} = l|S_{-i,1:t}X_{1:t}, \theta) &\propto \mathbb{P}(S_{it} = l|S_{-i,1:t-1}, X_{1:t-1}, \theta).f(X_{it}|S_{it} = l, X_{1:t-1}, \theta) \\ &= \mathbb{P}(S_{it} = l|S_{-i,1:t-1}, X_{1:t-1}, \theta)\mathcal{N}(\mu_{il}, \sigma_{il}^2) \qquad \text{(B.3)}\end{aligned}$$

The smoothing probabilities are obtained recursively and backward in time, once all the filtered probabilities $\mathbb{P}(S_{it} = l|X_{1:t-1}, \theta)$ for $t = 1, \ldots, T$ are calculated. If $t = T$, smoothing probability and filtered probability are equal.

For $t = T-1, T-2, \ldots, 1$ and for all $k = 1, \ldots, K$ the smoothing algorithm proceeds as follows:

$$\begin{aligned}\mathbb{P}(S_{it} = l|S_{-i,1:T}, X_{1:T}, \theta) &= \sum_{k=1}^{K} \mathbb{P}(S_{it} = l, S_{it+1} = k|S_{-i,1:T}, X_{1:T}, \theta) \\ &= \sum_{k=1}^{K} \mathbb{P}(S_{it} = l|S_{it+1} = k, S_{-i,1:T}, X_{1:t}, \theta)\mathbb{P}(S_{it+1} = k|S_{-i,1:T}, X_{1:T}, \theta) \\ &= \sum_{k=1}^{K} \frac{p_{it,lk}\mathbb{P}(S_{it} = l|S_{-i,1:T}, X_{1:t}, \theta)\mathbb{P}(S_{it+1} = k|S_{-i,1:T}, X_{1:T}, \theta)}{\sum_{j=1}^{K} p_{it,jk}\mathbb{P}(S_{it} = j|S_{-i,1:T}, X_{1:t}, \theta)}\end{aligned}$$

B.5 Metropolis-adjusted Langevin algorithm (MALA)

The implementation of the MALA requires some necessary expressions which we discuss in this section. We consider the logistic transformation on the parameter p_{lk}, $k = 1, \ldots, K$,

α, β and γ to deal with restrictions on parameters space.

$$\alpha = \frac{1}{1 + exp(-\tilde{\alpha})}$$

$$\beta = \frac{1}{1 + exp(-\tilde{\beta})}$$

$$\gamma = \frac{1}{1 + exp(-\tilde{\gamma})}$$

$$p_{lk} = \frac{1}{1 + exp(-\tilde{p_{lk}})}$$

where $\tilde{p_{lk}}$, $k = 1, \ldots, K$, $\tilde{\alpha}$, $\tilde{\beta}$ and $\tilde{\gamma}$ take value in the set of the real numbers. The derivatives of the parameter α, β and γ with respect to the logistic transformation are:

$$\frac{d\alpha}{d\tilde{\alpha}} = \frac{exp(-\tilde{\alpha})}{(1 + exp(-\tilde{\alpha}))^2} = \alpha(1 - \alpha)$$

$$\frac{d\beta}{d\tilde{\beta}} = \frac{exp(-\tilde{\beta})}{\left(1 + exp(-\tilde{\beta})\right)^2} = \beta(1 - \beta)$$

$$\frac{d\gamma}{d\tilde{\gamma}} = \frac{exp(-\tilde{\gamma})}{(1 + exp(-\tilde{\gamma}))^2} = \gamma(1 - \gamma)$$

$$\frac{dp_{lk}}{d\tilde{p_{lk}}} = \frac{exp(-\tilde{p_{lk}})}{(1 + exp(-\tilde{p_{lk}}))^2} = p_{lk}(1 - p_{lk})$$

The partial derivatives of the complete data log-likelihood

$$L = log\{\mathcal{L}(X_{1:T}, S_{1:T}, \theta)\}$$

$$= log\{\prod_{i=1}^{N}\prod_{t=1}^{T}\prod_{k=1}^{K}\prod_{l=1}^{K}(2\pi\sigma_{il}^2)^{-\frac{\xi_{l,it}}{2}} \exp\{-\frac{\xi_{l,it}}{2\sigma_{il}^2}(X_{it} - \mu_{il})^2\}(\alpha p_{lk} + \beta m_{it,k} + \gamma m_{t,k})^{\xi_{l,it}\xi_{k,it-1}}\} \tag{B.4}$$

with respect to the transformed parameters, after applying the chain rule are

$$\begin{aligned}\frac{\partial L}{\partial \tilde{\alpha}} =& \frac{\partial L}{\partial \alpha}\frac{d\alpha}{d\tilde{\alpha}} \\ =& \alpha(1-\alpha)\sum_{i=1}^{N}\sum_{t=1}^{T}\sum_{l=1}^{K}\sum_{k=1}^{K}\mathbb{I}_{\{l\}}(S_{it})\mathbb{I}_{\{k\}}(S_{it-1})\frac{p_{lk}}{\alpha p_{lk}+\beta m_{it,k}+\gamma m_{t,k}} \\ =& \alpha(1-\alpha)\sum_{i=1}^{N}\sum_{t=1}^{T}\sum_{l=1}^{K}\sum_{k=1}^{K}\mathbb{I}_{\{l\}}(S_{it})\mathbb{I}_{\{k\}}(S_{it-1})\mathbf{A}\end{aligned} \tag{B.5}$$

$$\begin{aligned}\frac{\partial L}{\partial \tilde{\beta}} =& \frac{\partial L}{\partial \beta}\frac{d\beta}{d\tilde{\beta}} \\ =& \beta(1-\beta)\sum_{i=1}^{N}\sum_{t=1}^{T}\sum_{l=1}^{K}\sum_{k=1}^{K}\mathbb{I}_{\{l\}}(S_{it})\mathbb{I}_{\{k\}}(S_{it-1})\frac{m_{it,k}}{\alpha p_{lk}+\beta m_{it,k}+\gamma m_{t,k}} \\ =& \beta(1-\beta)\sum_{i=1}^{N}\sum_{t=1}^{T}\sum_{l=1}^{K}\sum_{k=1}^{K}\mathbb{I}_{\{l\}}(S_{it})\mathbb{I}_{\{k\}}(S_{it-1})\mathbf{B}\end{aligned} \tag{B.6}$$

$$\begin{aligned}\frac{\partial L}{\partial \tilde{\gamma}} =& \frac{\partial L}{\partial \gamma}\frac{d\gamma}{d\tilde{\gamma}} \\ =& \gamma(1-\gamma)\sum_{i=1}^{N}\sum_{t=1}^{T}\sum_{l=1}^{K}\sum_{k=1}^{K}\mathbb{I}_{\{l\}}(S_{it})\mathbb{I}_{\{k\}}(S_{it-1})\frac{m_{t,k}}{\alpha p_{lk}+\beta m_{it,k}+\gamma m_{t,k}} \\ =& \gamma(1-\gamma)\sum_{i=1}^{N}\sum_{t=1}^{T}\sum_{l=1}^{K}\sum_{k=1}^{K}\mathbb{I}_{\{l\}}(S_{it})\mathbb{I}_{\{k\}}(S_{it-1})\mathbf{C}\end{aligned} \tag{B.7}$$

$$\begin{aligned}\frac{\partial L}{\partial \tilde{p_{lk}}} =& \frac{\partial L}{\partial p_{lk}}\frac{dp_{lk}}{d\tilde{p_{lk}}} \\ =& p_{lk}(1-p_{lk})\sum_{i=1}^{N}\sum_{t=1}^{T}\mathbb{I}_{\{l\}}(S_{it})\mathbb{I}_{\{k\}}(S_{it-1})\frac{\alpha}{\alpha p_{lk}+\beta m_{it,k}+\gamma m_{t,k}} \\ =& p_{lk}(1-p_{lk})\sum_{i=1}^{N}\sum_{t=1}^{T}\mathbb{I}_{\{l\}}(S_{it})\mathbb{I}_{\{k\}}(S_{it-1})\mathbf{D}\end{aligned} \tag{B.8}$$

For ease of presentation we defined

$$\mathbf{A} = \frac{p_{lk}}{\alpha p_{lk} + \beta m_{it,k} + \gamma m_{t,k}}$$

$$\mathbf{B} = \frac{m_{it,k}}{\alpha p_{lk} + \beta m_{it,k} + \gamma m_{t,k}}$$

$$\mathbf{C} = \frac{m_{t,k}}{\alpha p_{lk} + \beta m_{it,k} + \gamma m_{t,k}}$$

$$\mathbf{D} = \frac{\alpha}{\alpha p_{lk} + \beta m_{it,k} + \gamma m_{t,k}}$$

State	μ_{i1}	Bayesian CI	μ_{i2}	Bayesian CI	σ_{i1}	Bayesian CI	σ_{i2}	Bayesian CI
Alabama	-0.153	(-0.191, -0.115)	0.345	(0.330, 0.360)	0.247	(0.228, 0.266)	0.147	(0.140, 0.154)
Alaska	-1.032	(-1.125, -0.942)	0.234	(0.201, 0.266)	0.260	(0.210, 0.317)	0.367	(0.350, 0.383)
Arizona	-0.067	(-0.115, -0.016)	0.629	(0.600, 0.659)	0.356	(0.333, 0.380)	0.235	(0.221, 0.250)
Arkansas	-0.068	(-0.095, -0.040)	0.356	(0.342, 0.371)	0.187	(0.173, 0.201)	0.134	(0.127, 0.140)
California	0.002	(-0.024, 0.027)	0.380	(0.369, 0.391)	0.184	(0.172, 0.197)	0.095	(0.090, 0.101)
Colorado	-0.095	(-0.134, -0.055)	0.425	(0.410, 0.442)	0.230	(0.213, 0.248)	0.143	(0.135, 0.151)
Connecticut	-0.111	(-0.139, -0.083)	0.349	(0.333, 0.367)	0.182	(0.170, 0.196)	0.150	(0.142, 0.159)
Delaware	-0.084	(-0.113, -0.051)	0.409	(0.390, 0.429)	0.221	(0.206, 0.237)	0.176	(0.167, 0.186)
Florida	-0.001	(-0.057, 0.059)	0.425	(0.413, 0.438)	0.396	(0.367, 0.426)	0.116	(0.110, 0.123)
Georgia	-0.108	(-0.150, -0.067)	0.453	(0.432, 0.474)	0.263	(0.244, 0.284)	0.196	(0.186, 0.207)
Hawaii	-0.072	(-0.101, -0.044)	0.416	(0.386, 0.443)	0.211	(0.199, 0.223)	0.163	(0.150, 0.177)
Idaho	-0.216	(-0.290, -0.152)	0.526	(0.507, 0.543)	0.410	(0.381, 0.442)	0.144	(0.135, 0.155)
Illinois	-0.230	(-0.267, -0.193)	0.334	(0.316, 0.350)	0.251	(0.232, 0.271)	0.149	(0.141, 0.157)
Indiana	-0.410	(-0.477, -0.346)	0.359	(0.338, 0.379)	0.414	(0.380, 0.449)	0.193	(0.184, 0.203)
Iowa	-0.199	(-0.244, -0.153)	0.331	(0.314, 0.346)	0.295	(0.274, 0.316)	0.150	(0.142, 0.158)
Kansas	-0.280	(-0.347, -0.208)	0.306	(0.283, 0.329)	0.303	(0.274, 0.332)	0.198	(0.187, 0.209)
Kentucky	-0.255	(-0.303, -0.209)	0.344	(0.325, 0.361)	0.303	(0.280, 0.329)	0.174	(0.165, 0.183)
Louisiana	-0.483	(-0.585, -0.387)	0.280	(0.249, 0.308)	0.373	(0.336, 0.411)	0.235	(0.220, 0.251)
Maine	-0.209	(-0.255, -0.162)	0.509	(0.475, 0.544)	0.373	(0.351, 0.396)	0.293	(0.275, 0.313)
Maryland	-0.160	(-0.198, -0.123)	0.378	(0.356, 0.399)	0.223	(0.204, 0.241)	0.191	(0.180, 0.201)
Massachusetts	-0.158	(-0.196, -0.119)	0.379	(0.360, 0.398)	0.224	(0.206, 0.241)	0.171	(0.162, 0.182)
Michigan	-0.651	(-0.762, -0.539)	0.427	(0.392, 0.462)	0.714	(0.661, 0.772)	0.346	(0.327, 0.366)
Minnesota	-0.048	(-0.076, -0.018)	0.359	(0.346, 0.373)	0.204	(0.189, 0.220)	0.127	(0.120, 0.134)
Mississippi	-0.223	(-0.261, -0.190)	0.352	(0.330, 0.374)	0.209	(0.194, 0.225)	0.191	(0.181, 0.202)
Missouri	-0.171	(-0.205, -0.138)	0.325	(0.307, 0.343)	0.216	(0.201, 0.232)	0.160	(0.151, 0.168)
Montana	-0.373	(-0.421, -0.319)	0.378	(0.356, 0.401)	0.338	(0.314, 0.365)	0.212	(0.201, 0.224)
Nebraska	-0.085	(-0.118, -0.054)	0.335	(0.320, 0.350)	0.198	(0.183, 0.214)	0.140	(0.133, 0.147)
Nevada	-0.294	(-0.372, -0.211)	0.634	(0.611, 0.656)	0.515	(0.474, 0.553)	0.204	(0.193, 0.216)
New Hampshire	-0.079	(-0.132 , -0.028)	0.484	(0.460 , 0.508)	0.277	(0.256 , 0.299)	0.205	(0.194 , 0.218)
New Jersey	-0.093	(-0.123 , -0.064)	0.347	(0.331 , 0.365)	0.216	(0.200 , 0.232)	0.156	(0.147 , 0.164)
New Mexico	-0.083	(-0.140 , -0.018)	0.351	(0.333 , 0.371)	0.243	(0.221 , 0.265)	0.155	(0.147 , 0.163)
New York	-0.100	(-0.131 , -0.069)	0.270	(0.259 , 0.281)	0.186	(0.172 , 0.201)	0.100	(0.095 , 0.106)
North Carolina	-0.122	(-0.159 , -0.084)	0.421	(0.406 , 0.437)	0.250	(0.232 , 0.271)	0.145	(0.137 , 0.153)
North Dakota	-0.040	(-0.066 , -0.015)	0.291	(0.278 , 0.303)	0.148	(0.137 , 0.161)	0.119	(0.114 , 0.126)
Ohio	-0.376	(-0.491 , -0.265)	0.297	(0.275 , 0.319)	0.688	(0.634 , 0.749)	0.206	(0.196 , 0.217)
Oklahoma	-0.352	(-0.404 , -0.300)	0.308	(0.286 , 0.329)	0.291	(0.265 , 0.319)	0.213	(0.202 , 0.225)
Oregon	-0.188	(-0.272 , -0.107)	0.536	(0.510 , 0.561)	0.465	(0.432 , 0.503)	0.146	(0.130 , 0.162)
Pennsylvania	-0.166	(-0.204 , -0.130)	0.304	(0.288 , 0.320	0.248	(0.230 , 0.266)	0.149	(0.140 , 0.158
Rhode Island	-0.368	(-0.422 , -0.312)	0.356	(0.333 , 0.382)	0.308	0.282 , 0.336)	0.225	(0.212 , 0.236)
South Carolina	-0.219	(-0.263 , -0.171)	0.417	(0.396 , 0.438)	0.293	(0.270 , 0.315)	0.202	(0.192 , 0.213)
South Dakota	-0.060	(-0.090 , -0.027)	0.382	(0.367 , 0.396)	0.197	(0.181 , 0.213)	0.135	(0.128 , 0.142)
Tennessee	-0.123	(-0.177 , -0.074)	0.362	(0.345 0.379)	0.243	(0.222 , 0.264)	0.137	(0.128 0.145)
Texas	-0.111	(-0.147 , -0.073)	0.406	(0.392 , 0.420)	0.216	(0.198 , 0.234)	0.134	(0.127 , 0.141)
Utah	0.001	(-0.030 , 0.032)	0.466	(0.453 , 0.480)	0.230	(0.214 , 0.245)	0.126	(0.119 , 0.133)
Vermont	-0.146	(-0.195 , -0.095)	0.481	(0.452 , 0.510)	0.335	(0.312 , 0.358)	0.243	(0.229 , 0.258)
Virginia	-0.081	(-0.106 , -0.054)	0.410	(0.394 , 0.426)	0.176	(0.163 , 0.191)	0.146	(0.137 , 0.154)
Washington	-0.132	(-0.171 , -0.092)	0.355	(0.341 , 0.370)	0.224	(0.205 , 0.243)	0.137	(0.130 , 0.144)
West Virginia	-0.186	(-0.231 , -0.139)	0.336	(0.320 , 0.353)	0.290	(0.267 , 0.314)	0.150	(0.143 , 0.158)
Wisconsin	-0.680	(-0.885 , -0.474)	0.396	(0.361 , 0.432)	1.100	(0.998 , 1.201)	0.325	(0.303 , 0.347)
Wyoming	-0.770	(-1.004 , -0.532)	0.366	(0.344 , 0.386)	0.989	(0.878 , 1.108)	0.213	(0.199 , 0.226)

Table B.1: PMS-IC estimations coefficient for the US-States coincident indices.

Chapter 3

Macroeconomic Impacts of the Ebola Epidemic

3.1 Introduction and context

The Ebola Virus Disease (EVD) epidemic ravaged Guinea, Liberia and Sierra Leone (GLS) in 2014-15 with catastrophic humanitarian consequences. More than 27800 people have been infected by the virus over the two years since the appearance of the virus[1]. Fatalities now stand at over 11200 people in these three countries. Notable features of the disease include its high lethality, responsible for the panic in the countries affected and abroad, and the persistence [2] of the outbreak as illustrated by its resurgence in Liberia the 29th June 2015, which was declared Ebola-free the 9th May 2015.

The outbreak is estimated to have weakened growth, and increased domestic and external imbalances, inflation, and poverty. Possible channels include lower labor force partici-

[1] According to the World Health Organization (WHO), on December 26 2013, a 2-year-old boy in the remote Guinean village of Meliandou (at the border with Liberia and Sierra Leone) fell ill with a mysterious illness characterized by fever, black stools, and vomiting. He died 2 days later. The WHO later identified that child as West Africa's first case of Ebola virus disease. The circumstances surrounding his illness were ominous.

[2] While the basic reproduction number of the Ebola disease (the number of cases one case generates on average over the course of its infectious period estimated between 1.5 and 2.5 for the Ebola disease) is smaller than that of other well-known infectious diseases (2-5 for SARS and 12-18 for Measles), the lack of an effective vaccine made controlling its spread extremely difficult once it reached densely populated zones.

pation, productivity losses in affected communities and, more importantly, consumers and investors aversion behavior that impacted adversely trade and services. Estimating the economic impact of the outbreak is however difficult, because of the lack of comprehensive data linked to weak statistical capabilities, the difficulties in establishing an appropriate counterfactual giving the many other shocks facing the countries, the difficulties in identifying the behavioral effects, and the lack of parallels to draw from. Nonetheless, many expect the Ebola outbreak to have more profound repercussions on output potential and growth than previous pandemics (e.g., the 2002-04 SARS pandemic), which affected countries with strong public institutions and had modest growth effects.

The paper explores the economic impacts of the Ebola outbreak in GLS, after controlling for the policy responses to curtail its adverse macroeconomic consequences. The next section surveys the literature on the economic impact of public health catastrophes. Section III reviews stylized facts about EVD in GLS, and discusses the policy responses. The channels through which the disease affects economic performance are analysed in Section IV. Section V presents the empirical used for the estimation of a production function. The section also does a growth accounting exercise and assesses the impact of EVD separately via the channel of capital accumulation and total factor productivity. Section VI uses a scenario analysis to quantify the impact of EVD. It also uses a VAR approach to conduct scenario analysis over the horizon 2014-2018.

3.2 Literature Review

One of the by-products of the endogenous growth models popularized by Lucas (1988) is a myriad of work focused on capturing the role of human capital in economic outcomes. Several works have subsequently built on the notion that health, as part of human capital, is both an input as well as an outcome of economic development. Some pioneering works

by Pritchett and Summers (1996), Bloom et al. (1998) and many subsequent models have shown that health quality impacts on economic growth directly and indirectly and that population health, as measured by life expectancy, infant and child mortality and maternal mortality are positively related to economic growth. For the same reason, it is argued that poor health is costly for economic growth. Direct costs could come through the cost of medical care and the impact of mortality and morbidity on future incomes. Indirect costs include lost time and income of care givers during the care giving stage.

These models were however not designed to capture the impact on growth of diseases that reach epidemic or pandemic proportions. Epidemics and pandemics manifest differently from health or lifestyle diseases because they are often widespread, have high transmission rates and high fatality rates. Unlike personal health issues, they challenge public health policy and provision. In the 21st century, various countries have witnessed pandemics like HIV-AIDS, SARS, H1N1 influenza, Foot and Mouth disease, and Ebola Virus Disease (EVD). Because of the specific characteristics of epidemics, earlier models do not capture wider economic consequences from the diseases.

Quantification of the economic impact of widespread diseases is most systematically presented in the analysis of the macroeconomic impact of HIVAIDS in Sub Saharan Africa. Data on infection rates generated from epidemiological models are used in Solow-type growth models to develop scenarios of the impact of different levels of infection rates on labor force participation rate, efficiency of labor and capital accumulation (Over (1992), Cuddington (993a,b); Cuddington and Hancock (1995) , Haacker (2002), etc.). Some other models, based on computable general equilibrium were used in Arndt and Lewis (2001), and Bell et al. (2004), laid out the long-term costs of HIV/AIDS, and the vast scale on which social and economic effects are likely to be felt (because of decreased investment in human capital).

Available estimates of the impact of disease on economic growth are significant. Estimates by studies focused on Southern African countries (Haacker (2002), MacFarlan and Sgherri (2001)) suggest that HIV/AIDS reduces the rate of GDP growth by between 0.5 percent and 2.6 percent per annum. Estimates of the impact of pandemics on advanced and emerging market economies are also large, with Economic Round-up (2003) estimating East Asia's 2013 GDP loss from SARS at 0.5-1 percent, while Lee and McKibbin (2004) place the loss to Hong-Kong's economy at around 5.5 percent of GDP. The foot and mouth livestock disease -another widespread disease in advanced economies- is estimated by the European Association of Animal Production to have caused fewer than 200 deaths but cost at least $110 billion in 1996 (1 percent of the GDP of the 15 European Union states).

There are important differences between Low Income Countries (LICs) and advanced economies in the channels of transmission of the impact of pandemic diseases to the economy. Studies of pandemics in LICs found that the result of high prevalence rates is declining productivity, and lower human capital because of the increases in the death rate among the most economically active members of the population. The impact of pandemics in advanced and emerging economies seem to be manifested through large reductions in consumption, higher operating costs, and because of these countries' integration to the global economy, an increase in country risk premium which affects foreign direct investment flows. For example the 2003 Asian SARS outbreak claimed fewer than a thousand people but deterred investors and tourists. Lee and McKibbin (2004) found that the bulk of the loss (US$30bn to US$100bn) fell on Hong KongâĂŹs tourism and travel sectors, while foreign direct investment (FDI) fell by 62 percent in one quarter at the height of the crisis.

Pandemics differ also according to the durability of their economic effects. The impact of SARS appears to be contemporaneous or immediate (Hai et al. (2004),Beutels et al. (2009)), while HIV/AIDS has both medium term and long-term impact (Dixon et al.

(2001), Bell et al. (2004)). While this difference reflects in part the nature of the disease, another part is explained by the quality of health facilities and their ability to identify early on appropriate cures to stem the disease. In that regard strong external financing support, from both private and multilateral organizations helped many countries reduce the direct fiscal cost of public health programs, thereby moderating the impact through the capital accumulation channel (Masha (2004)).

If pandemic diseases have strong impact on economic growth, a key question is the extent to which country's factor endowment, and factor contribution to economic growth influence the severity of the outcome. While no research has undertaken such a comparison, a number of works have analysed the determinants of economic growth in the region, in a growth accounting framework. Tahari et al. (2004), estimated a Cobb-Douglass type production function in which the share of capital is assumed to be 0.4 [3] [4]. The study concluded that average real GDP growth in the region during 1960-2002 was driven primarily by factor accumulation with little or no role for total factor productivity, TFP. In another scenario based on different periods, and different sub-regional groups, the study found that some pick up in TFP growth was observed during 1997-2002, relative to 1990-96, namely in countries whose IMF-supported programs were adjudged to be on track, were part of the group of CFA franc zone, and were in the middle-income category.

A key weakness relates to the interpretation that the measured residual from the growth accounting exercise represents TFP growth. The regression results for GLS were in line with this conclusion, as it shows that TFP played a minor role in growth outcomes during

[3] This is in line with the literature on production functions for development countries. See Bosworth et al. (1995) for empirical support for this value.

[4] Other key assumptions of Tahari et al. (2004) are: population growth as a proxy for the labor force due to the paucity of employment data; capital stock series constructed using the perpetual inventory accumulation method ; depreciation assumed to be constant at 6 percent a year; and a capital-output ratio of 1.5 in 1980.

the period. Going by the experience of GLS, another possible interpretation is that the low/ negative TPF is explained by negative factors, including political disturbances and conflicts, institutional changes, external shocks, changes in government policies, and measurement errors due to paucity of data.

	2014	2015
Guinea	-1.44	-1.60
Liberia	-2.28	-0.84
Sierra Leone	-0.71	-1.29

The foregoing review of literature shows that epidemics manifest differently in different economic situations. While they could occur in different environments, their propagation depends crucially on the soundness of public health systems. Pandemics could be short term or endemic, and they can also have long-term economic consequences. Low income countries are particularly disposed to epidemics because most of the diseases are communicable diseases that are most likely to arise and persist under conditions commonly created by poverty. Nonetheless, there is no conclusive view on the economic impact. Even where an epidemics caused many deaths, it could happen suddenly and die out quickly, with the possible consequence that the economic dislocations that arise from morbidity, treatment, and higher fiscal cost did not last long enough to adversely impact growth. It is however also possible, that only in cases where epidemics are sustained over a long time period the effects could it create adverse macroeconomic consequences. In the next section, first, we examine the initial evidence on the impact of EVD epidemic to GLS countries.

3.3 Pre-Ebola economic prospects and policy responses

Guinea, Liberia and Sierra Leone were at different stages of the business cycle coming into the crisis: whereas in Guinea and Liberia the cycle had matured and was entering a

decelerating phase, output in Sierra Leone was expanding at historically high rates on the back of the commencement of iron ore mining and introduction of crude oil prospecting.

3.3.1 GLS Pre-Ebola economic environment and outlook

GLS countries belong to the lowest ranking countries on the UN Human Development Index, with dismal access to basic social services. All three countries are fragile, endowed with large mineral resources and an important agricultural potential. However these countries differ in their exchange rate regimes, and their policy frameworks[5]. Moreover, Sierra Leone and Liberia are heavily reliant on iron-ore mining for exports, while Guinea has a more diversified mining export base, which includes bauxite, gold and diamonds.

Data as of end-2013 show that the macroeconomic situation in GLS started to deteriorate before the Ebola outbreak. In Guinea, lagging structural reforms, energy shortages, political tensions and uncertainty in the run-up to the 2013 legislative elections added to the adverse economic effects of the slowdown in new mining investments. In Liberia, the weakening of macroeconomic conditions was even more evident. Mining activity and exports were declining in line with global prices, inflation was on an upward trend, and the exchange rate was depreciating at a fast rate. Difficulties in mobilizing revenue and external budget support were translating into fiscal policy slippages. Sierra Leone was the only country that went into the Ebola epidemic on an upswing in growth conditions. On account of new iron ore production coming on stream and strong growth in agriculture and services, economic output expanded by 20 percent in 2013. Against the backdrop of a good agricultural supply, the revenue-based fiscal consolidation and tight monetary policy stance helped reduce inflation to single digit levels in 2014 for the first time in nearly a decade.

[5] Stabilized regime in Guinea, dual currency arrangement in Liberia and floating in Sierra Leone.

Near and medium term outlook for the countries appeared risky, even before the outbreak of EVD. Given the slowdown in global demand conditions, it was apparent that macroeconomic conditions would weaken in the near and medium term. For Guinea, the overheated political environment was a major source of risk, and institutional weaknesses also imply that implementation of reforms would remain weak up to the end-2015 presidential elections. For Liberia and Sierra Leone, the near term outlook was already clouded by lower global iron prices. In the case of Sierra Leone, increased pressures from a higher public sector wage bill and a low revenue base also clouded the outlook.

3.3.2 Policy Response to EVD and Macroeconomic Outcome

To fight the outbreak and stem its economic consequences, all three countries adjusted their economic policies in the context of IMF-supported programs. Policies were loosened to allow more Ebola-related spending and provide countercyclical economic support to the private businesses and households, given the weak automatic stabilizers.

- **Fiscal policy** became accommodative across the board, allowing countries to incur higher Ebola-related expenditure in the midst of revenue shortfalls. In Liberia, revenue losses due to the Ebola amounted to -2.5 percent of GDP, in 2014, while Ebola related-spending rise to 4.1 percent of GDP (Text Table 3.1), and the change in fiscal deficit increased to -1.6 percent of GDP in 2014 and to -0.7 percent of GDP in 2015 (Figure 3.1).

- **Monetary policy** was also loosened in all countries. In Guinea, the reserve requirement was reduced in order to increase bank's liquid assets and channel sufficient liquidity for the government to finance the increased budget deficit. Financial sector credit to the government (including from the central bank) rose to 12 percent of

Table 3.1: Selected economic indicator

	Liberia			Sierra Leone		
PRE-EBOLA PROJECTION						
	2013	**2014**	**2015**	**2013**	**2014**	**2015**
revenue (percent of GDP)[1]	23.5	22.3	22.8	12.7	12.8	13.6
spending (percent of GDP)[1,2,3]	29.1	32	30.9	17.6	20.7	20.4
Ebola related spending[1,2,3]	n.a.	n.a.	n.a.	0	0	0
exchange rate	77.4	85.9	92.5	4334	-	-
inflation	7.6	8.3	7.7	9.8	7.8	6.7
CURRENT PROJECTION						
revenue (percent of GDP)[1]	23.5	22.5	22.5	12.7	11.1	9.6
spending (percent of GDP)[1,2,3]	29.1	39.3	37.7	17.6	20.1	18.8
Ebola related spending[1,2,3]	n.a.	4.1	n.a.	0	0.7	0.2
exchange rate	77.4	84.8	84.9	4334	4334	4953
inflation	7.6	9.9	7.7	9.8	8.3	10.2
IMPACT OF EBOLA (PERCENT OF GDP)						
revenue loss due to Ebola[4]	…	-2.5	-4.1	…	-1	-2
spending rise due to Ebola[4]	…	2.6	0.4	…	0	1.2

Note: There might be other factors than Ebola explaining the change in macroeconomic projections

[1] Fiscal year. 2013 refers to July 2013 to June 2014.

[2] Including off-budget revenue and expenditure.

[3] Cash base.

[4] Denominator is "pre-Ebola" GDP.

Source: IMF Staff calculations

GDP, from 0 percent previously. Despite the looser policy mix, inflation remained on a downward path, reflecting a high level of economic slack.

- **Exchange rate policy** was governed by reserves buffers. In Guinea and Sierra Leone, the central banks maintained a high level of interventions to slow the depreciation of the exchange rate and keep inflation low. In Liberia, the central bank lowered the foreign exchange injections in the market to preserve international reserve buffers.

- **Financial sector policy** was also supportive. As the economy weakened, banks' balance sheet deteriorated. In Liberia and Guinea, regulatory forbearance and one-off direct economic interventions in the financial system helped support credit to the private sector. In Sierra Leone, the central bank put two banks in administration, as their financial conditions deteriorated.

FIGURE3.1: Projections and estimates of selected economic indicators in GLS.

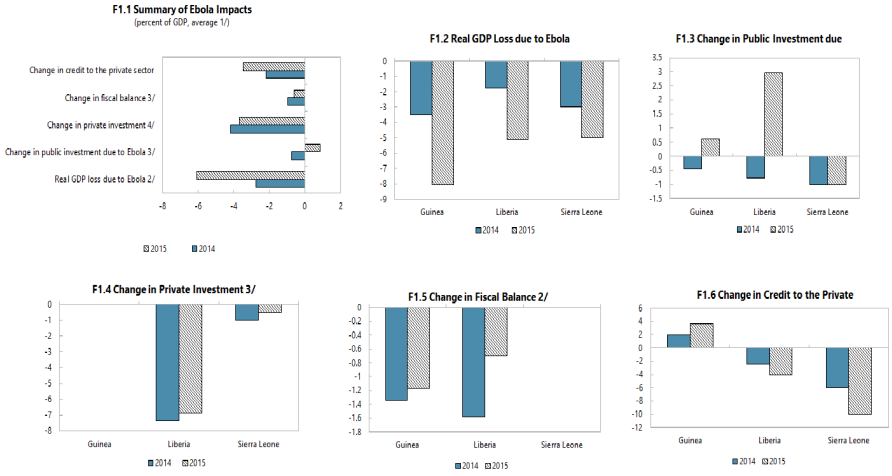

Source: Country authorities and IMF staff calculations. 1/ For Guinea, pre-Ebola data refer to the ECF Third Review for Guinea (Feb. 2014). 2/ For Liberia, the fiscal year covers July through June; e.g. 2013 refers to July 2013 to June 2014. 3/ For Liberia, refers to foreign direct investment. 4/ Real output loss due to Ebola as a % of real pre-Ebola GDP.

External support was instrumental to the implementation of these policy responses. Traditional donors, development partners and private foundations and individuals provided direct and indirect financial support. According to data available at the UN Office for the Coordination of Humanitarian Assistance website, total donor commitments to Ebola from April 2014 amounted to US$4.2 billion, out of which only US$0.7 billion was outstanding as of October 2015[6]. The IMF catalyzed donor support by providing 390 million in financial assistance to the three countries, including in the form of budget support and debt relief.

Notwithstanding the policy response economic growth fell precipitously in all three countries as a result of the Ebola impact, but also because of deteriorating external developments. Economic growth in Guinea is estimated to have fallen from 2.3 percent in 2013, to 1.1 percent in 2014 and zero in 2015. Despite looser policies, inflation in Guinea

[6] `https://fts.unocha.org/pageloader.aspx?page=emerg-emergencies&section=CE&Year=2014`

remained on a downward path, reflecting a high level of economic slack. Output growth in Sierra Leone fell from 20 percent in 2013 to 7 percent in 2014, and -23 percent in 2015. In Liberia output fell 8.7 percentage points to 0.7 percent in 2014 and 0.9 in 2015, while inflation rose by 7.6 basis points to 9.9 in 2014.

3.4 The Ebola epidemic and channels of its economic impact

As of December 31 2015, 28637 cases of Ebola infections were recorded in the three countries affected and 11315 deaths.

The epidemic adversely affected production factors, including labor and human and physical capital. Surveys conducted by the World Bank[7] provides insights into the impacts stemming from lower labor force participation and a lower quality of the labor force because of lower access to health and education services. As there was no systematic assessment of the impact of the Ebola outbreak on physical capital, the revisions to the investment projections provide some hints.

The World Bank surveys for Liberia and Sierra Leone suggest Ebola has cut employment, with a disproportionate impact on household enterprises[8]. In Liberia, about 40 percent of employed persons before the outbreak declare they are unemployed[9]. In Sierra Leone, employment fell from 83 percent in mid-2014 to around 78 percent by end-2014, before returning to pre-Ebola levels by mid-2015. Despite the return to work, hours worked among the employed fell from 47 hours per week in July 2014 to 42 hours in May 2015[10].

[7] The socio-economic impacts of Ebola in Liberia, Guinea, and Sierra Leone, 2014-15.

[8] Estimating Ebola-related changes in labor utilization is difficult given the paucity of labor force data prior to the epidemic, the presence of seasonal movements and the selection bias involved with cell-phones survey in which better-off households are overrepresented.

[9] The baseline for Liberia is comprised of those working at the time of the Liberian Household Income and Expenditure (HIES, January-August 2014).

[10] The baseline for Sierra Leone is the first national Sierra Leone Labor Force Survey (July-August 2014) and the Sierra Leone Demographic and Health Survey 2013).

Urban areas were worse off, with the sharpest crisis-period employment declines and slowest recoveries, particularly amongst non-farm/non-wage households (1/3 of the labor force). In Sierra Leone, non-farm enterprise failure rates more than quadrupled in the second half of 2014, household enterprise turnover fell by 2/3 by May 2015 and wages fell by Âij from mid-2014 to May 2015[11].

FIGURE3.2: Employment rates of household heads in Sierra Leone and Liberia

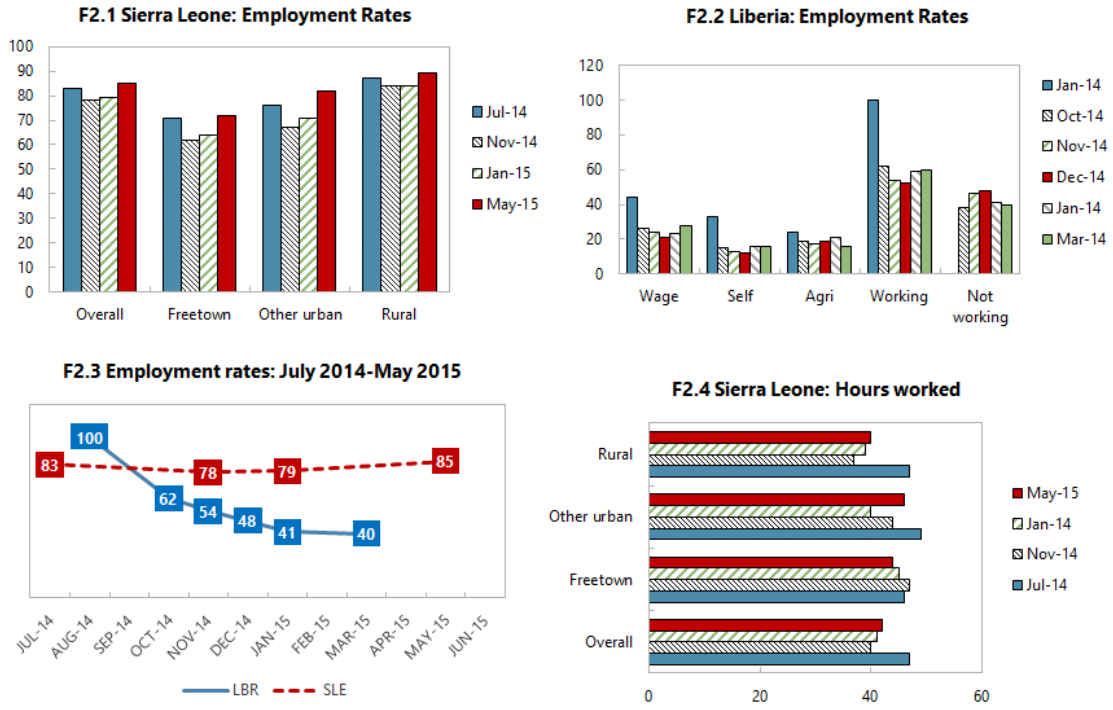

Source: Sierra Leone Labor Force Survey (LFS, July-August 2014), Liberia Household Income and Expenditure Survey (HIES, February-August 2014) and cell phone surveys round 1 (November 2014), round 2 (January-February 2015) and round 3 (May 2015).

The health sector in GLS, which were critically unprepared to deal with a crisis on the

[11] Wage labor represents 6 percent of labor according to the Labor Force Survey. The decline may be explained by layoffs in the mining sector, although direct mine employment accounts for 7 percent of wage labor.

scale of the Ebola epidemic, suffered massively (Table 3.2). With an infection rate in the health sector 32 times higher than in the general population, about 800 health workers were infected, of which 500 died. This exacerbated the pre-existing shortage of health care workers[12], and triggered a decline in the use of non-Ebola related health services and a worsening of health outcomes. In Sierra Leone, in-patient log books in the weeks following the onset of the epidemic show about 70 percent decline in admissions rates.

Table 3.2: EVD cases and physician density in GLS (up to 2-Aug-2015)

	Number of cases		**Number of deaths**		**Physicians (2010)**		
	Total	Health care workers **	Total	Health care workers **	Density per 1000	Total	Pop in 2014
Guinea	**3784**	**195**	**2522**	**97**	**0.1**	**1088**	**12043898**
Liberia	**10672**	**378**	**4808**	**192**	**0.014**	**56**	**4396873**
Sierra Leone	**13406**	**307***	**3951**	**221***	**0.022**	**127**	**6205382**

*Data as of 17 February 2015, **Data are until July 2015

Source: World Health Organization and World Development Indicators

School shutdowns ranged from 4.5-7.5 months (Table 3.3) leading to the loss of between 60-80 percent of the academic year[13], delaying instruction and graduation, possibly higher repeat rates, with some evidence pointing to a likely rise in dropouts. Schools were closed after the July/August 2014 resurgence in all three countries, encompassing 25,000 institutions and 4.8 million students. Schools reopened in 2015 as the epidemic subsided, beginning in Guinea in mid-January, followed by Liberia in mid-February, and Sierra Leone

[12] http://apps.who.int/iris/bitstream/10665/171823/1/WHO_EVD_SDS_REPORT_2015.1_eng.pdf?ua=1&ua=1

[13] This is in percent of the full academic year.

in mid-April. Following reopening of schools, in Sierra Leone, 87 percent of households with at least one school-aged report all children are attending. In Liberia, there appears to have been a reduction in school attendance by older children. Respondents indicate that 73 percent of 12+ children attending school last year returned this year, with 80 percent of those households citing a lack of money as the reason, and 14 percent indicating fear of Ebola. Cost constraints may be a more significant consideration for older children as fees are higher.

Table 3.3: Education in GLS

	School year		School stoppage			Academic year	Lost time			Out of school pre-Ebola	
	Start	End	Start	End	Months	Months	(% of academic year)	Schools	Students ('000)	% ages 6-11	% ages 12-17
Guinea	October	June	Oct-14	Jan-15	4.5	8	0.56	12000	2258	46	52
Liberia	September	June	Sep-15	Feb-15	5.5	9	0.61	5181	913	65	25
Sierra Leone	September	July	Sep-15	Apr-15	7.5	10	0.75	8100	1599	21	29
Total					*5.8*		*0.64*	*25281*	*4770*		

Source: UNICEF Guinea, UNICEF Liberia, UNICEF Sierra Leone

Through its impacts on labor, and human and physical capital, the epidemic affected severely economic growth. We need a table comparing the pre- and post-Ebola growth projections by sector. Services and trade were the most affected sectors, after the mining sector[14]. The aversion of tourists to public health concerns, coupled with suspension of many flights to the GLS contributed to a marked decline in tourism and tourism receipts. Figure 5 shows a clear loss in 2014 for Guinean and Sierra Leone tourism, where the decline in international tourist arrivals averaged 46 percent. In Sierra Leone, spending by international visitors on accommodation, food and drink, entertainment, shopping and other goods and services fell from US$ millions 66 in 2013 to US$ 32 million, a decrease of

[14] However, given the concomitant commodity price shock, it is difficult to identify the shock responsible for the decline in mining production.

60 percent in real terms.

FIGURE3.3: Tourism in Guinea and Sierra Leone

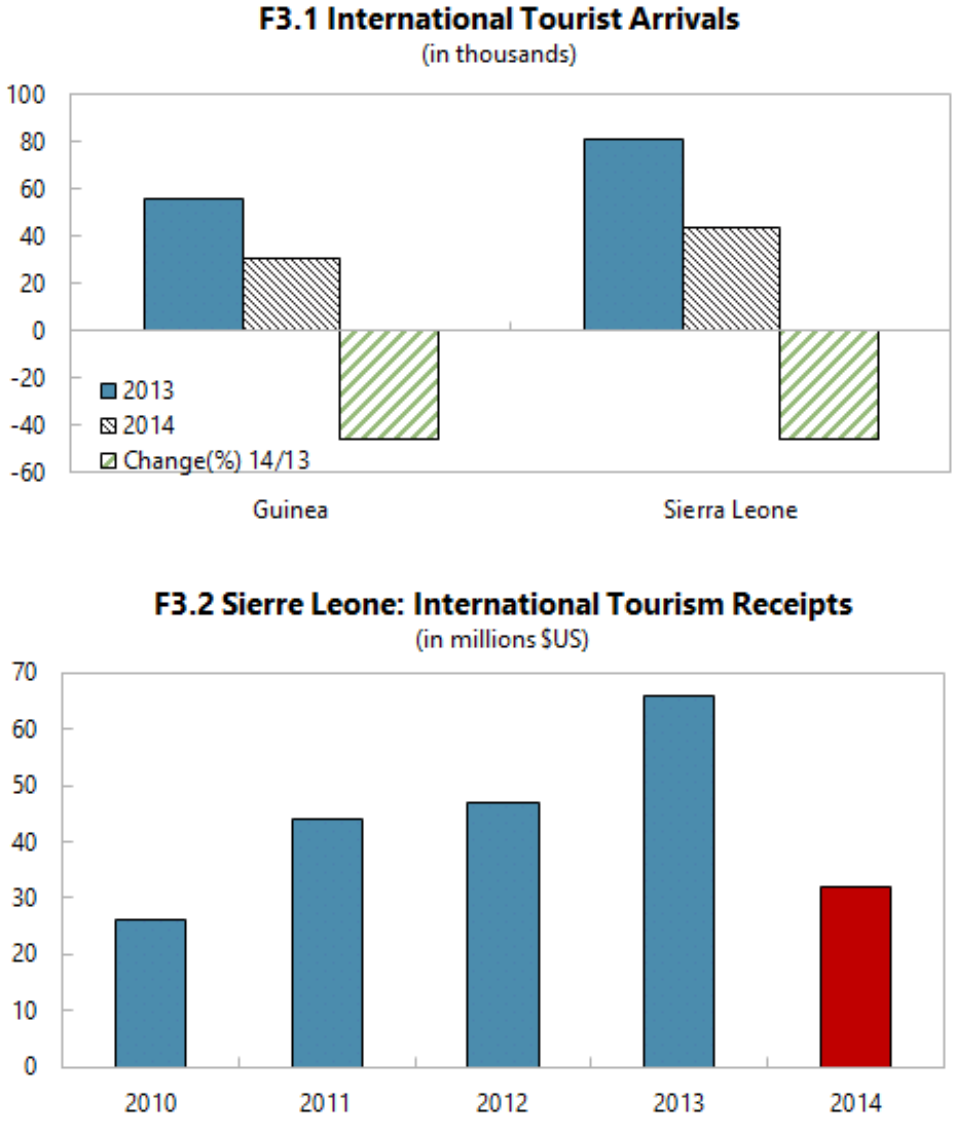

Source: World Tourism Organization, Ministry of Tourism of Guinea and Authors' calculations

3.5 Empirical methodology, estimation and results

We use panel data from 44 Sub-Saharan African countries in a Solow growth model to obtain robust estimates of these factors' contribution to GDP growth.

3.5.1 The Solow growth model

The theoretical framework for the exercise is based on a Cobb-Douglas-type function with constant return to scale which specifies output as a function of capital, labor, and total factor productivity:

$$Y_{it} = A_{it} K_{it}^{\alpha} L_{it}^{(1-\alpha)} \tag{3.1}$$

In equation (3.1), Y_{it} is the aggregate output, K_{it} is the stock of capital, L_{it} represents the labor force, A_{it} is the Solow residual. Factors shares are denoted by α, share of capital stock and $1-\alpha$, share of labor force, where $0 < \alpha < 1$. The Solow residual is multiplicatively related to both capital and labor, embodying both factor productivity and exogenous shocks. Taking the first difference of logs, Equation (3.1) can be rewritten as:

$$\widehat{y}_{it} = \alpha \widehat{k}_{it} + (1-\alpha)\widehat{l}_{it} + \widehat{a}_{it} \tag{3.2}$$

Thus, Equation (3.2) means that the growth rate of output depends on the growth rate of the capital stock, the growth rate of labor force and the growth rate of Solow residual. Under the assumed constant returns to scale, the weights of capital and labor in production are given by the shares of these two inputs in aggregate output. To define output in terms of the capital stock, l_{it} is subtracted from both sides of equation:

$$\widehat{y}_{it} - \widehat{l}_{it} = \alpha(\widehat{k}_{it} - \widehat{l}_{it}) + (1-\alpha)\widehat{a}_{it} \tag{3.3}$$

where the lowercase variable with a "hat" represent the log growth rate of the uppercase variables defined in equation (3.1). In a Cobb-Douglas production function, even though

the only parameter determining the contribution of physical capital and labor to growth of output is the parameter α, the growth of the Solow residual is an important element of growth outcomes through its indirect relation with α as stated in Equation (3.3). We can re-specify Equation (3.3) in terms of the Solow residual as follows:

$$\widehat{a}_{it} = \widehat{y}_{it} - \alpha\widehat{k}_{it} + (1-\alpha)\widehat{l}_{it} \tag{3.4}$$

Taking the first partial derivative of the Solow residual with respect to the share of capital, α, yields:

$$\partial\widehat{a}_{it}/\partial\alpha = -\widehat{k}_{it} + \widehat{l}_{it} \tag{3.5}$$

Equation (3.5) implies that an increase in the share of capital will decrease (increase) TFP growth if the growth rate of capital stock is larger (smaller) than the growth rate of labor. Since in most countries, capital grows much faster than labor, the second inequality holds in Equation (3.5). That is, countries with higher capital shares will tend to have lower TFP growth (for similar growth rates of capital and labor). Given that the Solow residual measures changes in total factor productivity, once changes to growth driven by capital and labor have been accounted for, it can be readily interpreted as a function of those influences on growth such as exogenous shocks, macroeconomic policy, institutional or environment policies and other influences not captured by factor inputs. Estimating the derived equations for GLS would be insightful, allowing us to decompose changes in growth to those driven by capital accumulation, labor force and factor productivity. However, as with growth regression estimation, the robustness of results is sensitive to sample size. Therefore, to obtain more robust estimates, the sample size is extended to all the Sub-Saharan African countries. Under the assumption that the share of capital is constant across these countries, a panel methodology is used to infer the value of α.

3.5.2 Data Set and Descriptive Statistics

The estimation of α through the growth accounting model uses data on real output, capital and labor.

- **Output** Real output is measured by GDP at constant prices as published by in the IMF *World Economic Outlook* (WEO) database.
- **Labor** Labor force data is available for all the countries and it is taken from the World Bank's *World Development Indicator* WDI database. Though the database covers 44 Sub-Saharan countries over a long sample period from 1990 to 2012, some countries - Eritrea, Liberia, Sao Tome and Principe and Zimbabwe are not covered. After considering an autoregressive model of order 1, data for these countries are backwardly extrapolated.
- **Capital** Using official data on real investment, a series on capital stock was computed based on the perpetual inventory accumulation method, consistent with past studies. Two further assumptions were made on the capital series and depreciation rate of capital. Firstly, the initial capital stock K_0 is related to the investment in initial year, the (steady state) growth rate of investment and the depreciation rate. Secondly, for each country, we assume a constant economic depreciation rate r=5% (Bu (2006)) and derive the physical capital series.

The significant economic contraction during the period up to 2001 in Sierra Leone reflects the civil. Overall growth performance in Liberia and Guinea is comparable to that of the SSA region, although these two countries' grew faster during the period up to 2001. Capital stock in proportion of output in GLS is much lower than the Sub-Saharan average. The non-linear trend of this indicator in these countries could reflect extended periods of

FIGURE3.4: Evolution of Real GDP Growth and Capital Stock in GLS.

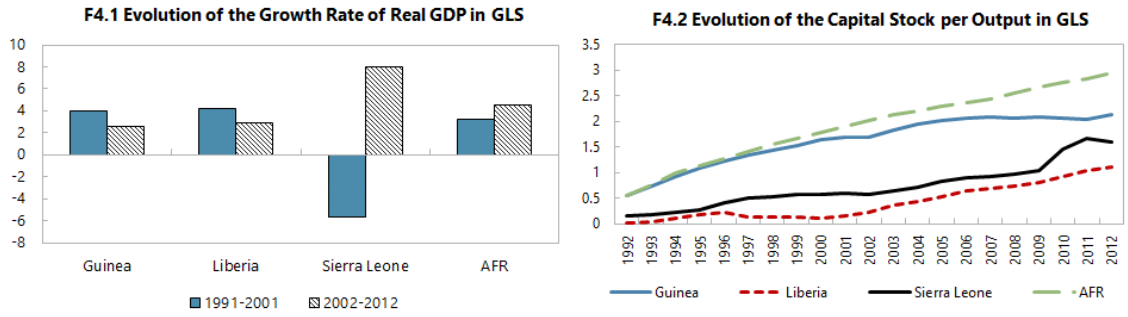

Sources: Country authorities and IMF sources.

civil strife and war. Liberia and Sierra Leone in particular, came out of civil war with significant amount of physical capital and infrastructure completely destroyed or wiped out.

3.5.3 Panel data estimation and results

To derive parameter estimates of the Solow production function, we estimate Equation (3.3) with $\widehat{y}_{it} - \widehat{l}_{it}$ as the dependent variable, and $\widehat{k}_{it} - \widehat{l}_{it}$ as the independent variable. To improve the robustness of the estimate, four different estimation methods are used: (i) Pooled least square augmented with year dummies (POLS), (ii) Pooled two-way fixed effects estimator (2FE) with time and country fixed effects, (iii) the Pesaran (2006), and (iv) the common correlated effects pooled estimators (CCEP). These estimators account for unobserved common factors with heterogeneous factors loadings by using cross section averages of the dependent and the explanatory variables as additional regressors. In the following, we replicate the intuition behind this approach considering the cross section average of the model in Equation (3.2) augmented with a common factor. As the cross section dimension gets large, the unobserved common factor can be captured by a combination of cross sectional averages of y, k and l (Eberhardt et al. (2013)).

Table 3.4: Production Function Estimates of Sub-Saharan African Countries

Dependent variable: ln(Yit)-ln(Lit)				
	POLS	2FE	CCEP	CCEP
	(1)	(2)	(3)	(4)
ln(Kit)-ln(Lit)	0.562	0.505	0.386	0.352
	(5.02)***	(3.94)***	(4.2)***	(3.87)***
Year dummies	Included	Implicit		Included
AB Test AR(2)	0.000	0.0031	0.0023	0.0056
AB Test AR(3)	0.0012	0.0413	0.2583	0.1963
CD Test	0.001	0.000	0.223	0.404
Order of integration	I(0)	I(0)	I(0)	I(0)
RMSE	0.06983	0.06916	0.06704	0.06654
R-squared	0.2219	0.2698	0.3312	0.357
Observations	1012	1012	1012	1012
Countries	44	44	44	44

Source: Authors' calculations. POLS: pooled OLS (with year fixed effects); 2FE: two-way fixed effects CCEP: Pooled Pesaran (2006); CCE: common correlated effects Absolute t-statistics in parenthesis are based on White heteroscedasticity robust standard errors. Significance level at **5% and ***1%

The results of the estimates of Labor productivity (Table 3.4) range from 0.35 to 0.56, which is within the range commonly found in growth accounting exercises. The variation across estimation methods is also minimal. However, the results of the pooled type estimators, POLS and 2FE suffer from cross section dependence as indicated by the fact that the CD Test Statistic confirms that the value of α is overestimated. This suggests the importance of the use of common correlated factor estimators, CCE, to get an unbiased estimate for α . The inclusion of common correlated factor improves the fit of the regression: the adjusted R-squared of the two CCE increases from 0.22 and 0.27 to 0.33 and 0.36.

Diagnostic tests performed on the regressions support the quality of the estimates. The tests include the Arellano and Bond (1991) test for no residual serial correlation (p-values); the Pesaran (2004) test of cross-sectional independent residuals (p-values). The order of integration of the residuals is determined using the Baltagi and Hashem Pesaran (2007) CIPS test.

Table 3.5 reports the decomposition of real output for the value of α=0.352 from the CCE model (4) regression. This value is assumed to be the same for all countries. The table shows the decomposition of real output growth into the contribution of the stock of capital, the contribution of labor input growth rate, and that of the Solow residual, broken down into Total Factor Productivity (TFP), and exogenous shocks. The evidence emerging from the decomposition of growth suggests that out of the 44 Sub-Saharan African countries, 24 report positive contribution of TFP to output growth. Over the period 1991-2012, TFP contributed 0.52 percent to an annual average real growth rate of 3.8 percent.

Figure 3.5 shows the evolution of the estimated TFP of Guinea, Liberia and Sierra Leone. The TFP for Guinea was very volatile compared to that of Liberia and Sierra Leone. This is not an uncommon finding in fragile and post-conflict states, where the growth of TFP is unlikely to be secular. Senhadji (2000) found similar evidence supporting excess volatility of TFP in developing countries. The graph also reveals that productivity performance was not constant over the sample period. Although, on average productivity growth was negative in Liberia and Sierra Leone, it was positive during some period (see Figure 3.5).

3.5.4 The impact of Ebola: the physical capital accumulation channel

In order to analyze the impact of EVD on growth through physical capital, we compare the values predicted by Equation (3.2) for growth assuming physical capital takes the values

FIGURE3.5: Evolution of Total Factor Productivity in GLS.

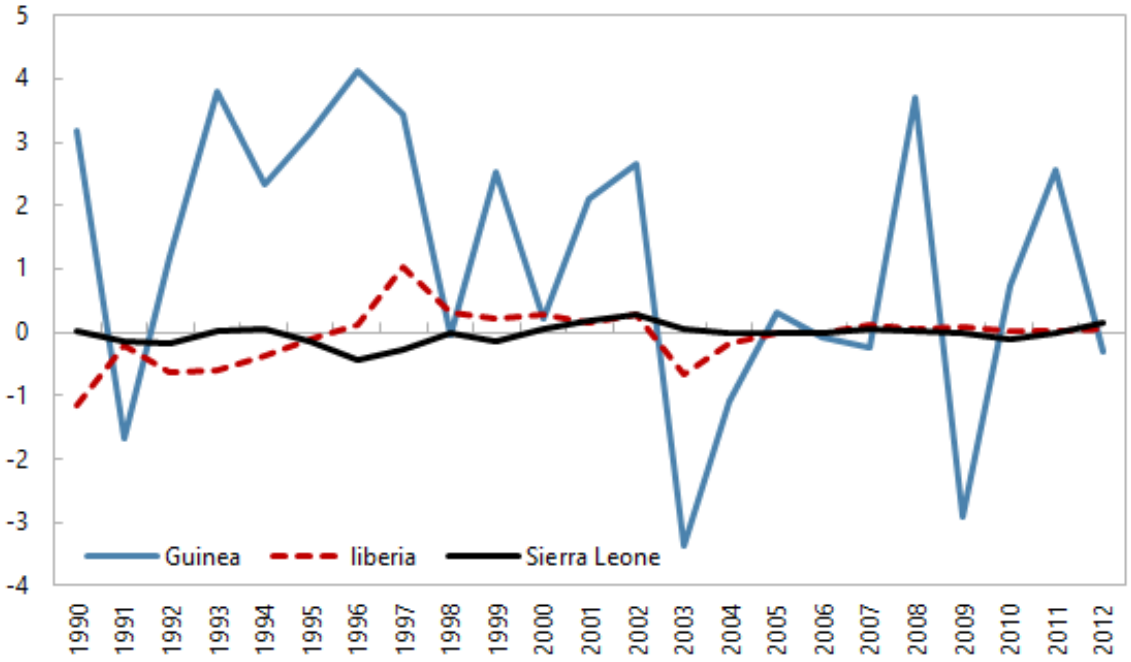

Sources: Authors' estimations.

in 2014-15 projected before the Ebola outbreak ($\widehat{k}_{it}^{(PRE-EBOLA)}$) and the values projected after taking into account the Ebola outbreak ($\widehat{k}_{it}^{(POST-EBOLA)}$)[15]. Assuming the same growth rate of labor force and productivity, then the difference in growth predicted by Equation (3.2) can be attributable to the Ebola outbreak through the physical capital accumulation channel. We do also the same exercise by setting in the growth equation the projected growth rate of physical capital to its historical average.

$$\widehat{y}_{i2014(POST-EBOLA)} - \widehat{y}_{i2014(PRE-EBOLA)} = \alpha(\widehat{k}_{i2014(POST-EBOLA)} - \widehat{k}_{i2014(PRE-EBOLA)})$$

[15] For 2014 we compare the estimates with the projection before the outbreak.

Figure 3.6 shows that differences are much larger between the two periods considered. In GLS, even though pre and post Ebola capital stocks share the same upward trends the capital stocks levels are much lower during post Ebola periods.

Table 3.6 shows a small impact of EVD on GLS capital accumulation. Indeed, the shocks affected contemporaneously the capital stocks but their relative importance differs by country and has changed over time. Given the low value of capital accumulation channel in propagating EVD shocks, it is appropriate to investigate another transmission channel. In the next section, we explore the human capital accumulation channel indirectly via the total factor of productivity.

FIGURE3.6: Capital stock in billions of national currencies pre and post Ebola in GLS.

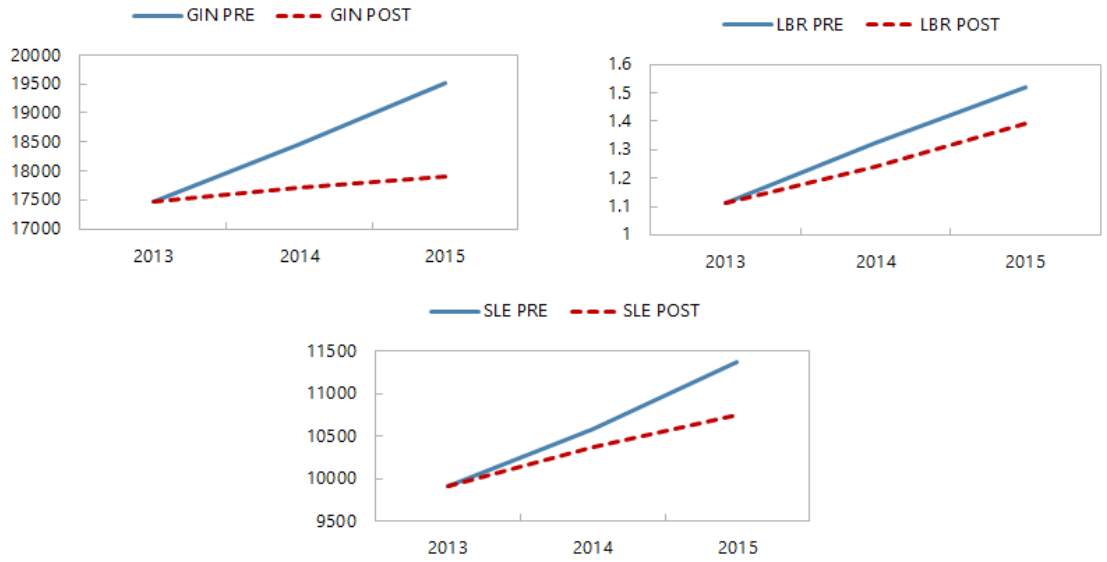

Sources: Authors' estimations.

3.5.5 The impact of Ebola: the total factor productivity Channel

Part of the impact of pandemics affecting low-income countries goes through lower productivity due to disruptions in the allocation of resources imposed by the dramatic health

situation. To quantify the impact of the Ebola outbreak through this channel, we first estimate the relation between TFP growth and the growth rate of the human capital stock, after controlling for some other variables. We calculate the stock of human capital accumulated through education as suggested in the endogenous growth theory. The average years of schooling (or equivalently the level of educational attainment), is the most popular and most commonly used specification of the human capital stock in the literature because it reflects the accumulated educational investment embodied in the current labor force. Thus, following the literature, we adopt the level of educational attainment as proxy for the human capital stock.

There are two main global data sets on the mean year of schooling. The first dataset provided by Barro and Lee (1993, 2001, 2013) covers 187 countries and contains information on educational attainment for people aged 25 and more spanning the period 1980 to 2013. The second global data set for average years of schooling is maintained by Cohen and Soto (2007), covers 95 countries, and spans the period 1960 to 2020. To transform the mean years of schooling into a human capital stock variable we follow the specification adopted in the Penn World Table 8.0 by taking into account the Mincerian rate of return to education. The data on Mincerian rates of return to an additional year of schooling were obtained from Psacharopoulos (1994).

The specification of the function is as follows:

$$hc_{it} = \exp(\phi(S_{it})) \tag{3.6}$$

where hc_{it} is the average human capital stock per worker of country i at time t, $\phi()$ is a function of the Mincerian rate of return to an additional year of schooling. The function $\phi()$ is chosen in accordance with previous studies, which found that early years of education have higher return than later years (Caselli (2005)).

$$\phi(s) = \begin{cases} 0.134 * s & \text{if } s \leqslant 4 \\ 0.134 * 4 + 0.101(s-4) & \text{if } 4 < s \leqslant 8 \\ 0.134 * 4 + 0.101 * 4 + 0.068(s-8) & \text{if } s > 8 \end{cases} \tag{3.7}$$

FIGURE3.7: Evolution of Human Capital Stock per unit of Output in GLS.

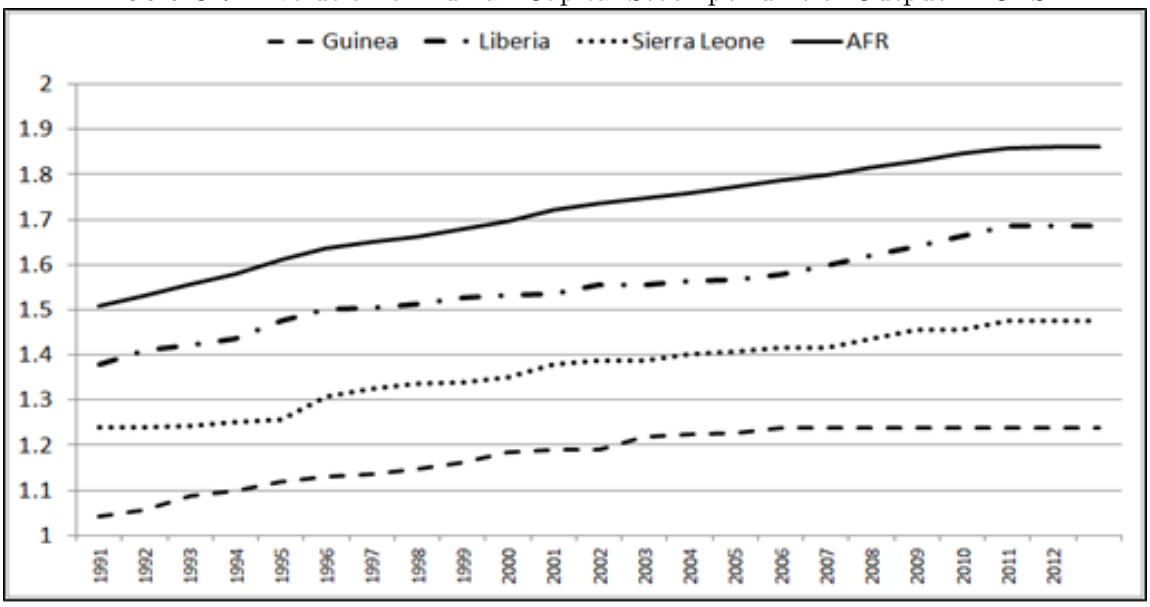

Sources: Authors' estimations.

The derived stock of human capital for GLS over time is presented in the Figure 3.7. The series on TFP growth estimated from the sources of growth equation reported in Table 3.5 is regressed on three categories of independent variables.

- **Human capital stock** from 1990 to 2012.
- **Macroeconomic variables** found in the literature to have a significant correlation with TFP growth, and comprised of the log of inflation, the log difference of credit to private sector (in percent of GDP) and the log difference of the economy's openness.

- **Institutional variables** are comprised of an indicator of democracy, an indicator of government effectiveness; and an indicator of the control of corruption[16].

Table 3.7 shows the results of two sets of three equations. Most variables have the expected sign.

- Human capital endowment is the most important determinant of TFP growth of the Sub-Saharan African countries, and the estimate consistently ranges from 50 to 63.
- The macroeconomic variables also have their expected signs, except the openness of the economy, which seems to affect negatively TFP growth.
- Institutionalized democracy and government effectiveness significantly improve TFP growth, while the variable "corruption" is negatively related to TFP growth.

To improve statistical properties of the residual, we drop the variables domestic credit to private sector, openness of the economy and democracy from the second set of equations in alternative specifications. The resulting model displays better overall fit and statistical properties.

3.6 Calibration of the impact of EVD

In order to calibrate and identify the impact of Ebola on TFP and output growth, we quantify first the country specific shock to human capital stock.

3.6.1 Deriving the shock to human capital stock in 2014

To derive the size of the shock to human capital stock we focus on the total number of EVD cases, the population potentially at risk and the total population in 2014. Unlike a model

[16] Indicator of Democracy (1992-2012) is from the Center for Systemic Peace, while Indicator of government effectiveness and the control of corruption (1996-2012) are from the Worldwide Governance Indicators (WGI) over the period.

that focuses only on the working population that was infected, this approach allows us to focus on the overall impact on human capital stock, rather than just the labor force. The population at risk is approximated by the number of contacts under follow up per EVD case. Table 3.8 shows the population potentially at risk during the period from July 6th to July 26th 2015. The size of the shock[17], significantly differs across the three countries. Overall, the results in Table 8 indicates, that the shock is severe in Sierra Leone with 11% negative impact on stock of human capital and less pronounced in Guinea with 3% negative impact.

3.6.2 Estimating the impact of EVD on TFP and output growth

In the no-Ebola scenario, TFP growth is set at the average of the period 1991-2012. The impact of Ebola on economic growth is assumed to come through the reduction in human capital stock. As indicated in Section 3.3, at the height of the epidemic, school closure ranged from 4.5 to 7.5 months in the three countries. The number of hours worked by employed declined by 12.8 percent between July 2014 and May 2015 in Sierra Leone and the other countries are assumed to have faced a similar drop in hours worked. In the Ebola scenario, we consider a negative shock on human capital stock. Based on the estimated size of shock to human capital, we assume 3% negative shock to human capital stock in Guinea and 10% negative shock in Liberia and Sierra Leone. In addition, we assume constant factors accumulation and infer their contributions based on no-Ebola scenario. We then calculate the resulting TFP growth after shock to human capital stock based on equation:

$\widehat{TFP}$= 52.283*$HumanCapitalStock$ - 3.134*$\overline{Inflation}$

-6.012*$\overline{Credittoprivatesector}$-9.985*$\overline{Opennessofeconomy}$

[17] The size of the Ebola shock is defined as the population at risk in percent of the total population. The population at risk is the contacts under follow up per case multiplied by the total cases. We focus on the period from July 6th to July 26th 2015.

$+0.045*\overline{Democracy}$

Table 3.9 shows that under the assumption of no Ebola, on average between 2014 and 2015 real GDP would increase by 4.73 percent in Guinea, 6.40 percent in Liberia and 10 percent in Sierra Leone (IMF Staff estimates). Capital accumulation would drive real GDP growth and offset the decline in TFP (by 1.58 percent in Guinea, 4.92 percent in Liberia and 7.19 percent in Sierra Leone). With Ebola, real output growth would slow to 1.3 percent in Guinea, 0.63 percent in Liberia and 6.57 percent in Sierra Leone. This confirms that the impact of Ebola on growth, coming through the shock to human capital is substantial.

3.6.3 Further evidence from a VAR model

In the following section, we assess the impact of the disease on other macroeconomic indicators such as the fiscal balance, private sector credit, and the current account. The approach consists of assessing the response to a human capital shock in the context of a Vector Auto-Regressive model. The baseline VAR model predicts the future evolution of the key macroeconomic variables, when the human capital stock is set at its historical value. The alternative VAR scenario explores the dynamics of the macroeconomic variables after implementing a shock to the human capital variable. In particular we assess the deviations of these variables from the level predicted under the steady state (historical values). The size of the shock is specific to the country and reflects the severity of the impact of the Ebola shock on human capital as estimated in Table 3.8 above. We quantify the first round effects of the shock to human capital over the horizon 2014-2018 for GLS.

Each reduced form country-specific VAR(1) model can be written as:

$$D(y_t) = B * D(y_{t-1}) + A * hcs_t + u_t \tag{3.8}$$

where $y_t = (g_t, cre_t, fb_t, ca_t)$ is the vector of endogenous variables and hcs_t denotes the

human capital stock variable. The vector y_t includes real GDP growth (g_t), domestic credit to private sector (cre_t), overall fiscal balance (fb_t) and balance on current account (ca_t)[18]. The operator $D()$ denotes the first difference operator which applied for stationarity since our VAR model is nonstationary in levels. The error term u_t is uncorrelated at different time periods and follows a white noise process.

Since our interest is limited to baseline scenario and alternative scenario under unexpected EVD shock, and not to inferring standard VAR results such as impulse response functions and variance decomposition, there is no need to postulate for identification restriction to recover the structural parameters of the models. Furthermore, given data limitations, we consider a VAR of order 1 which allows us to achieve model stability and residuals normality (see Annex). These conditions are paramount for conditional forecasting of the impact of an adverse external shock such as negative shock to the human capital stock.

This size of the unexpected negative shock to human capital stock in GLS in 2014-15 is assumed to be proportional to the size of shock. Exploring this alternative allows us to analyze the extent to which, under a negative shock to human capital stock, the economy would be pushed away from baseline expectations. We first examine the trajectories in GLS under the VAR baseline forecast of real GDP growth, balance on current account, fiscal balance and credit to private sector.

Guinea: In the baseline scenario real GDP increases from 3.67 percent in 2014 to 4.10 percent in 2018. The deficit on current account is projected to deteriorate to under 30 percent of GDP by 2018. The overall fiscal balance strengthens to -3.52 percent of GDP by 2018 and the ratio of credit to the private sector to GDP increases from 10.15 percent

[18] Data on real GDP, current account balance, and the overall fiscal balance are from the IMF *World Economic Outlook* (WEO) database, while the data on human capital stock comes from the World Bank's *World Development Indicator* (WDI).

in 2014 to 13.39 percent in 2018. The results in Table 3.10 suggest that a temporary shock to human capital stock has an immediate and high impact on the macroeconomic aggregates in Guinea. Economic growth slows down to 0.86 percent from 3.67 percent in the baseline. Associated with the slowdown are weaker overall fiscal balance and lower credit growth. Consistent with the expected impact of reduced economic activity on import, a strengthening of the balance on current account is forecast.

Liberia: Under the VAR baseline scenario, real GDP hovers around an average of 7.5 percent over the 5-year period. The current account deficit would deteriorate, while the fiscal deficit narrows gradually from 6.89 in 2014 to 4.23 percent of GDP by 2018. The ratio of domestic credit to private sector to GDP will increase from 18.59 percent in 2014 to 24.50 percent in 2018. In the adverse scenario, (Table 3.11) the impact of the shock to human capital stock on growth is quite large, accounting for more than a 5 percentage point decline in real growth. As a result, all other macroeconomic variables are similarly affected.

Sierra Leone: The analysis of the VAR baseline forecast reveals real GDP growth and the balance on current account to GDP would follow the similar pattern, as they reach a trough in 2016 and subsequently, reversal of trend. Similarly, overall fiscal balance will improve gradually during the baseline, until 2016, when deterioration of the fiscal accounts commences. This is similar to private sector credit, which expands until 2016 before contracting. The shock results in an immediate high impact on the macroeconomic variables (Table 3.12). Though real GDP growth would moderate in 2014, it reaches a trough of 2.5 percent 2015 before rebounding. The impact on fiscal balances is somewhat smaller than on external balances, but the slow down in credit growth is quite substantial.

3.7 Conclusion and policy recommendations

Following an extended period of economic stability, GLS countries became suddenly engulfed in the EVD epidemic, which exerted catastrophic human tolls. At the same time, the measures introduced to curb the disease, such as curfews, quarantines, restrictions of international travel and closure of schools and educational institutions contributed to a slowdown in economic activities, with important consequences for macroeconomic outcomes. The large outlay of resources channeled towards eradicating the disease as well as mitigating its adverse consequence took its toll on public finances, in countries that were already financially strained. Availability of external support from traditional donors and private organizations, both directly and indirectly moderated the impact, and contributed to lower rates of infection, and eventually eradiation of the disease.

The stylized facts suggest that human capital was strongly affected by the disease. The closure of schools, reduction in work hours, fatality and morbidity, all combine to degrade the human capital stock of the affected countries. Our evidence suggests that the epidemic also contributed to a small decline in capital accumulation due to investors' risk averse behavior and decline in government expenditure on capital investments. However, the bulk of the adverse impact was driven by the shock of the disease to the GLS human capital stock. Our quantification of the population at risk confirms that the size of the shock to human capital stock ranges from 4 percent in Guinea to 12 percent in Liberia.

The empirical model estimated is a Solow type production function, whose results were then used to undertake a growth accounting exercise for 44 SSA countries. The growth accounting framework which allowed us to derive the impact on capital accumulation and to conduct scenario analysis to assess the extent to which a shock to human capital stock affects TFP growth and output. Our empirical estimates confirm that while Ebola had

a small impact on capital accumulation due to investor's risk-averse behavior, the bulk of the negative impact on economic growth was propagated through the TFP channel, which declined due to the shocks to human capital. The result is therefore lower growth outcomes, than previously projected.

Additional evidence from a VAR model allowed us to assess the impact of a low probability event or an extreme shock on key macroeconomic variables. The EVD shock is presented as an unexpected shock to the stock human capital of the GLS economies and a scenario analysis is used to quantify the first round effects of the shock. Our results demonstrate that the methodology is appropriate for GLS economy and the information on human capital stock was sufficient to explain most of the variation in macroeconomic aggregate such as real GDP growth, the balance on current account, the overall fiscal balance and the domestic credit to private sector. While other factors, such as adverse external environment were at play during the same period, the fact that the model delivered shocks through changes in human capital arrived at through a quantification of at risk EVD population, confirms that the growth outcome simulated is more directly linked to EVD.

Given the demonstration of the vulnerability of GLS countries to human capital shock, the key policy implication is the need to increase investment in human capital, namely health and education. The positive donor sentiments exhibited during the epidemic needs to be harnessed to improve future donor support.

Table 3.5: Sub-Saharan African Countries: Sources of Growth, 1991-2012

Country	Real GDP growth	Contribution of :				*Memorandum*	
	(%)	Capital stock	Labor Force	TFP	Exogenous shocks	Investment to GDP ratio	Real Investment growth
Angola	5.42	3.08	1.92	0.65	-0.23	1.159	0.121
Benin	4.33	1.84	2.14	0.54	-0.19	0.179	0.062
Botswana	4.85	1.87	1.7	1.98	-0.7	0.444	0.062
Burkina Faso	5.28	1.15	1.85	3.53	-1.24	0.197	0.015
Burundi	1.34	0.95	1.49	-1.7	0.6	0.304	0.043
Cabo Verde	5.4	2.29	1.89	1.89	-0.66	0.351	0.07
Cameroon	2.11	0.97	1.93	-1.22	0.43	0.186	0.036
Central Afr. Rep.	1.21	0.28	1.42	-0.75	0.26	0.109	0.025
Chad	5.76	3.33	1.99	0.69	-0.24	0.359	0.099
Comoros	1.79	0.55	1.92	-1.04	0.37	0.123	0.034
Congo, Dem. Rep.	-0.23	0.68	1.82	-4.21	1.48	0.037	0.011
Congo, Rep	2.94	1.51	1.55	-0.19	0.07	0.099	0.063
Côte d'Ivoire	2.08	1.35	1.94	-1.87	0.66	0.148	0.004
Equatorial Guinea	18.15	7.23	1.82	14.04	-4.94	1.543	0.189
Eritrea	2.64	1.35	1.96	-1.04	0.37	0.2	0.018
Ethiopia	5.74	2.24	2.07	2.21	-0.78	0.631	0.079
Gabon	2.01	0.82	1.57	-0.59	0.21	0.282	0.029
Gambia, The	3.72	2.94	1.9	-1.73	0.61	0.227	0.116
Ghana	5.46	1.85	1.73	2.9	-1.02	0.805	0.085
Guinea	3.33	0.88	1.71	1.15	-0.4	0.215	0.046
Guinea-Bissau	1.95	-0.48	1.89	0.83	-0.29	0.156	-0.036
Kenya	3.17	1.38	1.76	0.04	-0.01	0.249	0.055
Lesotho	4.11	0.72	0.71	4.13	-1.45	0.564	0.023
Liberia	1.82	3.03	2.1	-5.11	1.8	0.087	0.134
Madagascar	2.17	1.37	2.06	-1.94	0.68	0.181	0.048
Malawi	3.9	1.55	1.68	1.03	-0.36	0.49	0.052
Mali	4.28	3.59	2.44	-2.7	0.95	0.118	0.12
Mauritius	4.74	1.31	0.81	4.05	-1.43	0.398	0.026
Mozambique	6.75	2.78	1.84	3.28	-1.16	0.26	0.077
Namibia	4.29	1.87	1.81	0.95	-0.34	0.212	0.04
Niger	3.23	2.31	2.49	-2.42	0.85	0.184	0.076
Nigeria	6.45	2.24	1.58	4.06	-1.43	0.569	0.058
Rwanda	4.2	1.85	1.56	1.22	-0.43	0.406	0.073
São Tomé and Príncipe	3.02	1.8	1.89	-1.02	0.36	0.34	0.046
Senegal	3.25	1.94	1.93	-0.95	0.33	0.173	0.067
Seychelles	3.69	1.06	1.21	2.19	-0.77	0.578	0.025
Sierra Leone	1.21	1.64	1.37	-2.76	0.97	0.123	0.082
South Africa	2.48	0.94	1.45	0.14	-0.05	0.367	0.026
Swaziland	2.7	-0.15	1.56	1.99	-0.7	0.19	-0.077
Tanzania	4.76	1.86	1.84	1.65	-0.58	0.388	0.084
Togo	2.03	0.61	2	-0.89	0.32	0.163	0.025
Uganda	6.6	2.73	1.86	3.1	-1.09	0.401	0.081
Zambia	3.56	2.78	1.6	-1.26	0.44	0.33	0.097
Zimbabwe	-0.13	-0.31	1.54	-2.11	0.74	0.094	0.013
AFR	3.81	1.72	1.76	0.52	-0.18	33.22%	5.50%

Source: IMF sources and Authors' calculations.

Table 3.6: Impact of EVD on capital accumulation (in percentage point)

	2014	2015
Guinea	-1.44	-1.60
Liberia	-2.28	-0.84
Sierra Leone	-0.71	-1.29

Sources: Authors' estimations.

Table 3.7: Empirical Results of the panel estimation of the determinants of TFP

Dependent variable: Total Factor Productivity						
	POLS	POLS	2FE	2FE	CCEP	CCEP
	(1)	(2)	(3)	(4)	(5)	(6)
Human Capital Stock	51.217	51.076	49.310	54.617	52.283	62.793
	(2.13)**	(-1.56)	(1.97)**	(2.02)**	(2.18)**	(2.44)**
Inflation	-1.314	-2.163	-1.441	-2.227	-3.134	-1.896
	(-3.41)***	(-2.28)**	(-2.40)**	(-2.42)**	(-2.81)***	(-2.30)**
Credit to private sector	-5.270		-4.783		-6.012	
	(-2.75)***		(-2.41)**		(-2.99)***	
Openess of economy	-9.397		-8.391		-9.985	
	(-2.30)**		(-2.12)**		(-2.03)**	
Democracy	0.042		0.042		0.045	
	(2.33)**		(1.72)*		(1.87)*	
Government efficiency		2.877		7.099		4.610
		(2.96)***		(2.86)***		(1.82)*
Corruption		-2.724		-3.668		-3.893
		(-1.96)*		(-1.79)*		(-1.68)*
Year dummies	Included	Included	Implicit	Implicit		
AB Test AR(1)	0.007	0.000	0.0804	0.0443	0.8406	0.36
AB Test AR(2)	0.0547	0.0128	0.2342	0.7305	0.2026	0.6767
CD Test	0.959	0.93	0.621	0.975	0.997	0.721
Order of integration	I(0)	I(0)	I(0)	I(0)	I(0)	I(0)
RMSE	8.7738	6.9134	8.3809	6.3732	7.856	5.7113
R-squared	0.1172	0.086	0.233	0.2792	0.3634	0.4553
Observations	840	364	840	364	840	364
Countries	40	27	40	27	40	27

Source: Authors' calculations. POLS: pooled OLS (with year fixed effects); 2FE: two-way fixed effects CCEP: Pooled Pesaran (2006); CCE: common correlated effects Absolute t-statistics in parenthesis are based on White heteroscedasticity robust standard errors. Significance level at **5% and ***1%

Table 3.8: Size of the Population Potentially at Risk and Shock

New cases	Guinea	Oct 19th 2014	25
	Liberia	Sept 07th 2014	110
	Sierra Leone	Jan 28th 2015	12
New contacts under follow up	Guinea	Oct 19th 2014	3223
	Liberia	Sept 07th 2014	6145
	Sierra Leone	Jan 28th 2015	773
Contacts under follow up per case	Guinea		129
	Liberia		56
	Sierra Leone		64
cumulative cases	Guinea	up to Dec 31st, 2014	2707
	Liberia	up to Dec 31st, 2014	8018
	Sierra Leone	up to Jan 28th, 2015	10518
Population potentially at risk	Guinea	up to Dec 31st, 2014	348986
	Liberia	up to Dec 31st, 2014	447915
	Sierra Leone	up to Jan 28th, 2015	677535
Size of the shock	Guinea	up to Dec 31st, 2014	3%
	Liberia	up to Dec 31st, 2014	10%
	Sierra Leone	up to Jan 28th, 2015	11%

Sources: Ministries of Health of Guinea, Liberia, and Sierra Leone, WHO, and authors' calculations.

Table 3.9: Decomposition of Growth Rate of Real GDP (alpha=0.352 %)

	Average 1991-2012			Baseline scenario [1]			Scenario 1		
	GIN	LBR	SLE	GIN	LBR	SLE	GIN	LBR	SLE
Real GDP growth	3.33	1.82	1.21	**4.73**	**6.4**	**10**	**1.26**	**0.63**	**6.57**
Capital acc	0.88	3.03	1.64	1.98	6.12	16.3	1.98	6.12	16.3
Labor force acc	1.71	2.1	1.37	1.71	2.1	1.37	1.71	2.1	1.37
Solow residual	0.74	-3.31	-1.79	1.04	-1.82	-7.67	-2.43	-7.59	-11.1
TFP growth	**1.14**	**-5.11**	**-2.76**	**1.14**	**-5.11**	**-2.76**	**-1.58**	**-4.92**	**-7.19**
Exogenous shocks	-0.4	1.8	0.97	**-0.1**	**3.29**	**-4.91**	**-0.86**	**-2.67**	**-3.91**
Memorandum items									
Investment to GDP	21.5	8.7	12.3						
Real investment growth	4.6	13.4	8.2						

Sources: IMF sources and authors' calculations. [1] We consider the average of the latest WEO projections 2014-2015 as our baseline of the real GDP growth rate in GLS.

Table 3.10: Guinea: Alternative Ebola Scenario

No Ebola baseline scenario				
Guinea	GDP growth	Balance on Current Account (% of GDP)	Overall Fiscal Balance (% of GDP)	Domestic credit to private sector (% of GDP)
2014	3.67	-20.18	-4.37	10.15
2015	4.10	-21.88	-4.39	10.89
2016	4.48	-24.17	-4.23	11.67
2017	5.29	-26.62	-3.75	12.49
2018	6.03	-29.04	-3.52	13.39
Memorandum items				
2014*	4.50		-2.76***	10.45
Ebola scenario (3% negative shock to human capital stock)				
Guinea	GDP growth	Balance on Current Account (% of GDP)	Overall Fiscal Balance (% of GDP)	Domestic credit to private sector (% of GDP)
2014	0.86	-17.14	-6.01	9.07
2015	-0.05	-17.08	-5.83	8.98
2016	1.27	-19.78	-4.82	10.00
2017	1.54	-21.84	-5.07	10.84
2018	2.43	-24.63	-4.46	11.72
Memorandum items				
2014**	1.10	-18.03	-4.35	12.50

Sources: IMF sources and authors' calculations. (*) IMF Staff projections, (**) IMF Staff estimates, (***) grant included.

Table 3.11: Liberia: Alternative Ebola Scenario

No Ebola baseline scenario				
Liberia	GDP growth	Balance on Current Account (% of GDP)	Overall Fiscal Balance (% of GDP)	Domestic credit to private sector (% of GDP)
2014	7.33	-31.41	-6.89	18.59
2015	5.99	-43.01	-5.28	21.17
2016	9.02	-36.01	-3.95	21.92
2017	7.50	-43.13	-5.13	23.53
2018	8.32	-42.76	-4.23	24.50
Memorandum items				
2014*	5.90		-7.08	20.24
Ebola scenario (-10% negative shock to human capital stock)				
Liberia	GDP growth	Balance on Current Account (% of GDP)	Overall Fiscal Balance (% of GDP)	Domestic credit to private sector (% of GDP)
2014	2.56	-36.80	-2.73	18.35
2015	3.39	-40.66	4.69	20.63
2016	12.52	-26.36	1.80	21.99
2017	6.85	-42.98	-5.31	23.53
2018	7.49	-42.96	-3.38	24.20
Memorandum items				
2014**	0.69	-36.35	-4.49	18.18

Sources: IMF sources and authors' calculations. (*) IMF Staff projections, (**) IMF Staff estimates.

Table 3.12: Sierra Leone: Alternative Ebola Scenario

No Ebola baseline scenario				
Sierra Leone	GDP growth	Balance on Current Account (% of GDP)	Overall Fiscal Balance (% of GDP)	Domestic credit to private sector (% of GDP)
2014	10.96	-10.45	-4.83	5.89
2015	5.02	-17.88	-3.99	7.37
2016	3.85	-24.87	-3.81	7.53
2017	11.16	-23.09	-3.91	6.67
2018	14.53	-18.28	-4.39	6.09
Memorandum items				
2014*	11.30		-4.2	12.10
Ebola scenario (10% negative shock to human capital stock)				
Sierra Leone	GDP growth	Balance on Current Account (% of GDP)	Overall Fiscal Balance (% of GDP)	Domestic credit to private sector (% of GDP)
2014	8.05	-12.14	-4.50	5.44
2015	1.38	-18.80	-2.85	5.37
2016	12.20	-13.43	-3.02	4.70
2017	15.67	-8.27	-4.31	5.65
2018	3.54	-17.38	-4.31	7.31
Memorandum items				
2014**	7.10	-10.94	-3.12	4.83

Sources: IMF sources and authors' calculations. (*) IMF Staff projections, (**) IMF Staff estimates.

Bibliography

Allen, F. and Babus, A. (2009), "Networks in Finance," *The network challenge: strategy, profit, and risk in an interlinked world*, p. 367.

Arellano, M. and Bond, S. (1991), "Some tests of specification for panel data: Monte Carlo evidence and an application to employment equations," *The review of economic studies*, 58, 277–297.

Arndt, C. and Lewis, J. D. (2001), "The HIV/AIDS pandemic in South Africa: Sectoral impacts and unemployment," *Journal of International Development*, 13, 427–449.

Artis, M., Krolzig, H.-M., and Toro, J. (2004), "The European business cycle," *Oxford Economic Papers*, 56, 1–44.

Baltagi, B. H. and Hashem Pesaran, M. (2007), "Heterogeneity and cross section dependence in panel data models: theory and applications introduction," *Journal of Applied Econometrics*, 22, 229–232.

Bańbura, M., Giannone, D., and Reichlin, L. (2010), "Large Bayesian vector auto regressions," *Journal of Applied Econometrics*, 25, 71–92.

Barro, R. J. and Lee, J.-W. (1993), "International comparisons of educational attainment," *Journal of monetary economics*, 32, 363–394.

Barro, R. J. and Lee, J.-W. (2001), "International data on educational attainment: updates and implications," *oxford Economic papers*, 53, 541–563.

Barro, R. J. and Lee, J. W. (2013), "A new data set of educational attainment in the world, 1950–2010," *Journal of development economics*, 104, 184–198.

Barthélemy, J. and Poncet, S. (2008), "China as an integrated area?" *Journal of Economic Integration*, 23, 896–926.

Bell, C., Devarajan, S., and Gersbach, H. (2004), "Thinking about the long-run economic costs of AIDS," *The macroeconomics of HIV/AIDS*, 96, 128–129.

Beutels, P., Jia, N., Zhou, Q.-Y., Smith, R., Cao, W.-C., and De Vlas, S. J. (2009), "The economic impact of SARS in Beijing, China," *Tropical Medicine & International Health*, 14, 85–91.

Billio, M., Casarin, R., Ravazzolo, F., and van Dijk, H. K. (2012), "Combination schemes for turning point predictions," *The Quarterly Review of Economics and Finance*, 52, 402–412.

Billio, M., Casarin, R., Ravazzolo, F., and Van Dijk, H. K. (2016a), "Interconnections between Eurozone and US booms and busts: A Bayesian panel Markov-switching VAR Model," *Journal of Applied Econometrics*.

Billio, M., Casarin, R., Ravazzolo, F., and Van Dijk, H. K. (2016b), "Interconnections Between Eurozone and US Booms and Busts Using a Bayesian Panel Markov-Switching VAR Model," *Journal of Applied Econometrics*.

Bloom, D. E., Sachs, J. D., Collier, P., and Udry, C. (1998), "Geography, demography, and economic growth in Africa," *Brookings papers on economic activity*, pp. 207–295.

Bosworth, B., Collins, S. M., and Chen, Y.-c. (1995), *Accounting for differences in economic growth*, no. 115, Brookings Institution.

Brémaud, P. (2013), *Markov chains: Gibbs fields, Monte Carlo simulation, and queues*, vol. 31, Springer Science & Business Media.

Bry, G. and Boschan, C. (1971), "Cyclical Analysis of Time Series: Selected Procedures and Computer Programs," *New York: National Bureau of Economic Research*.

Bu, Y. (2006), "Fixed capital stock depreciation in developing countries: Some evidence from firm level data," *Journal of Development Studies*, 42, 881–901.

Burda, M. (2015), "Constrained Hamiltonian Monte Carlo in BEKK GARCH with Targeting," *Journal of Time Series Econometrics*, 7, 95–113.

Burda, M. and Maheu, J. M. (2013), "Bayesian adaptively updated Hamiltonian Monte Carlo with an application to high-dimensional BEKK GARCH models," *Studies in Nonlinear Dynamics and Econometrics*, 17, 345–372.

Burns, A. F. and Mitchell, W. C. (1946), "Measuring business cycles," *New York: National Bureau of Economic Research*.

Byström, H. N., Olofsdotter, K., and Söderström, L. (2005), "Is China an optimum currency area?" *Journal of Asian Economics*, 16, 612–634.

Çakmaklı, C., Paap, R., and van Dijk, D. (2013), "Measuring and predicting heterogeneous recessions," *Journal of Economic Dynamics and Control*, 37, 2195–2216.

Camacho, M. and Leiva-Leon, D. (2014), "The Propagation of Industrial Business Cycles," Tech. rep., Working paper n. 2014-48, Bank of Canada.

Candelon, B., Piplack, J., and Straetmans, S. (2009), "Multivariate Business Cycle Synchronization in Small Samples," *Oxford Bulletin of Economics and Statistics*, 71, 715–737.

Caselli, F. (2005), "Accounting for cross-country income differences," *Handbook of economic growth*, 1, 679–741.

Celeux, G. (1998), "Bayesian inference for mixture: The label switching problem," pp. 227–232.

Chengyong, W. and Chunrong, A. (2010), "Nonlinear Smooth Transition of Chinese Business Cycle," *Economic Research Journal*, 3, 008.

Chib, S. (1996), "Calculating posterior distributions and modal estimates in Markov mixture models," *Journal of Econometrics*, 75, 79–97.

Christensen, O. F., Roberts, G. O., and Rosenthal, J. S. (2005), "Scaling limits for the transient phase of local Metropolis–Hastings algorithms," *Journal of the Royal Statistical Society: Series B (Statistical Methodology)*, 67, 253–268.

Cohen, D. and Soto, M. (2007), "Growth and human capital: good data, good results," *Journal of economic growth*, 12, 51–76.

Cuddington, J. T. (1993a), "Modeling the macroeconomic effects of AIDS, with an Application to Tanzania," *The World Bank Economic Review*, 7, 173–189.

Cuddington, J. T. (1993b), "Further results on the macroeconomic effects of AIDS: the dualistic, labor-surplus economy," *The World Bank Economic Review*, 7, 403–417.

Cuddington, J. T. and Hancock, J. D. (1995), "The macroeconomic impact of AIDS in Malawi: a dualistic, labour surplus economy," *Journal of African Economies*, 4, 1–28.

Dixon, S., McDonald, S., and Roberts, J. (2001), "AIDS and economic growth in Africa: a panel data analysis," *Journal of International Development*, 13, 411–426.

Eberhardt, M., Helmers, C., and Strauss, H. (2013), "Do spillovers matter when estimating private returns to R&D?" *Review of Economics and Statistics*, 95, 436–448.

Föllmer, H. and Horst, U. (2001), "Convergence of locally and globally interacting Markov chains," *Stochastic Processes and Their Applications*, 96, 99–121.

Francis, N., Owyang, M. T., Savascin, O., et al. (2012), "An endogenously clustered factor approach to international business cycles," *Federal Reserve Bank of St. Louis Working Paper*.

Friedman, M. (1993), "The "plucking model" of business fluctuations revisited," *Economic Inquiry*, 31, 171–177.

Frühwirth-Schnatter, S. (2001), "Markov chain Monte Carlo estimation of classical and dynamic switching and mixture models," *Journal of the American Statistical Association*, 96, 194–209.

Frühwirth-Schnatter, S. (2006), *Finite Mixture and Markov Switching Models*, Springer, New York.

Gatfaoui, J. and Girardin, E. (2015), "Comovement of Chinese provincial business cycles," *Economic Modelling*, 44, 294–306.

Gelfand, A. E. and Dey, D. K. (1994), "Bayesian model choice: Asymptotics and exact calculations," *Journal of the Royal Statistical Society. Series B (Methodological)*, pp. 501–514.

Gerlach-Kristen, P. (2009), "Business cycle and inflation synchronisation in Mainland China and Hong Kong," *International Review of Economics & Finance*, 18, 404–418.

Giannone, D., Lenza, M., and Reichlin, L. (2008), "Business cycles in the euro area," Tech. rep., NBER Working Paper No. 14529.

Girardin, E. (2005), "Growth-cycle features of East Asian countries: are they similar?" *International Journal of Finance & Economics*, 10, 143–156.

Girardin, E. and Kholodilin, K. A. (2011), "Are geese flying by themselves inside China? An LSTR-SEM approach to income convergence of Chinese counties," *Working Paper n. 1124, German Institute for Economic Research.*

Girolami, M. and Calderhead, B. (2011), "Riemann manifold Langevin and Hamiltonian Monte Carlo methods," *Journal of the Royal Statistical Society: Series B (Statistical Methodology)*, 73, 123–214.

Guo, F., Ozyildirim, A., and Zarnowitz, V. (2009), "On the measurement and analysis of aggregate economic activity for China: The coincident economic indicators approach," *China Economic Journal*, 2, 159–186.

Haacker, M. (2002), "The economic consequences of HIV/AIDS in Southern Africa," 38.

Hai, W., Zhao, Z., Wang, J., and Hou, Z.-G. (2004), "The short-term impact of SARS on the Chinese economy," *Asian Economic Papers*, 3, 57–61.

Hamilton, J. D. (1989), "A New Approach to the Economic Analysis of Nonstationary Time Series and the Business Cycle," *Econometrica*, 57, 357–384.

Hamilton, J. D. and Owyang, M. T. (2012), "The propagation of regional recessions," *Review of Economics and Statistics*, 94, 935–947.

Harding, D. and Pagan, A. (2002), "Dissecting the cycle: A methodological investigation," *Journal of Mononetary Economics*, 49, 365–381.

Harding, D. and Pagan, A. (2006), "Synchronization of cycles," *Journal of Econometrics*, 132, 59–79.

Holz, C. A. (2004a), "China's statistical system in transition: Challenges, data problems, and institutional innovations," *Review of Income and Wealth*, 50, 381–409.

Holz, C. A. (2004b), "Deconstructing China's GDP statistics," *China Economic Review*, 15, 164–202.

Hsiao, F. S. and Mei-Chu, W. H. (2003), ""Miracle Growth" in the Twentieth Century - International Comparisons of East Asian Development," *World Development*, 31, 227–257.

Kaufmann, S. (2010), "Dating and forecasting turning points by Bayesian clustering with dynamic structure: A suggestion with an application to Austrian data," *Journal of Applied Econometrics*, 25, 309–344.

Kaufmann, S. (2015), "K-state switching models with time-varying transition distributions - Does loan growth signal stronger effects of variables on inflation?" *Journal of Econometrics*, 187, 82–94.

Kim, C.-J. and Nelson, C. R. (1998), "Business cycle turning points, a new coincident index, and tests of duration dependence based on a dynamic factor model with regime switching," *Review of Economics and Statistics*, 80, 188–201.

Kim, C.-J. and Nelson, C. R. (1999), "Has the US economy become more stable? A Bayesian approach based on a Markov-switching model of the business cycle," *Review of Economics and Statistics*, 81, 608–616.

Kose, M. A., Otrok, C., and Whiteman, C. H. (2003), "International business cycles: World, region, and country-specific factors," *american economic review*, pp. 1216–1239.

Kose, M. A., Otrok, C., and Whiteman, C. H. (2008), "Understanding the evolution of world business cycles," *Journal of international Economics*, 75, 110–130.

Krolzig, H.-M. and Toro, J. (2005), "Classical and modern business cycle measurement: The European case," *Spanish Economic Review*, 7, 1–21.

Langnana, C. and Hongweib, L. (2007), "Empirical investigation on the asymmetry and persistence of Chinese business cycle," *Economic Research Journal*, 4.

Lee, J.-W. and McKibbin, W. J. (2004), "Globalization and disease: The case of SARS," *Asian Economic Papers*, 3, 113–131.

Leiva-Leon, D. (2014), "A New Approach to Infer Changes in the Synchronization of Business Cycle Phases," .

Lemoine, F., Mayo, G., Poncet, S., and Ünal, D. (2014), "The Geographic Pattern of China's Growth and Convergence within Industry," .

Liu, J.-q. and Zheng, T.-g. (2008), "Recognition of Phases of China s Business Cycle and Forecasting for the Growth Trend," *China Industrial Economics*, 1, 32–39.

Liu, L. (2009), "Impact of the global financial crisis on China: Empirical evidence and policy implications," *China & world economy*, 17, 1–23.

Lucas, R. E. (1988), "On the mechanics of economic development," *Journal of monetary economics*, 22, 3–42.

MacFarlan, M. and Sgherri, S. (2001), *The macroeconomic impact of HIV/AIDS in Botswana*, vol. 1, International Monetary Fund.

Masha, I. (2004), "An economic assessment of Botswana's national strategic framework for HIV/AIDS," *The macroeconomics of HIV/AIDS*, p. 287.

Nilsson, R. and Brunet, O. (2006), "Composite Leading Indicators for Major OECD Non-Member Economies: Brazil, China, India, Indonesia, Russian Federation, South Africa," Tech. rep., Working Paper n. 2006-1, OECD.

Over, M. (1992), "The macroeconomic impact of AIDS in Sub-Saharan Africa." .

Owyang, M. T., Piger, J., and Wall, H. J. (2005), "Business cycle phases in US states," *Review of Economics and Statistics*, 87, 604–616.

Ozyildirim, A. and Wu, H. X. (2013), "Modeling Trends, Cyclical Movements and Turning Points of the Chinese Economy," Tech. rep., Working Paper n. 13-02, The Conference Board, Economics Program.

Paap, R., Segers, R., and van Dijk, D. (2009), "Do leading indicators lead peaks more than troughs?" *Journal of Business & Economic Statistics*, 27, 528–543.

Pesaran, M. H. (2004), "General diagnostic tests for cross section dependence in panels," *Working Paper Series No. 1229, CESifo. IZA Discussion Paper No. 1240. Available at SSRN:* `http://ssrn.com/abstract=572504`.

Pesaran, M. H. (2006), "Estimation and inference in large heterogeneous panels with a multifactor error structure," *Econometrica*, 74, 967–1012.

Pritchett, L. and Summers, L. H. (1996), "Wealthier is healthier," *Journal of Human resources*, pp. 841–868.

Psacharopoulos, G. (1994), "Returns to investment in education: A global update," *World development*, 22, 1325–1343.

Scott, S. L. (2011), "Data augmentation, frequentist estimation, and the Bayesian analysis of multinomial logit models," *Statistical Papers*, 52, 87–109.

Senhadji, A. (2000), "Sources of Economic Growth: An Extensive Growth Accounting Exercise," *International Monetary Fund Staff Papers*, 47, 129–129.

Sichel, D. E. (1994), "Inventories and the three phases of the business cycle," *Journal of Business & Economic Statistics*, 12, 269–277.

Stock, J. H. and Watson, M. W. (2014), "Estimating turning points using large data sets," *Journal of Econometrics*, 178, 368–381.

Tahari, A., Akitoby, B., and Aka, E. B. (2004), "Sources of growth in Sub-Saharan Africa," *IMF Working Paper*, 176.

Tang, K.-K. (1998), "Economic integration of the Chinese provinces: a business cycle approach," *Journal of Economic Integration*, 13, 549–570.

Tisdell, C. (2009), "Economic reform and openness in China: China's development policies in the last 30 years," *Economic Analysis and Policy*, 39, 271.

Vesper, A. J. (2013), "Three Essays of Applied Bayesian Modeling: Financial Return Contagion, Benchmarking Small Area Estimates, and Time-Varying Dependence," Ph.D. thesis.

Virbickaite, A., Ausín, M. C., and Galeano, P. (2015), "Bayesian inference methods for univariate and multivariate GARCH models: A survey," *Journal of Economic Surveys*, 29, 76–96.

Wall, H. J. (2007), "Regional Business Cycle Phases in Japan." *Federal Reserve Bank of St. Louis Review*, pp. 61–80.

Wang, P. and Theobald, M. (2008), "Regime-switching volatility of six East Asian emerging markets," *Research in International Business and Finance*, 22, 267–283.

Williams, D. (1991), *Probability with martingales*, Cambridge University Press.

Yao, Y. (2014), "The Chinese growth miracle," *Handbook of Economic Growth*, 2, 943–1031.

Young, A. (2003), "Gold into Base Metals: Productivity Growth in the PeopleâĂŹs Republic of China during the Reform Period," *Journal of Political Economy*, 111, 1220–1261.

Zheng, T., Teng, Y., and Song, T. (2010), "Business cycle asymmetry in China: evidence from Friedman's plucking model," *China & World Economy*, 18, 103–120.